An off-lattice derivation and thermodynamic consistency consideration for the Sanchez-Lacombe equation of state

by

Kier von Konigslow

A thesis
presented to the University of Waterloo
in fulfillment of the
thesis requirement for the degree of
Doctor of Philosophy
in
Physics - Nanotechnology

Waterloo, Ontario, Canada, 2017

Examining Committee Membership

The following served on the Examining Committee for this thesis. The decision of the Examining Committee is by majority vote.

External Examiner:	Constantinos G. Panayiotou Professor, Dept. of Chemical Engineering, Aristotle University of Thessaloniki
Supervisors:	Russell B. Thompson Associate Professor, Dept. of Physics & Astronomy, University of Waterloo
	Chul B. Park Adjunct Professor, Dept. of Mechanical & Industrial Engineering, University of Toronto
Internal Member:	Bae-Yeun Ha Professor, Dept. of Physics & Astronomy, University of Waterloo
Internal-External Member:	Nasser M. Abukhdeir Associate Professor, Dept. of Chemical Engineering, University of Waterloo
Other Member:	David Yevick Professor, Dept. of Physics & Astronomy, University of Waterloo

I hereby declare that I am the sole author of this thesis. This is a true copy of the thesis, including any required final revisions, as accepted by my examiners.

I understand that my thesis may be made electronically available to the public.

Abstract

The application of the Sanchez-Lacombe equation of state (SL-EOS) to homogeneous polymeric mixtures is requisite for the application of some types of Self-Consistent Field Theory (SCFT) to inhomogeneous mixtures. It has recently been observed that the SL-EOS fails to adequately describe the saturated polymer-solvent mixtures considered in polymeric foaming. This observation portends poor outcomes for the application of SCFT to the inhomogeneous polymer mixtures that constitute foams. In order to investigate this failure, an off-lattice method for deriving the SL-EOS is presented. In doing so, it is shown that the phase equilibrium inconsistencies introduced into the mixture formulation through hole volume mixing rules cannot be corrected, as previously proposed. Rather, it is found that any mixing rule applied to the hole volume introduces impermissible thermodynamic inconsistencies to the theory.

A new variant of the theory for use with saturated polymer-solvent mixtures is proposed, eliminating mixing rules in favour of a constant hole volume. This variant is successfully applied to the solubility data of saturated binary and ternary polymer-solvent mixtures, indicating that the previously observed poor performance of the SL-EOS for such mixtures was partly the result of the thermodynamic inconsistencies. Fair agreement is also achieved for swelling data for the same mixtures.

A physical interpretation of hole volume is put forward, characterizing them in terms of rudimentary averaged correlations. The interpretation relates these correlations to the architecture of polymer molecules, evidenced by consideration of both pure fluids and mixtures.

The large number of conflicting literature parameters is addressed by proposing a best practice parameter estimation procedure based on nonlinear least-square fitting, for both for pure fluids and mixtures. Poor performance in some literature parameters is found to be related to sub-optimal parameter estimation practices, namely those that include few data points and those that encompass the critical point.

An additional constraint is proposed for semi-empirical statistical thermodynamical theories that include features without physical basis and use thermodynamic principles to derive material properties, asserting that ensemble equivalence should be imposed. This constraint is applied through the imposition that equations of state derived from each thermodynamic potential be consistent.

Acknowledgements

I would first like to thank my supervisors, Professors Russell B. Thompson and Chul B. Park. This work would not have been possible without their skilful guidance and wholehearted support.

In addition, I would like to thank my Graduate Committee members, Professors Nasser M. Abukhdeir and Bae-Yeun Ha as well as my Examination Committee members, Professors Constantinos G. Panayiotou and David Yevick.

This thesis would not have been possible without the support of my loving wife Azadeh Bagheri.

This research was financially supported by the Natural Sciences and Engineering Research Council of Canada (NSERC) as well as by the Consortium for Cellular and Microcellular Plastics (CCMCP).

Dedication

To my loving family.

Table of Contents

List of Tables

List of Figures

Acronyms

BPP Branched Polypropylene.

CBA Chemical Blowing Agent.

DME Dimethyl Ether.

EOS Equation of State.

FH Flory-Huggins.

FOV Flory-Orwoll-Vrij.

HN Hong-Noolandi.

LCST Lower Critical Solution Temperature.

LDPE Low-Density Polyethylene.

LPP Linear Polypropylene.

MFT Mean Field Theory.

PBA Physical Blowing Agent.

PC Perturbed-Chain.

PLA Polylactic Acid/Polylactide.

PS Polystyrene.

PVT Pressure-Volume-Temperature/Pressure-Density-Temperature.

SAFT Self-Associating Fluid Theory.

SCFT Self-Consistent Field Theory.

SL Sanchez-Lacombe.

SS Simha-Somcynsky.

UCST Upper Critical Solution Temperature.

Nomenclature

Symbol	Description	Unit
F	Helmholtz free energy	J
G	Gibbs free energy	J
P^*	characteristic pressure	MPa
P	pressure	MPa
Q_{conf}	configurational partition function	
Q_{int}	internal partition function	
Q	canonical partition function	
T^*	characteristic temperature	K
T	temperature	K
Λ_h	normalization factor for partition function	cm
Λ_i	thermal de Broglie wavelength associated with component i	cm
α_i	volume ratio of component i with respect to the volume of a hole	
$\alpha_{i,r}$	volume ratio of component i with respect to a constant, arbitrary reference volume	
χ_i	solubility of solvent i in a polymer-solvent mixture	
χ_s	total solubility of solvent in a saturated polymer-solvent mixture	

Symbol	Description	Unit
ϵ_{ii}^*	interaction energy between neighbouring segments of species i on a lattice	J
ϵ_{ij}^*	interaction energy between neighbouring segments of species i and species j on a lattice	J
ϵ_{ii}	energy characterizing interaction between segments of species i	J
ϵ_{ij}	energy characterizing interaction between segments of species i and species j	J
ϕ_i	volume fraction occupied by component i	
ψ_i	segment fraction occupied by component i	
ρ^*	characteristic density	$\mathrm{g\,cm^{-3}}$
ρ	density	$\mathrm{g\,cm^{-3}}$
$\tilde{F}$	reduced Helmholtz free energy	
$\tilde{G}$	reduced Gibbs free energy	
$\tilde{P}$	reduced pressure	
$\tilde{T}$	reduced temperature	
$\tilde{\rho}$	reduced density	
k_B	Boltzmann's constant	$\mathrm{J\,K^{-1}}$
r_i^0	number of lattice sited occupied by component i in the pure fluid	
r_i	number of lattice sited occupied by component i in the mixture	
v^*	lattice characteristic volume	$\mathrm{cm^3}$
v_0	hole volume	$\mathrm{cm^3}$
v_i	segment volume of species i	$\mathrm{cm^3}$
v_r	arbitrary constant reference volume	$\mathrm{cm^3}$

"All models are wrong; some models are useful."

– George E. P. Box

Chapter 1

Introduction

1.1 Motivations

The ability to predict phase equilibria in homogeneous polymer-solvent mixtures is important to many applications, especially the manufacture of polymeric foams. While many theories exist that are capable of making such predictions, industrial applications such as process control favour theories with high accuracy and low complexity. This is achieved by reducing the information content of the theory to include only the molecular information relevant to the desired properties, often thermodynamic Pressure-Volume-Temperature (PVT) data, while excluding unnecessary model features [101]. This trade-off must be considered carefully. On one hand, a theory that is too simplistic will not be capable of explaining and predicting the system's behaviour and will not satisfactorily predict observables [119]. On the other hand, a theory containing a large amount of information does not *necessarily* imply that it offers greater accuracy or a wider range of applicability. In general, a theory should strike a balance that is appropriate for its given purpose [101].

The widely used Sanchez-Lacombe equation of state (SL-EOS) offers an excellent balance between correlation to experiment and complexity for the polymer-solvent mixtures considered in polymeric foaming. The earlier cell theories attribute inappropriate solidlike entropies to amorphous fluids [28, 29], while the contemporaneous Simha-Somcynsky theory includes additional arbitrary features and added complexity [56, 113]. The perturbed-chain self-associating fluid theory (PC-SAFT) features dozens of model parameters and dozens of terms in its equation of state [38, 39]. Inclusion of only PVT considerations makes the SL-EOS ideal for process control applications that need consider only PVT-related parameters.

The SL-EOS is not only capable of predicting thermodynamic changes upon mixing, but also pure fluid properties [66, 103–105]. The SL-EOS was first advanced in a 1974 publication in *Nature* [103] preliminary to more detailed publications outlining a theory for pure fluids [104] and for mixtures [66]. The theory applies to both macromolecules and small molecules by treating them as chains of segments distributed on a lattice. The presence of lattice vacancies, known as holes, allows for the treatment of volumetric effects not typically included in earlier lattice-based mixture theories [26, 54]. The holes absorb residual equation of state effects not explicitly included in the theory, making it semi-empirical in nature. Since its introduction, the SL-EOS has been ubiquitous, with applications ranging from hydrogen storage [2] to drug delivery [59] to dark energy [21].

Many statistical mechanical equations of state, those that are semi-empirical in particular, make use of assertions that can only be validated through comparison with experimental observation [119]. The SL-EOS makes several such assertions, including the assumption introduced by Prigogine [98] of the independence of internal and translational modes of energy, the inclusion of holes to absorb residual equation of state effects [66, 104], and the mean field discounting of correlations [41]. In the past, technological limitations impeded the ability to obtain accurate and independent solubility and swelling data for polymer-solvent mixtures, where solubility is defined as the mass fraction of solvent in a saturated polymer-solvent mixture and swelling is defined as the ratio of the volume of a polymer-solvent mixture to the volume of the original polymer sample. Accurate magnetic-balance-based solubility measurement requires knowledge of volumetric changes. Since this was not directly observable, buoyancy corrections to the experimental data could be made only with reference to theoretical equations of state, making verification of those equations using such data impossible [68]. Recently, novel methods for the observation of such volumetric changes have made independent buoyancy corrections, and thus accurate experimental solubility data, possible [47, 68, 73, 80]. It has therefore only recently been possible to experimentally verify the SL-EOS for polymer-solvent mixtures.

Through comparison with independent experimental solubility and swelling data, it has become apparent that the SL-EOS produces unsatisfactory predictions at high pressures [47, 68, 73–75, 80]. Due to the importance of the high-pressure regime for the manufacture of micro- and nano- cellular foams as well as the use of more environmentally friendly blowing agents, this failure has led to the abandonment of the theory, in some applications, in favour of alternatives that offer better agreement at the cost of greater complexity and greater demands on computing power [47, 67, 69–71, 76, 79, 90, 134, 139]. In some cases, such as the Simha-Somcynsky equation of state [56, 113], the better agreement may be simply due to additional unphysical free parameters, such as the equation governing the solidlike and gaslike contributions to free volume. In other cases, such as with perturbed-

chain self-associating fluid theory (PC-SAFT) [38, 39], the greatly increased complexity of the theory and resulting greater demand on computing power is not justified, since much of the increased information content is not used in industrial process control. On the other hand, the quality of the SL-EOS predictions does not necessarily indicate the failure of the *fundamental* theory assertions.

The failure of the SL-EOS could be attributed to several possible sources. For example it could be the result of poor quality parameters. It has been noted in the literature that the degree of success the pure fluid parameters exhibit in predicting pure fluid properties has a great effect on the success of the subsequent multicomponent mixture predictions [5]. Conventional wisdom has been that no single set of parameters is capable of good agreement with experiment over a large range of pressures and temperatures. At the same time no consensus exists on how best to perform parameter estimation, with a multitude of procedures employed to varying degrees of success. The combination of these factors has led to large numbers of competing parameters for the same materials, without agreement on appropriate thermodynamic ranges or fitting practices [4, 12, 20, 34, 36, 45, 58, 63, 87, 95, 135, 138]. Many of these parameters make poor predictions outside of the thermodynamic range from which they were estimated.

The failure could also be attributed to the use of the theory outside of its known limitations. In statistical mechanics, systems of many interacting particles rarely yield to exact solution [50, 119]. In the pursuit of physical predictions, it is often necessary to apply simplifying assumptions to produce more tractable mathematics [50, 64, 119]. Often as a consequence, these assumptions impose limitations on the resulting theory. Agreement of the theoretical predictions with experiment can be affected by such assumptions, particularly if predictions are made outside of these limits. In the case of the SL-EOS, low solvent density assumptions appropriate for gaseous blowing agents may begin to break down at high pressure, particularly in the supercritical regime [107]. The application of the mean field statistics makes application of the theory near second-order phase transitions, such as the critical point, problematic.

Failure of the theory could also be the result of concealed inconsistencies. Phase dependence of the reference energies and reference chemical potentials based on the Sanchez-Lacombe equation of state for fluid mixtures has been shown by Neau [88] to cause inconsistent phase equilibrium calculations. Despite an attempt by Neau to correct the issue with the aid of fugacity coefficients, the inconsistency runs deeper than currently appreciated and cannot be corrected.

On the other hand, success of the SL-EOS affects more than the homogeneous systems originally considered. In 1981, Hong and Noolandi [53] created a version of Self-Consistent

Field Theory (SCFT) for inhomogeneous mixtures that similarly features a fluid of incompressible segments and holes. The theory has been applied to polymeric foams in order to calculate interfacial tension and cell densities [60–62, 91, 116]. The authors observed that the Hong-Noolandi Self-Consistent Field Theory (HN-SCFT) reduces to the SL-EOS in the homogeneous limit [53], implying that validation of the SL-EOS is a required prerequisite for the application of HN-SCFT [53, 117]. Significantly, since HN-SCFT was derived through a functional integral construction, it serves as proof that the SL-EOS can be decoupled from the lattice.

1.2 Objectives and scope

Since the SL-EOS is the homogeneous limit of HN-SCFT, failure of the SL-EOS to apply to the homogeneous mixtures considered in the polymeric foaming process would cast doubt upon the ability of HN-SCFT to successfully describe the inhomogeneous mixtures that comprise polymeric foams. Therefore, the primary purpose of the present work is to determine if the SL-EOS for polymeric mixtures, in its original form or a variant thereof, is capable of successful application to the homogeneous mixtures considered in foaming. To this end, the present work sets three aims.

The first aim is to investigate whether the unsatisfactory predictions of the SL-EOS are the result of the essential elements of the model, or rather could be caused by a sub-optimal implementation or unsuitable ancillary assumptions. Investigation of the implementation is to be accomplished through the examination of pure fluid and mixture parameter estimation procedures and careful tracking of simplifying assumptions. Investigation of ancillary assumptions is to be accomplished through the examination of mixing rules and the noted thermodynamic inconsistencies.

The second aim is to determine if an alternative formulation of the theory allows for the calculation of phase equilibria for the polymer-solvent systems typically considered in polymer foaming. Specifically, to determine if a variant of the theory can be contrived to predict solubility and swelling information for saturated polymer-solvent mixtures.

The third aim is to determine whether a thermodynamic consistency verification is warranted for semi-empirical theories that include features without a physical basis.

To achieve these aims, the present work undertakes to derive the Sanchez-Lacombe equation of state using off-lattice statistical thermodynamics methods. Such a derivation allows for the severance of the SL-EOS from possible lattice artefacts as well as the

application of modern statistical mechanical methods. This is done for the purpose of applying the theory to polymer-solvent mixtures relevant to polymer foaming, in the hopes of making accurate phase equilibrium calculations for such systems. Success of the theory is indicated by correct prediction of PVT behaviour in pure fluids, including first-order phase transitions, as well as solubility and swelling in saturated polymer-solvent mixtures.

1.3 Outline

The goal of Chapter 2 is to lay the foundations for the present work. A brief description of polymer foaming is given, followed by a brief outlining of the principles of thermodynamic mixtures. Next, descriptions are given of the statistical mechanics techniques used to derive physical properties from molecular considerations. Finally, the theoretical context and details of the SL-EOS are described.

Chapter 3 derives the present theory. This is first done for pure fluids, beginning with a description of the model followed by derivation of thermodynamic quantities. Next, the procedure is repeated for multicomponent fluids, first with the expansion of the model to mixtures, similarly followed by a derivation of thermodynamic quantities. This leads directly to an investigation of mixing rules and the thermodynamic inconsistencies of the SL-EOS. Finally, a variant of the theory is proposed applicable to saturated polymer-solvent mixtures.

The purpose of Chapters 4 and 5 is the validation of the present theory and the interpretation of observed phenomena. First, a new parameter estimation procedure is proposed for pure fluids based on observations from the literature, with new parameters calculated for several materials. Next, the present theory is applied to mixtures, with solubility and swelling calculated for binary and ternary polymer-solvent and polymer-co-solvent systems followed by a preliminary investigation into the temperature dependence of solubility. Finally, a procedure for validating semi-empirical theories is outlined.

Readers approaching this work with a knowledge of statistical thermodynamics that are more interested in theoretical considerations may want to focus their attention on a subset of sections. Section 2.5.3 outlines the on-lattice version of the Sanchez-Lacombe equation of state, while Sections 3.2 and 3.4 outline the off-lattice molecular treatment for pure fluids and mixtures, respectively. Discussion of the significance of holes has its foundation in free volume theory found in Section 2.5.2, with the mechanics of their treatment found in Section 3.3.1 and possible physical interpretation discussed in Section 5.2. A discussion of the SL inconsistencies is begun in Section 2.5.4, with the deeper significance found in

Section 3.7. Considerations applicable to general semi-empirical statistical thermodynamic theories are found in Sections 2.4.3 and 3.7.

Readers approaching from an engineering perspective may similarly want to focus on an alternate set of sections. The applicability of the present work to polymer foaming process control is introduced in Section 2.2 with a discussion of the thermodynamics of foaming. The advantages of the Sanchez-Lacombe theory over other theories for this purpose are outlined in Section 2.5.6. The correlation of the theory to quantities relevant for foam processing is discussed in Sections 4.1.6 and 5.1.2. Just as importantly, the limitations of the theory and areas to exercise caution are discussed in Section 2.5.3. The methodology for determination of parameters from experimental data is discussed in Sections 3.9, 4.1.5, 5.1.2 and the methodology for calculating phase equilibria and mixture composition is found in Section 3.10.

Chapter 2

Background

2.1 Introduction

While the thermodynamic study of fluids and solutions date to the 19^{th} century, by the 1930's it had become clear that the existing theories that applied to low molecular weight fluids did not sufficiently explain the properties of the then newly-discovered macromolecules [57]. The solution theories of the time were not able to satisfactorily explain the smaller than expected vapour depression, smaller than expected boiling point elevation, lower than expected osmotic pressures, and much higher than expected viscosities [57]. Moreover, it was found that the greater the molecular weight of the polymer, the larger the deviation from ideal solution theory [57].

Theories describing the properties of polymeric fluids and mixtures belong to a field of study known as statistical thermodynamics, which is a marriage of the earlier theories of thermodynamics, the study of heat and energy, with statistical mechanics, the derivation of material properties from molecular considerations [119]. Without the benefit underlying molecular theory, thermodynamical considerations only allow for relationships between the different properties of a material [119]. In the statistical thermodynamics paradigm, it is typical to derive a thermodynamic property from statistical mechanics, then use thermodynamic principles to calculate all other thermodynamic properties [119]. It is reasonable to assume that following such a procedure relies on agreement between the two theories.

In order to properly discuss the larger space into which this work fits, this section is divided into four parts. The first part is a discussion of polymeric foams. This section outlines the systems to which the present work applies. The second part is a discussion of the

thermodynamic principles and quantities of interest for polymeric fluids and mixtures. The principles discussed in this section are of particular importance to the present work, since they play a central role in the verification methodology of the statistical thermodynamical theories to follow. The third part is an explanation of the statistical mechanical methodology used to derive thermodynamic properties from molecular considerations. Together, the first, second, and third parts establish a context for the theories in the literature. The fourth part is a description and comparison of the existing theories in the literature, including the Sanchez-Lacombe equation of state.

2.2 Polymeric foams

Foams are defined to be materials that feature gaseous voids, referred to as cells, dispersed in a solid medium. Applications of polymeric foams are extensive, ranging from packaging and insulation to aircraft components and medical materials [67]. Polymer foam materials are known for their physical, mechanical and thermal properties, which are a function of their polymer matrices, cellular structures, and gas compositions [67]. The fluids introduced into polymeric materials for the purpose of creating the gaseous voids are known in the foaming industry as blowing agents.

The primary methods for the introduction of blowing agents into polymer melts is through chemical reaction and physical mixing [67]. The present work focuses on the latter method. Physical Blowing Agent (PBA) foaming makes up roughly 38% of the polymer foaming market as of 2006, and offers advantages over Chemical Blowing Agent (CBA) foaming in terms of speed and continuous processing [67]. Since blowing agent molecules are much smaller than those of polymer molecules, blowing agents are often referred to in theoretical considerations as solvents. Solvents in the context of polymeric mixtures are molecules that are much smaller that the polymers with which they are mixed. The present work will often refer to blowing agents as solvents.

Polymeric foams are created from saturated polymer-solvent mixtures by forcing the system into an unstable configuration then locking the resulting structure into place. This is done in four steps over three phases as follows [67]:

1. (Implementation phase) A polymer and blowing agent mixture of pre-determined proportions is brought from low pressure and temperature to high pressure and temperature.

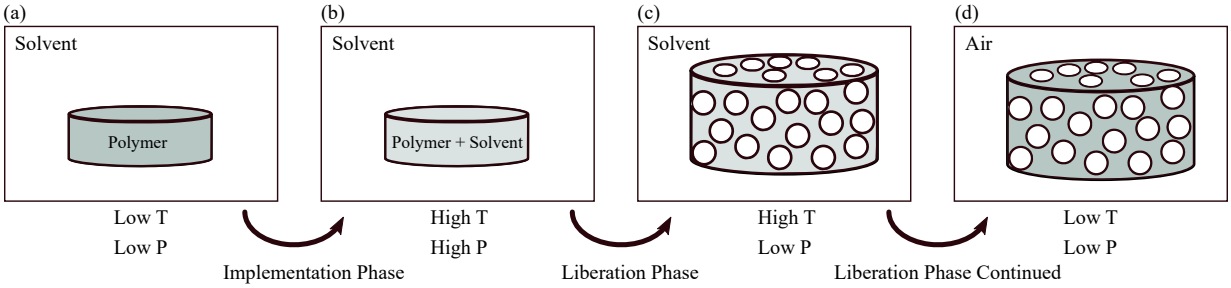

Figure 2.1 An illustration of the foaming process considered in the present work. In the implementation phase, a polymer sample (a) is brought to high pressure and high temperature in a solvent environment (b). The solvent diffuses into the polymer matrix until saturation is reached. In the liberation phase the pressure is rapidly decreased, driving the mixture into a supersaturated configuration and allowing for the nucleation and growth of gaseous solvent bubbles (c). The temperature is decreased before the bubbles are allowed to consolidate (d). In the evacuation phase (not shown), the solvent in the bubbles diffuses into the environment, leaving air-filled bubbles behind.

2. (Liberation phase) The mixture is driven into an unstable configuration by decreasing the pressure from high to low, providing conditions necessary for nucleation and growth of blowing agent bubbles.

3. (Liberation phase continued) The temperature is decreased to below the melting or glass transition to solidify the structure before the blowing agent bubbles are able to consolidate or condense.

4. (Evacuation phase) The blowing agent is allowed to diffuse from the foam into the environment.

An illustration of the foaming process can be found in figure 2.1.

The present work deals with the implementation phase only. Polymeric foaming requires knowledge of of the Pressure-Volume-Temperature properties (PVT properties), also known as equation of state properties, for the design and implementation of such materials. Knowledge of the phase equilibrium behaviour of polymer-blowing-agent mixtures, referred to in the present work as polymer-solvent mixtures, is also requisite.

2.3 Thermodynamics of pure fluids and mixtures

2.3.1 General thermodynamic principles

The way in which a thermodynamic system behaves and interacts is governed by the laws and principles of thermodynamics. A system can interact with its surroundings, depending on the manner in which they are either coupled or isolated. The most common system interactions are work done on/by the system, heat exchanges with surroundings, and/or mass exchanges with surroundings. Consideration of these interactions determines if a system is open, closed, isolated, etc. In the thermodynamic study of materials, a system is said to be described by a set of macroscopic properties which are referred to as state variables. Further, the state of a system can be characterized using an extensive quantity known as a thermodynamic potential, such as the internal energy U, the Helmholtz free energy F, the Gibbs free energy G, the grand potential Φ_G, etc. Potentials can be used to calculate the flow of heat and work into and out of the system, with the choice of potential depending on how the system is expected to evolve. In the same vein, potentials can be used to calculate the relationship between the state variables in an equilibrium state.

For a thermodynamic system characterized by internal energy U and containing a set of r thermodynamic coordinates, let the extensive variables of state be denoted Y_i and the intensive variables be denoted X_i where $i = 1, ..., r$. Let Y_i and X_i be conjugate variables, so that

$$X_i = \left(\frac{\partial U}{\partial Y_i} \right)_{\{Y_{j \neq i}\}}.$$

One of the central principles of thermodynamics is that the thermodynamic potentials are derivable from the internal energy U via Legendre transformation [64], so that the k^{th} potential is defined

$$\psi_k = U - \sum_{l=1}^{k} X_l Y_l, \tag{2.1}$$

or equivalently

$$\psi_k = \sum_{j=k+1}^{r} X_j Y_j, \tag{2.2}$$

where $k < r$. The thermodynamic potentials are therefore first-power homogeneous functions of the extensive variables, meaning that $\psi_k(\{\lambda Y_i\}) = \lambda^1 \psi_k(\{Y_i\})$. While equations 2.1 and 2.2 are general, the common thermodynamic potentials that are used in this work

are defined in table 2.1. Here entropy S, volume V, and particle numbers $\{n_i\}$ are extensive state variables and temperature T, pressure P, and chemical potentials $\{\mu_i\}$ are the respective conjugate intensive state variables. Each potential is associated with a set of natural variables, which are determined from the fundamental thermodynamic relation in combination with Legendre transformation. While the thermodynamic potentials are first-power homogeneous functions of the extensive variables, this does not imply that these same variables form the set of natural variables for the thermodynamic potential. In some cases, one or more of these extensive variables is a function of the natural variables. The complete set of natural variables for a given thermodynamic potential are referred to in the present work as a set of thermodynamic coordinates.

Thermodynamic potential	Equation	Natural variables
Helmholtz free energy	$F = U - TS = -PV + \sum_i \mu_i n_i$	T, V, $\{n_i\}$
Gibbs free energy	$G = U + PV - TS = \sum_i \mu_i n_i$	T, P, $\{n_i\}$
Grand potential	$\Phi_G = U - TS - \sum_i \mu_i n_i = -PV$	T, V, $\{\mu_i\}$

Table 2.1 Common thermodynamic potentials and their natural variables.

An equation of state establishes a relationship between the thermodynamic coordinates when the system is at equilibrium, taking the form of an intensive state variable as a function of extensive state variables [64]. In other words, the general form of an equation of state is

$$X_i = X_i(\{Y_i\}).$$

In general, equations of state are derived from partial derivatives of the thermodynamic potentials. Since the thermodynamic potentials are first-power homogeneous equations of the extensive variables, this implies that the equations of state are zeroth-power homogeneous equations of the extensive variables, meaning that $X_i(\{\lambda Y_i\}) = \lambda^0 X_i(\{Y_i\})$ [10]. Once again, the set of extensive variables does not need to coincide with the set of natural variables, with one or more of the extensive variables being a function of the natural variables in such cases. For example, the present work makes use of the mechanical equation of state

$$P = P(S, V, \{n_i\}),$$

where the set $\{n_i\}$ refers to the number of particles in a multicomponent system. If the equation of state is derived from the Gibbs free energy in table 2.1, with natural variables T, P, and $\{n_i\}$, then the extensive variables S and V will be functions of the natural variables.

In effect, the equation of state defines a surface in the thermodynamic coordinate space. The system can only be considered in equilibrium if the current state lies on the surface. Knowledge of all the equations of state of a system constitutes complete knowledge of its thermodynamic properties [10]. It is of critical importance to note that the equilibrium surface of a given system does not depend on which thermodynamic potential is used to derive it [120–122]. This point is discussed further in Section 2.4.3. The nature of, and relationships between, the state variables, thermodynamic potentials, and equations of state, form the set of thermodynamic principles often referred to in the present work.

2.3.2 Common fluid properties

The properties of polymeric fluids can be derived from the thermodynamic potentials. The common properties of interest for fluids include liquid-vapour equilibria, critical phenomena, and PVT behaviour. The material properties that are most easily observable tend to be the second derivatives of the thermodynamic potentials, known as thermodynamic response functions [99]. The response functions are so called because they describe the way in which a thermodynamic system changes in response to small variations in the variables of state. A list of the most common response functions and their definitions can be found in table 2.2.

2.3.3 Thermodynamic considerations for mixtures

In the thermodynamic study of mixtures, it is not strictly necessary to describe the properties of the system as a whole, but rather it suffices for some applications to describe the properties of the system only with reference to the pure fluids [119]. Such quantities are known as quantities of mixing. In examining the quantities of mixing, however, it is not possible to gain information about the properties of the individual pure fluids [25]. The purpose of this section is to show that the thermodynamic properties of mixing obey the same thermodynamic principles described in Section 2.3.1, albeit with the properties of mixing substituted for the properties of the fluid.

In general, quantities of mixing can be derived for any extensive parameter [64]. Let Y be any extensive parameter of the mixture. The quantity of mixing of ΔY_{mix} is defined

$$\Delta Y_{\text{mix}} \equiv Y - \sum_i Y_{i,\text{pure}}, \tag{2.3}$$

where $Y_{i,\text{pure}}$ is the corresponding parameter in the i^{th} pure fluid under identical external conditions.

Property	Relationship	Description
Thermal expansivity	$\alpha_V = \frac{1}{V}\left(\frac{\partial V}{\partial T}\right)_P = \frac{1}{V}\frac{\partial^2 G}{\partial P \partial T}$	Establishes a relationship between the heat added to the system and the change in temperature when pressure is held constant.
Adiabatic compressibility	$\beta_S = -\frac{1}{V}\left(\frac{\partial V}{\partial P}\right)_S = -\frac{1}{V}\frac{\partial^2 F}{\partial P^2}$	Describes the rate of change of the volume in response to changes in pressure when no heat or matter is exchanged with surroundings.
Isothermal compressibility	$\beta_T = -\frac{1}{V}\left(\frac{\partial V}{\partial P}\right)_T = -\frac{1}{V}\frac{\partial^2 G}{\partial P^2}$	Describes the rate of change of the volume in response to changes in pressure when temperature is held constant.
Isochoric heat capacity	$C_V = T\left(\frac{\partial S}{\partial T}\right)_V = -T\frac{\partial^2 F}{\partial T^2}$	Establishes a relationship between the heat added to the system and the change in temperature when volume is held constant.
Isobaric heat capacity	$C_P = T\left(\frac{\partial S}{\partial T}\right)_P = -T\frac{\partial^2 F}{\partial T^2}$	Establishes a relationship between the heat added to the system and the change in temperature when pressure is held constant.

Table 2.2 A list of commonly used thermodynamic response functions, which tend to be material properties most accessible to observation.

In mixtures, it is sometimes practical to deal with intensive mean molar quantities rather than extensive properties. The mean molar quantity corresponding to Y is defined

$$\bar{Y} \equiv \frac{Y}{\sum_i n_i},$$

which is an intensive quantity. The partial molar quantity associated with Y is defined

$$\bar{Y}_i \equiv \left(\frac{\partial Y}{\partial n_i}\right)_{T,P,\{n_{j\neq i}\}}.$$

It can be shown that [64]

$$Y = \sum_i \bar{Y}_i n_i.$$

Finally, the molar fraction can be defined

$$x_i = \frac{n_i}{\sum_i n_i}.$$

Using these definitions, it is possible to show that [64]

$$\Delta\bar{Y}_{\text{mix}} = \bar{Y} - \sum_i x_i \bar{Y}_{i,\text{pure}} = \sum_i x_i \left(\bar{Y}_i - \bar{Y}_{i,\text{pure}}\right). \tag{2.4}$$

Using the definitions of equations 2.3 and 2.4 the free energy of mixing is defined

$$\Delta\bar{G}_{\text{mix}} \equiv \bar{G} - \sum_i x_i \bar{G}_{i,\text{pure}},$$

where $\bar{G}$ represents the mean molar free energy of the mixture and $\bar{G}_{i,\text{pure}}$ represents the molar free energy of the i^{th} pure fluid. The free energy of mixing can further be divided into an enthalpy of mixing and an entropy of mixing. The relation between these terms is

$$\Delta G_{\text{mix}} = \Delta H_{\text{mix}} - T\Delta S_{\text{mix}} = \sum_i n_i \Delta\mu_i,$$

where ΔH_{mix} is the enthalpy of mixing and ΔS_{mix} is the entropy of mixing [64].

Ideal mixtures

An ideal mixture is one in which the components of the mixture behave as though they are in their individual states [64]. Such mixtures are defined by their zero enthalpy of mixing as well as their characteristic entropy of mixing.

The free energy of such a mixture is derivable from thermodynamic principles in combination with the ideal gas equation of state $PV = nk_BT$ [64]. The entropy of mixing is calculated to be

$$\Delta\bar{S}_{\text{mix,ideal}} = -k_B \sum_i x_i \ln x_i, \tag{2.5}$$

where i is the index over species. The molar fraction can be related to the pressure P by Raoult's law and Dalton's law to be

$$x_i = \frac{P_i}{P},$$

where P_i is the vapour pressure of component i [64]. It can further be shown [64] that the enthalpy of mixing is

$$\Delta\bar{H}_{\text{mix,ideal}} = 0.$$

This zero enthalpy of mixing is the direct result of the fact that there are no interactions between particles [64].

Mixture classification

Real mixtures are often characterized by their degree of deviation from the ideal mixture [64]. Such quantities are often referred to as excess quantities, and are defined

$$W_{i,\text{excess}} = W_i - W_{i,\text{ideal}},$$

where W_i is any thermodynamic quantity. This practice dates to a time when the ideal mixture was thought to be one to which all mixtures should conform [119]. The deviation from the ideal is related to the character of interactions between the particles [119].

A regular mixture is one in which the system exhibits interactions between particles, but the interactions are assumed not to be strong enough to affect the entropic considerations [64]. This results in a system that has a non-zero enthalpy of mixing, but an entropy of mixing identical to that of an ideal mixture. Regular solutions themselves represent a type of idealized solution, as many real solutions are likely to exhibit non-zero excess enthalpy and entropy under experimental observation [119]. A complete list of the mixture classifications based only on excess enthalpy and entropy is found in table 2.3.

	$\Delta H_{\text{mix,excess}} = 0$	$\Delta H_{\text{mix,excess}} \neq 0$
$\Delta S_{\text{mix,excess}} = 0$	Ideal mixture	Regular mixture
$\Delta S_{\text{mix,excess}} \neq 0$	Athermal mixture	General mixture

Table 2.3 The classification of mixtures with reference to the ideal mixture, where the ideal entropy of mixing is given by equation 2.5 [119].

2.3.4 Common mixture properties

The common mixture properties of interest are heat and volume change upon mixing, multicomponent phase equilibria for saturated mixtures, stability considerations for homogeneous mixtures, and upper critical solution temperature (UCST) or lower critical solution temperature (LCST).

Consideration of solubility and swelling in saturated mixtures are especially important for polymer foaming. Solubility is defined as the total mass fraction of blowing agent that can be dissolved into the polymer matrix at saturation. Swelling is defined as the ratio of the volume of saturated polymer-blowing-agent mixture to the volume of the pure polymer. A list of common mixture properties and their definitions are found in table 2.4.

2.4 Principles of statistical mechanics

2.4.1 Foundation

Thermodynamics allows for connections between the material properties, but does not allow the calculation of these properties independently of the others [119]. The relations provided by thermodynamics are entirely independent of any consideration of the material, and therefore cannot be expected to provide insight into molecular or atomic considerations [119]. Statistical mechanics, on the other hand, concerns itself with the derivation of material properties from particular, atomic, or molecular considerations [119]. Its original purpose was to derive these properties at equilibrium, although it has since expanded beyond its original scope [119].

Statistical thermodynamical theories begin with assertions about the structure, properties, forces, etc. of the constituent particles of a system [119]. These assertions are referred to as a model of the constituent particles of the system. Generally, these assertions are simplified in order to allow for more manageable treatment, making statistical mechanics a study of idealized systems [119].

Property	Definition	Description
Mean molar heat of mixing	$\Delta\bar{H}_{\text{mix}} = \bar{H} - \sum_i x_i \bar{H}_{\text{pure},i}$	The difference in the enthalpy of the mixture and the sum of the enthalpies of the pure components.
Volume change upon mixing	$\Delta V_{\text{mix}} = V - \sum_i V_{\text{pure},i}$	The difference in volume of the mixture and the sum of the pure components.
Solubility	$\chi_{\text{BA}} \equiv \frac{\sum_i^{\text{BA}} n_i M_i}{\sum_i^{\text{BA}} n_i M_i + \sum_j^{\text{P}} n_j M_j}$	The total mass fraction of blowing agent that can be dissolved into a polymer matrix at saturation.
Swelling	$S_W = \frac{V(T,P,t_{eq})}{V(T,P,t_{ini})} = \frac{\rho^{\text{polymer}}}{\rho^{\text{mix}}(1-m_{\text{BA}})}$	The ratio of the saturated polymer-blowing-agent mixture volume to the volume of the pure polymer.

Table 2.4 A list of common mixture properties and their definitions.

The purpose of statistical mechanics is manifold. One purpose is to gain insight into the nature of the particles of a system of interest through comparison with experimentally obtained properties [119]. Assertions are made about the constituent particles of a system using a model, then statistical mechanical principles are applied to calculate material properties. Agreement with corresponding experimental properties is then used to justify the assertions or, if they disagree, to refine the model [119]. The process is then repeated, producing information about the physical system with each iteration [119]. Another important purpose is to relate a particular property of a physical system to a particular property of the constituent particles [119]. By constructing a model with this property and an equivalent model without, comparison of the material properties through statistical mechanics can be used as evidence [119].

While thermodynamics describes the state of a system using the averaged thermodynamic properties, as described in Section 2.3.1, statistical mechanics describes states with much more detail [119]. For statistical mechanics, it is necessary to begin with a description of the spatial coordinates, internal coordinates, velocities, etc. of each of the constituent

particles of the system. For this reason, thermodynamic states are sometimes referred to as *macrostates*, while such statistical mechanical microscopic states are referred to as *microstates*. While quantum mechanics contains bounds on the accuracy of such microstate information, these bounds disappear in the classical limit [119].

Connecting thermodynamic properties to the microscopic description is done through statistical averaging of microscopically described properties using Boltzmann thermodynamic probabilities. At its core, statistical mechanics asserts that, at temperature T, the probability of a system being in a given microstate that has total energy E is proportional to e^{-E/k_BT}, the Boltzmann factor [119]. The average value of a quantity Z is found using the relation

$$\langle Z \rangle = \frac{\sum_i Z_i e^{-E_i/k_BT}}{\sum_i e^{-E_i/k_BT}}, \tag{2.6}$$

where the sum is over all microstates and Z_i is the value of the property in microstate i. The sum in the denominator is of particular importance. It is a sum of the Boltzmann factor over all states, known as the partition function. The partition function is defined to be

$$Q = \sum_i e^{E_i/k_BT}, \tag{2.7}$$

where E_i is the total energy of state i, and k_B is Boltzmann's constant. It can be shown that the averaged energy $\langle E \rangle$ is equal to the thermodynamic energy U [119]. It can also he shown that the Helmholtz free energy is related to the partition function by the equation

$$F = -k_BT \ln Q. \tag{2.8}$$

While averaged thermodynamic properties can be determined for each quantity using equation 2.6, it is more typical in statistical thermodynamical theories to calculate only a thermodynamic function such as the Helmholtz free energy in equation 2.8. All other material properties are then calculated from the resulting thermodynamic function using the principles of thermodynamics [119].

Since the thermodynamic properties are the result of averaged statistical mechanical properties, then the probability that the system can be found away from those values, known as thermal fluctuations, merits discussion. The probability of finding the system at a fixed deviation from its thermodynamic average decreases with the number of particles [119]. Generally, for systems with particles on the order of 1 cm^3 of liquid, the probability of finding the system deviating observably from the average is negligible [119]. In other words, the thermodynamic probability of the averaged state is overwhelming for macroscopic systems, except under certain conditions, which are discussed further in Section 2.4.2. This observation leads to convenient simplifying assumptions.

2.4.2 Simplifying assumptions

In general, statistical mechanical equations for systems of interacting particles do not yield easily to exact analytical solution, even for heavily idealized models [119]. This necessitates the use of numerical methods, simplifying assumptions, or often both. Numerical methods, such as Monte-Carlo methods, do allow for the calculation of properties of complex models with fewer simplifying assumptions, but at a cost of greater numerical complexity [18].

Independent energy assumption

It is sometimes possible to split the total energy of a system into the sum of independent parts [98, 119]. Such decompositions can be used to produce simplifying assumptions. For example, let the total energy be divided into independent translational and internal energies:

$$E = E_{\text{translational}} + E_{\text{internal}}.$$

It follows that the partition function will then be similarly divided, with

$$Q = \sum_i e^{-(E_{\text{translational}}+E_{\text{internal}})/k_B T} = Q_{\text{configurational}} \cdot Q_{\text{internal}},$$

and finally

$$F = F_{\text{configurational}} + F_{\text{internal}}.$$

The partition function associated with the translational degrees of freedom is known as the configurational partition function, and is commonly the only one considered in statistical mechanics of mixtures [119]. If it is assumed that the internal degrees of freedom of the particles are not affected by their environment, then it can be assumed that the internal energy of the molecules is the same in all configurations [119]. The permissibility of splitting the energy into independent terms is not something statistical mechanics can determine *a priori*. Rather, it can only be decided *a posteriori* through comparison of calculated properties and observed properties [119]. It has been proposed that only the external, or configurational, modes contribute to the PVT properties of polymeric liquids and mixtures [100].

Mean field assumption

As mentioned previously, for systems with large numbers of particles, the system becomes overwhelmingly likely to be found in its thermodynamic averaged state. This is because

the most probable state contributes the largest term to the partition function [84]. For extremely large systems of particles, the replacement of the logarithm of the sum over states with the logarithm of the largest term is an acceptable approximation [119, 140]. Such approximations are known as mean field approximations.

In general terms, mean field theories reduce many-body problems to one-body problems by reducing interactions to an averaged effect on a single considered particle [18]. Such an approach neglects the effects of fluctuations [18], which is justifiable in many situations. Taking this approach also has the effect of neglecting correlations [13]. Mean field assumptions, therefore, are justifiable in situations where fluctuations are not important and correlations are very short-ranged. On the other hand, these approximations break down when correlation lengths increase, such as near critical points [6, 13, 18, 92].

2.4.3 Ensemble equivalence

It is often argued from a thermodynamic standpoint that the potentials derived from the microcanonical and canonical ensembles always yield the same predictions for equilibrium properties [122]. This is indeed true if the thermodynamic potentials in table 2.1 are assumed to obey the Legendre transformations outlined in Section 2.3.1 [121]. These arguments tend to be related to one originally put forward by Gibbs in which the canonical ensemble becomes identical to the microcanonical ensemble as the system volume tends to infinity, thus implying that the ensembles produce the same equilibrium predictions in the thermodynamic limit [122].

While exotic statistical mechanical systems lacking ensemble equivalence in the thermodynamic limit have been studied by Touchette [121], these systems are beyond the scope of the present work. Such systems do not obey the Legendre transformations between thermodynamic potentials, in violation of the principles of thermodynamics. Given the use of these same principles to calculate all quantities of interest in the present work, disagreement with these fundamental relations is considered impermissible. It is here required that the theory exhibit equivalence in the thermodynamic limit in all ensembles, for example the microcanonical, canonical, and grand-canonical ensembles.

2.5 Statistical thermophysics of polymeric mixtures

2.5.1 Flory-Huggins theory

The problem of describing polymer-solvent mixtures in the case of large polymer-solvent molecular size disparity was considered independently by several scientists, including P. J. Flory [26], M. L. Huggins [54], and others [57]. The theory takes into consideration properties of the mixture relative to the pure fluids, hence the Gibbs free energy calculated corresponds to the free energy of mixing, rather than the free energy of the fluid.

The Flory-Huggins (FH) theory describes a binary mixture of polymer and solvent species of very different size. The model behind the theory begins with a lattice populated by segments of each species, with solvent molecules occupying a single lattice position and polymer molecules occupying several [50]. The volume of a single lattice site is determined by the solvent species, which in turn affects the level of coarse-graining of the polymer chains. Segments of a polymer molecule occupy sites in a "random walk" [50]. The model asserts that interactions are restricted to nearest-neighbour. Letting the subscript 1 represent the solvent and 2 the polymer, interaction energies are fixed to be ϵ_{11} between solvent segments, ϵ_{22} between polymer segments, and ϵ_{12} between segments of polymer and solvent. The relative interaction energy is defined to be $\epsilon = \epsilon_{11} + \epsilon_{22} - 2\epsilon_{12}$.

Importantly, the statistical arguments produced from the model assume random mixing, after the Bragg-Williams approximation [50]. In the Bragg-Williams approximation, it is assumed that the molecules are randomly distributed over the lattice [50]. The random mixing assumption ignores correlations, and belongs to the family of mean-field assumptions discussed in Section 2.4.2.

The model of the system can be used to generate a free energy of mixing [50]. The expression for the mean molar Gibbs free energy of mixing is given by

$$\frac{\Delta \bar{G}_{\text{mix}}}{k_B T} = \phi_1 \ln \phi_1 + \frac{\phi_2}{\alpha_2} \ln \phi_2 + \chi_{12} \phi_1 \phi_2,$$

where ϕ_1 and ϕ_2 correspond to the volume fractions occupied by solvent and polymer, respectively, and α_2 corresponds to the ratio of the volume of a polymer to the volume of a solvent [64]. The interaction parameter is related to the relative segment interaction energies by

$$\chi_{12} = \frac{z\epsilon}{k_B T},$$

which is known as the "mixing parameter" [50]. It should be noted that, in the special case that $\epsilon_{11} + \epsilon_{22} = 2\epsilon_{12}$, the mixing parameter vanishes and the theory reduces to the ideal mixture discussed in Section 2.3.3.

Despite the appearance of entropic terms similar to those of the ideal mixture as well as an additional apparently enthalpic term, the classification of the mixture depends on the nature of the mixing parameter χ_{12}. Normally, the interaction parameter ϵ is taken to be temperature-independent, implying that it does not contain entropic considerations and is purely enthalpic in nature. In such a case, the Flory-Huggins model yields a theory of the regular mixture type. In practice, while the Flory derivation originally assumed the segment interactions led purely to a heat of mixing, there is no *a priori* justification for that assumption [27]. On the contrary, there may be a contribution to entropy from effects of interaction on the orientation of the components [27]. In this case, the relative binary interaction may contain an entropic component. This would mean it would be possible for the interaction energy to be broken into an enthalpic and an entropic component of the form

$$\epsilon = \epsilon_H - T\epsilon_S.$$

In general, therefore, the mixing parameter takes the form of a free energy, with the most general interpretation taking both the enthalpic and entropic portions to be functions of composition. Given this interpretation, FH would not be considered a theory of the regular mixture type, but rather a general mixture.

The Flory-Huggins theory has been used with some success to calculate quantities of mixing in a qualitative or semiquantitative way [50]. Quantities that can be derived from the theory include heats of mixing, stability of mixtures, as well as upper- and lower-critical solutions temperatures.

Because of its consideration only of quantities relative to the pure components, it is unable to provide insight into the pure fluids. Indeed, the theory yields a uniformly zero free energy if the molar fraction of either component is taken to be one. Since the lattice is by nature incompressible, the volume and particle number are not independent thermodynamic variables, meaning that the model does not allow for Pressure-Volume (PV) effects [50]. This means that FH does not include a capacity to describe volume changes upon mixing, an important consideration in the polymer foaming industry [67].

2.5.2 Free volume theory

Unlike solids, fluids feature molecules that can migrate thermally over macroscopic distances [33]. This migration is often attributed to interstitial space between molecules, al-

lowing them to move freely [33]. The measure of this space is known as "free volume". No such consideration is included in a molecular theory of classical particles in a close-packed configuration, such as the Flory-Huggins theory. A model incorporating free volume is said by Fujita to feature a *hole volume assumption* [33]. In keeping with the language of the present work, it is referred to here as a *hole volume assertion* and is expressed as follows:

- (Hole volume assertion) There exists interstitial space in the liquid not occupied by the cores of constituent molecules.

This assertion is common to all free volume theories, such as the Fujita [32], Vrentas-Duda [130–132], and Fox-Flory [30] theories, which differ only in their treatment of this volume [33]. Free volume theories allow for the calculation of diffusion equations in liquids [32, 33, 130, 131] as well as provide a quantitative treatment of glass transitions [14, 30, 123].

2.5.3 Sanchez-Lacombe theory

Molecular theory of solutions

The Sanchez-Lacombe (SL) theory is a molecular theory of solutions that expands on the earlier Flory-Huggins lattice-fluid theory by incorporating free volume. Free volume is assumed to be entirely the result of lattice vacancies, as opposed to being incorporated into lattice cells as in the Flory-Orwoll-Vrij (FOV) theory [28, 29, 100]. Importantly, the inclusion of free volume allows the inclusion of PV considerations in the lattice fluid model. The theory is applicable to general liquid and vapour solutions, and predicts a first-order phase transition, volume changes upon mixing, as well as the complete phase behaviour of both pure fluids and fluid mixtures [103]. The details of the theory are outlined in two separate papers: a paper describing the pure fluid case [104] and a paper expanding the theory to multicomponent fluids [66]. Due to inherent differences in the pure fluid and multicomponent fluid theories, it is helpful to parallel the original presentation by Sanchez and Lacombe, first outlining the model for pure fluids, then expanding the pure fluid model to include multiple species. This is done to highlight the difficulties of such an expansion.

In the SL pure fluid construction [104], the system is modelled by a lattice with coordination z and per-site volume v^*. The system is composed of n molecules each divided into r segments occupying a site on the lattice, as well as n_0 lattice vacancies known as "holes". The molecules are assumed to be linear or branched, with each interior segment having $z-2$ nonbonded nearest neighbours and 2 bonded neighbours. Chain ends have

$z-1$ nonbonded neighbours and 1 bonded neighbour. The model asserts that the close-packed volume of a molecule, given by rv^*, is independent of pressure and temperature. It should be noted that while the statistics are derived under the assumption that molecules have either linear or branched structures, this requirement is eventually relaxed, with the molecules treated simply as groupings of segments. Since the volume of a lattice site is v^*, and holes are assumed to be vacant lattice sites, then it follows that the volume of a hole is v^*. Interactions are restricted to nearest-neighbour, nonbonded segments and given a termperature-independent interaction energy ϵ. Bonded segment-segment, segment-hole, and hole-hole pairs do not interact. Molecular interactions are characterized by $r\epsilon^*$, where $\epsilon^* = z\epsilon/2$ is the energy required to create a lattice vacancy. A pure fluid is completely characterized by the molecular model parameters ϵ^*, v^*, and r or equivalently the thermodynamic scaling parameters T^*, P^*, and ρ^*. The molecular and thermodynamic parameters are related by $T^* = \epsilon^*/k_B$, $P^* = \epsilon^*/v^*$, and $\rho^* = M/rv^*$ (or $V^* = nrv^*$), where M is the molecular weight of the molecule.

An essential feature of the model merits comment before discussion of multicomponent fluids begins. While not explicitly stated, it is implicit in the derivation of the pure fluid SL-EOS that the volume v^* is independent of temperature and pressure. This it also implied from the treatment of v^* as a parameter that characterizes the pure fluid, with the parameter treated as constant in table I of the pure fluid paper [104]. Therefore changes in free volume due to changes in temperature and pressure correspond only to changes in the *number* of holes.

Mixing rules

Scaling the pure fluid to a multicomponent fluid is for the most part straightforward, as most model assertions are readily scaled to multiple species [104]. The most obvious difficulty is the population of a mixture lattice with elements of pure component lattices of different characteristic volumes. This issue is a direct result of the hole volume in the pure fluid being constant and characteristic of that fluid. The multicomponent fluid characteristic volume should adopt the hole volumes of each of the disparate pure component values in each of the pure fluid limits in order for the theory to be internally consistent. To this end, the characteristic volume is taken to be an average, with all parameters defined per lattice site requiring translation from the pure fluid into the mixture. The fluid is assumed to be composed of molecules of species i, each with a number of molecules n_i. Holes are once again associated with the subscript 0. For clarity, is assumed that the set $\{n_i\} = \{n_i \mid i \neq 0\}$ is the set of the number of molecules of each species in the system, excluding the number of holes n_0.

The set of rules for translation into the mixture is referred to in the SL paper [66] as "combining rules", but referred to in the much of the literature as "mixing rules". Some mixing rules are derived, but others are arbitrary in nature [66, 105]. For the sake of generality, derived mixing rules are expressed here explicitly where possible, while arbitrary mixing rules are only outlined.

The characteristic lattice volume v^* in the mixture is taken to be some average of those of the pure components [66]. It is stated that this is, in general, some function of the characteristic volumes of the pure components and the composition of the mixture [66], implying the characteristic volume has the form of a function

$$v^* = v^*(\{v_i^*\}, \{n_i\}),$$

where v_i^* is the lattice characteristic volume in the pure component i. This mixing rule will be referred to as the *volumetric mixing rule*. As stated in the description of the model, the close-packed volume $r_i^0 v_i^*$ is preserved for each pure component, where the superscript 0 denotes a value for the pure fluid. It follows from this assertion and the volumetric mixing rule that the number of lattice sites occupied by a molecule of species i in the mixture is given by

$$r_i = r_i^0 \left(\frac{v_i^*}{v^*} \right).$$

In lattice terms, this is tantamount to changes in composition leading to changes in the level of coarse-graining of the polymer molecules. Due to the self-similar nature of polymer molecules, changes in the level of coarse-graining should have no effect on the physical results *provided that the segment size is large on the lengthscale of a monomer and small on the lengthscale of the polymer itself* [102]. While not typically considered in the literature, this should be taken into account when studying mixtures of polymers, especially those of very diverse size and characteristic volume. Table 2.5 gives a selection of volumetric mixing rules found in the literature.

The definition of the averaged characteristic energy ϵ^*, not originally considered a mixing rule in the original publication [66], was later enforced in order for the cohesive energy density to be consistent between pure and multicomponent fluids [105]. This mixing rule, which will be referred to as the *energetic mixing rule*, is therefore derived depending on the specific form of the volumetric mixing rule. This dependence on the volumetric mixing rule is a result of the characteristic energy being defined as the interaction energy per segment of volume v^*, the segment size being subject to mixing rules. In general, the characteristic energy will be a function of the pure fluid interactions ϵ_{ii}^*, the pair interactions ϵ_{ij}^* where $i \neq j$, as well as the composition $\{n_i\}$. Dependence on the set of characteristic

Source	Volumetric mixing rule	Justification
Sanchez and Lacombe [104]	$v^* = \sum \psi_i v_{ii}^*$	Result of constraining the total number of pair interactions in the mixture to be equal to the sum of those of the component in their pure states. Creates surface area effect.
Poser and Sanchez [96]	$v^* = \sum \psi_i v_{ii}^* - \sum \sum_{j<j} \psi_i \psi_j v_{ij}^*$	Linear mixing rule with quadratic correction. Models hole volume as expansion of unknown function of composition. Keeps first- and second-order terms.

Table 2.5 A selection of volumetric mixing rules proposed in the literature as well as their sources and justifications. Here, ψ_i represents the occupied segment fraction.

volumes of the pure fluids $\{v_i^*\}$ is only indirectly through the definitions of the pure fluid interactions. In general, the energetic mixing rule has the form

$$\epsilon^* = \epsilon^*(\{\epsilon_{ii}^*\}, \{\epsilon_{ij}^*\}, \{n_i\}).$$

It should be noted that the definition of this characteristic energy differs here from that used later on in Chapter 3 due to differences in their respective definitions.

Sanchez-Lacombe Equation of State

Derivation of the SL-EOS relies on lattice statistics, outlined by Guggenheim [41, 43, 44], in order to calculate the configurational partition function of the canonical system under a mean field random mixture assumption. The Guggenheim approach assumes "that when two sites are not occupied by the same molecule the probabilities of being occupied or vacant are independent for the two sites" [44]. In standard form, the Gibbs free energy and equation of state are then calculated from the configurational partition function. It should be noted that the expression for the number of accessible states is applicable only to linear and branched r-mers, with cyclic r-mers requiring a different formula [66].

The SL-EOS takes the form of the equation

$$\tilde{P} + \tilde{\rho}^2 + \tilde{T}\left[\ln(1-\tilde{\rho}) + \left(1 - \frac{1}{r}\right)\tilde{\rho}\right] = 0, \tag{2.9}$$

where the reduced variables of state are defined in terms of the characteristic thermodynamic parameters $\tilde{P} \equiv P/P^*$, $\tilde{T} \equiv T/T^*$, and $\tilde{\rho} \equiv \rho/\rho^* = V^*/V$. The theory gains a corresponding states principle in the limit $r \to \infty$.

Determination of parameters

The pure fluid is fully characterized by a set of three parameters, as described previously, as well as the molecular weight. The three parameters can either be the set of molecular parameters r, v^*, and ϵ^*, or equivalently by the set of thermodynamic parameters P^*, T^*, and ρ^* (or V^*) [104]. These parameters are obtained from comparison with experimental observation, typically PVT data [104]. Sanchez and Lacombe provide a method of determining these molecular parameters with the use of readily available vapour-pressure data for gases [104]. For polymers, where such data is not possible due to the large size of the molecules, the data can be calculated from PVT data.

Mixtures are fully characterized by the set of pair interaction parameters $\{\epsilon^*_{ij}\}$ where $i \neq j$. These parameters are obtained from comparison with experimental mixture data, typically from thermodynamic data obtained from binary mixtures of each pair [66].

Success of the SL theory

For pure fluids, the SL theory predicts the first-order liquid-vapour phase transition for many fluids from the triple point to the near the critical point, PVT data in the single-phase liquid and vapour regions as well as in the supercritical regime [104]. It yields successful predictions for thermodynamic response functions such as isothermal compressibility and thermal expansivity. It also also agrees well with predecessors, such as the VdW fluid, arriving at the same result for the second virial coefficient [104].

In mixtures, SL theory has successfully been applied to binary as well as ternary fluid mixtures at low pressures. It has been applied with some success to predict spinodal curves, binodal curves, lower critical solution temperature and/or upper critical solution temperature for many fluids [66, 105].

Limitations of the SL theory

The assumptions made in order to achieve an analytical expression for the partition function give rise to several limitations that merit being made explicit. Limitations also arise from the simplicity of the molecular treatment.

It is well known that mean-field theories break down near second-order phase transitions. As such, the SL theory is not expected to yield accurate results near the critical point, due to the importance of correlations in that regime. Indeed, in their determination of molecular parameters using vapour-pressure data, SL deliberately choose not to include experimentally obtained data within $15 - 20^{\circ}$C of the critical point [66].

Since SL theory does not contain consideration of internal molecular degrees of freedom, it should not be expected to produce accurate predictions of thermodynamic quantities dependent on them [104]. For example, SL theory does not accurately describe heat capacities. In fact, refinements to the theory that include consideration of a flexibility parameter δ are deliberately ignored by SL, due to the fact that such considerations do not contribute to the PVT properties predicted by the theory [66].

2.5.4 Neau correction

In her 2002 paper, Neau [88] found that the previously used methods for calculating phase equilibria were thermodynamically inconsistent. Wherever characteristic lattice volumes differ, such as under mixing rules, the chemical potentials generated from the configurational partition function can not then be used to perform equilibrium calculations due to differing reference values [88].

If it is assumed that the the equations of state calculated from the configurational partition function match those calculated from the canonical partition function, then it follows that phase equilibria can be calculated using fugacities rather than chemical potentials [88]. Fugacities are defined as effective partial pressures, providing an alternative to chemical potentials for the purpose of calculating phase equilibria [42, 64]. Fugacity coefficients can be derived from the equation of state by integration, using the ideal gas as reference [88].

The foundation of this approach is that the partition function calculated from the lattice statistics is not the canonical partition function Q, but the configurational partition function Q_{conf} [88]. If consideration of the incompressibility of the lattice is temporarily put aside, these two partition function are generally related by the equation

$$Q_{\text{conf}}(T, V, n_0, \{n_i\}) = \frac{Q(T, V, n_0, \{n_i\})}{Q_{\text{int}}(T, n_0, \{n_i\})},$$

where Q_{int} corresponds to the internal degrees of freedom of the canonical partition function. The Neau correction requires that

$$\left(\frac{\partial Q_{\text{int}}(T, n_0, \{n_i\})}{\partial V}\right)_{T,\{n_i\}} = 0.$$

While this argument is sound for a typical canonical ensemble, special consideration must be made for incompressible systems that include holes. Incompressibility is a constraint on the system, establishing a relationship between the total volume and the number of mers given by $V = (n_0 + \sum_i r_i n_i)v^*$ [66]. On the surface, incompressibility seems to be at odds with the typical canonical ensemble assumption that volume and particle number are independent. Since the set $\{n_i\}$ and the volume V are assumed to be independent variables in the canonical ensemble, incompressibility implies that the number of holes is a function of the total volume, or $n_0(V)$. This means that in reality, $Q = Q(T, V, \{n_i\})$ and $Q_{\text{conf}} = Q_{\text{conf}}(T, V, \{n_i\})$. As a consequence of the volume dependence of the number of holes, it must be that

$$\left(\frac{\partial Q_{\text{int}}(T, n_0(V), \{n_i\})}{\partial V}\right)_{T,\{n_i\}} \neq 0.$$

This result implies that the equation of state derived from the canonical partition function will be different from that derived from the configurational partition function. It therefore follows that the fugacities cannot be used to calculate phase equilibria, as postulated by Neau.

2.5.5 Hong-Noolandi construction

In 1981, Hong and Noolandi put forward a statistical mechanical theory describing inhomogeneous mixtures of polymers and small molecules [52]. The theory is based on the earlier works of Edwards [24] and others, dealing with the statistical mechanics of polymers featuring excluded volume [24, 31, 48, 49]. In the work of Edwards [24], the polymer molecule is modelled as a freely-jointed chain, with links of a fixed length l and excluded volume v. The Hong-Noolandi (HN) theory expands on these earlier models to incorporate solvent molecules, treated as single-segment "polymer" molecules [52].

HN theory uses a functional integral over density functions to calculate the partition function, under the constraint that there is no volume change locally under mixing [52]. The theory applies self-consistent field theory (SCFT) to derive their results, allowing

for the calculation of structures and interfacial properties for many polymer and solvent systems [52].

It was noted in the original publication that in the limit of homogeneous density, the theory reduced to that of Flory-Huggins due to the similarity in molecular treatment [52]. In short, the excluded segment volume and freely-jointed chain treatment, combined with the disallowed volume change upon mixing, parallels the incompressible lattice "random walk" segment treatment of FH.

In a second publication, Hong and Noolandi expand upon their earlier theory, adding a solvent species representing vacancies [53]. It was noted in this second construction that the theory produced an equation of state identical to that of SL in a homogeneous limit [53]. While it had earlier been observed that the Flory entropy of mixing is derivable without reference to lattice statistics [57], this result helped to prove that the SL-EOS was similarly derivable without a lattice construction [106].

2.5.6 Alternative theories

A comprehensive discussion of theories for polymer fluids and mixtures would be a prohibitively large task. Rather, the present work considers alternative theories to be only those that provide treatment of a comparable set of material properties derived from theories in line with the original motivation outlined in Chapter 1. As even the task of describing these theories comprehensively would be much too great, only a selection of the equation of state theories are presented here. Many of the statistical mechanical theories for polymeric fluids found in the literature can be broadly organized into families based on their treatment of molecular considerations [40, 100]. Within the family of lattice fluid theories, cell theories such as the Flory-Orwoll-Vrij (FOV) equation of state [28, 29] and cell-hole theories such as the Simha-Somcynsky (SS) equation of state [56, 113] offer alternative treatments of free volume. Outside of the lattice fluid family, cubic theories such as the Peng-Robinson (PR) equation of state [94] and perturbation theories such as the perturbed-chain self-associating fluid theory (PC-SAFT) [38, 39] generate equations of state that are simpler and more complex than SL, respectively.

Flory-Orwoll-Vrij theory

In the Flory-Orwoll-Vrij theory, as with all cell theories, molecular segments are assumed to occupy discrete spaces within a close-packed structure [28, 29, 100]. Like the SL theory, FOV imposes structure on the fluid, taking the form of volume elements in a simple square

lattice. In contrast with SL, however, the earlier FOV theory does not contain lattice vacancies. Rather, free volume is treated via vacant space within each cell [28, 98]. Segments are assumed to occupy the centre of their cell, ignoring fluctuations in line with other mean field theories. In comparison with SL theory, the FOV model has been found to perform much more poorly over a large pressure range. This is attributable to the imposition of the solid-like lattice on the fluid, which tends to underestimate entropy [113].

Simha-Somcynsky theory

The Simha-Somcynsky theory is a hybrid of the earlier cell model treatment and SL theory [56, 113, 137]. Like the cell theories that preceded it, each segment is assumed to occupy a cell that also contains vacant space [113]. The free volume is split, however, between contributions from each cell ("solidlike") as well as cell vacancies ("gaslike") [113]. The cells are assumed to be arranged in a hexagonal close-packed configuration with a Lennard-Jones 6-12 potential characterizing the interactions between segments. Unlike SL theory, the SS theory considers nonnearest neighbour interactions [100]. Each pure fluid is characterized by four parameters: a chain length parameter s, a parameter characteristic of the external degrees of freedom per chain c, a parameter characterizing the maximum attractive energy ϵ^*, and a characteristic repulsion volume v^*, although an additional constraint exists relating s and c [56]. For chain-like molecules, $3c/(s+3) = 1$ and for spherical molecules $c = s = 1$ [56]. The relationship dictating the relative contributions to free volume from gaslike and solidlike modes takes the form of an arbitrary equation, with variants chosen by comparison of theory with experiment [113]. In order to extend the pure fluid theory to a multicomponent mixture, SS applies mixing rules, with each of the parameters becoming a compositional average of those of the pure components [56].

The equation of state is derived from the configurational partition function using a random mixture mean field assumption [56]. Since the equation of state is a function not only of the reduced variables of state, but also a "structure function" y, material properties are found by simultaneously solving the equation of state as well as an additional equation minimizing the partition function as a function of occupied sites [56, 100, 113].

The SS-EOS performs extremely well in comparison to many other lattice-based theories [100]. This improved performance comes at a price of greatly increased complexity. In comparison with SL theory, the divided free volume and nonnearest neighbour interactions introduces much greater complexity to the molecular model. In addition, rather than merely satisfying the equation of state, equilibrium calculations should simultaneously satisfy the equation of state and structure function conditions. In practice, this requires the use of nonlinear optimization techniques. One could also argue that the arbitrary

division of the free volume, tuned through comparison with experiment, constitutes an additional degree of freedom.

Peng-Robinson equation

The Peng-Robinson equation of state belongs to the cubic equation of state family of theories. The theory is based on expanding the earlier van der Waals equation of state to describe multicomponent fluids, and as such eschews statistical mechanical methods by assuming *a priori* knowledge of the form of the equation of state [94]. At a microscopic level, the theory treats molecules as interacting hard spheres [94]. Each pure fluid is characterized by two parameters: one characterizing the intermolecular attraction force having units of energy and the other characterizing the the size of the hard-spheres having units of volume [94]. In general, the hard-sphere parameter is taken to be a constant, whereas the interaction parameter is taken to be a function of temperature [94]. Since parameter estimation procedures for cubic equations of state typically require knowledge of critical parameters, the usual parameter estimation procedures require modification for polymeric fluids [40]. The pure fluid equation of state is expanded to allow for multicomponent mixtures using mixing rules on both parameters [94].

Compared to SL theory, the PR approach offers much greater simplicity, albeit at a cost of accuracy due to the more simplistic treatment of polymer molecules [40]. The PR-EOS allows for the calculation of PVT properties and phase-equilibria in both pure fluids and multicomponent fluid mixtures, especially for vapour pressures and densities [40, 94]. On the other hand, predictions of liquid densities, while better than the preceding cubic equations of state, have limited accuracy for large molecules [94].

Perturbed-chain self-associating fluid theory

The perturbed-chain self-associating fluid theory differs from the lattice-based theories in terms of statistical mechanical method and molecular model sophistication. Perturbation theories are based upon the expansion of the Helmholtz free energy in terms of inverse temperature about that of a reference system [38]. In PC-SAFT, the fluid is composed of spheres subject to a modified square-well interaction [39]. Pure fluids are fully characterized by four parameters: a segment diameter σ, an attractive interaction parameter ϵ, the number of segments per chain m, and a hard-core repulsion length s_1, although an additional constraint typically sets $s_1/\sigma = 0.12$. In the modified square-well, the potential

is a step-wise function of the radial distance of the form [39]:

$$u(r) = \begin{cases} \infty & r < (\sigma - s_1) \\ 3\epsilon & (\sigma - s_1) \leq r < \sigma \\ -\epsilon & \sigma \leq r < \lambda\sigma \\ 0 & r \geq \lambda\sigma \end{cases}$$

The reference fluid is taken to be a fluid of hard-sphere chains [38, 39]. The central model feature that reflects real molecular behaviour is the soft repulsion exhibited when $r < \sigma$ [39]. The equation of state is derived from the Helmholtz free energy, which is in turn derived from the hard-chain free energy calculated in earlier works [39]. The derivation is not discussed here in detail as it is beyond the scope of the present work. Just as with the cubic and lattice theories, mixing rules are used to extend the pure fluid theory to a multicomponent fluid, although a rigorous expansion is in principle possible [39].

In addition to the pure fluid parameters, a set of model parameters are required to make predictions of material properties. PC-SAFT contains 24 model parameters in addition to the three parameters required for each pure component [39]. These model parameters are determined from comparison with experimental pure fluid data, and are taken to be universal [39].

The SAFT theories tend to outperform SL theory predictions in all thermodynamic ranges [40]. PC-SAFT, however, requires the simultaneous satisfaction of a large set of nonlinear equations in order to make predictions, which in turn requires the use of nonlinear optimization techniques that must be performed numerically at great computational cost.

Chapter 3

Theory

3.1 Introduction

In statistical thermodynamics, averaged system properties, known as thermodynamic properties, are calculated using Hamiltonian mechanics and combinatorics derived from a molecular model. In general, modern statistical thermodynamical theories arrive at conclusions about materials by first developing a model for the constituent particles based on theories about the nature of molecules, then using statistical mechanics to derive one of the thermodynamic functions, then using thermodynamic principles to further derive the other properties [119].

Use of thermodynamics in the procedures of statistical thermodynamics implies that the resulting theories should agree with the older and independently derived principles and laws of thermodynamics within its domain of applicability.

The statistical considerations require knowledge of the states accessible to the system. In order to facilitate the enumeration of states in the statistical mechanical construction, it is necessary to make some assumptions about the structure of the system, generally as one of the aspects of the molecular model. This requirement is inherently more difficult to satisfy in models of amorphous fluids than it is in models of crystalline solids. Models in the lattice fluid family, as the name implies, satisfy the requirement by imposing a regular structure on the amorphous fluid. Such an assumption comes at a price, as modelling an amorphous fluid with a lattice will as a rule tend to underestimate the number of possible configurations [82].

Success of the model is indicated, although not proven, by agreement between calculated

and observed properties [119]. Violation of the principles or laws of thermodynamics implies falsification of the theory.

It is useful to split the discussion of the model into a pure fluid portion and a multicomponent fluid portion, as Sanchez and Lacombe had done in their original publications [66, 104, 105]. The primary reason for this division is that, while the two theories are not in and of themselves incompatible, the application of mixing rules to the multicomponent theory heralds a departure from the pure fluid theory's treatment of free volume, the significance of which has not fully been appreciated. This is evidenced by the fact that mixing rules introduce thermodynamic inconsistencies to the mixture theory that are not present in the pure fluid theory. A more detailed discussion of the model differences is found in Section 3.4 and a discussion of mixing rules is found in Section 3.7.

The chapter begins with the pure fluid and mixture theories treated as distinct, reconciling them only in due course. Next, contact is made with the Sanchez-Lacombe equation of state by identifying analogous model parameters, followed by a discussion of the problematic mixing rules and their alternatives. In the absence of mixing rules, special considerations are taken to translate the constituent pure fluid parameters into the multicomponent fluid theory, followed by the outlining of parameter estimation procedures. Finally, the chapter is concluded with procedures for calculating the composition of saturated fluid mixtures necessary for polymer foaming applications.

3.2 Description of the pure fluid model

The fundamental assertions of the pure fluid theory are reduced to elementary statements and presented here in an order convenient for discussion. Comparison with the lattice-centric language in the SL paper is found in Appendix A. The model assertions are:

1. (Segment excluded volume) The fluid is composed of polymer molecules each divided into N equal segments of volume v that cannot overlap.

2. (Preserved close-packed volume) The volume occupied by a polymer molecule is constant, given by the product of the quantities Nv, and is a characteristic of a given polymer species.

3. (Short-ranged segment interaction) Interactions are limited to those between polymer segments only. The strength of the interactions are assumed to be temperature- and pressure- independent. Interactions are short-ranged, so that they become negligible

beyond a segment size. Such interactions are a characteristic of a given polymer species.

4. (Free volume partition) The fluid contains free volume not occupied by molecular segments. The free is volume partitioned into equal segments, each having a volume of v_0. These segments are referred to as "holes".

5. (Hole character) Holes are treated as a distinct chemical species rather than simple vacant space. The species contains translational degrees of freedom only.

6. (Incompressibility) The system of polymer molecules and holes is assumed to fill all space, so that if a given location is not occupied by a polymer segment, it is occupied by a hole.

7. (Constant hole volume) The volume of a hole v_0 is constant and a characteristic of a given polymer species. Changes in free volume correspond solely to changes in the number of holes.

It is worth mentioning that these assertions do not address several details that may typically be included when modelling polymers. These should not be viewed as oversights, but rather deliberate omissions made in accordance with the motivations impelling the theory (see Section 1.1). For example, no mention is made of the structure of the polymer molecules. Indeed, Sanchez and Lacombe include rudimentary considerations of polymer structure, symmetry, and flexibility into their model [104]. However, the internal degrees of freedom, as formulated in their construction, did not contribute to the ultimate results [66, 104], likely due to the consideration of only the configurational portion of the partition function via lattice statistics. Rotational, vibrational, and other internal degrees of freedom are not considered in their construction at all, leaving only translational degrees of freedom for each chemical species. Since the aim of this current work is to yield an off-lattice construction of the model, producing a theory of equivalent simplicity, such degrees of freedom are similarly ignored here.

As will be discussed in greater detail later on, it is assumed that the model need not be limited to polymer macromolecules. Small molecules can be represented by trivially setting $N = 1$. Further, in the homogeneous limit, small molecules and oligomers of equal size produce identical results in terms of translational entropy. It should also be noted that in the homogeneous limit, the requirement that segments do not overlap is relaxed, with the *segment excluded volume* assertion enforced only in an ensemble averaged manner.

The SL theory for pure fluids was conceived to describe PVT behaviour in the single phase region and to describe first-order liquid-vapour phase transitions from the triple point

to the critical point [104]. It is just as important to note its limitations as its purpose, in order to avoid misinterpretation of results. The limitations of the theory can be broadly categorized into two distinct sources: limitations due to details not considered in the model and limitations due to approximations for mathematical tractability.

Keeping track of the simplifying assumptions made in the pursuit of desired properties can be of great importance. For example, Sanchez and Rodgers described a method for determining the solubility of solvent in a polymer-solvent mixture by invoking the use of Henry's law [107]. To that end, they required that the mass fraction of solvent absorbed into the polymer be small, which is true for the coexistence of a gaseous solvent phase and mixture phase at low pressure. Such an assumption may break down in the case of a supercritical solvent phase at high pressure, necessitating the abandonment of the resulting equations in favour of other avenues. For this reason, all assumptions used in this work are clearly marked and tracked. For the purpose of clarity, all assertions that together form the essential components of the model are labelled "assertions". All assertions that do not form essential components of the theory, but whose purpose is primarily for the tractability of the mathematics, are labelled as "assumptions" and marked at the points in the derivations where they are used.

As an example of the former, the original SL model does not contain effective consideration of internal degrees of freedom. As such, it is expected to be deficient in predicting thermodynamic quantities that are dominated by these considerations, such as heat capacity [104].

As an example of the latter, the mean-field approximation applied to the partition function introduces the assumption that correlations are unimportant and can be ignored. This assumption limits the theory to conditions where correlations are unimportant despite the fact that this is not inherent to the molecular model.

3.3 Statistical thermodynamics of pure fluids

3.3.1 Partition function based on the canonical ensemble

The thermodynamic properties of the system are derived from the model assertions by generating a partition function. Several mathematical expressions for important quantities are created to describe the microscopic state of the fluid. Based on both the *segment excluded volume* and *free volume partition* assertions, it is possible to define an expression for both a number density and a volume density for the segments of the polymer species and

the holes, denoted 0. Let it be assumed that there are n polymer molecules and n_0 holes in the system. If the set of positions of the centres of holes is defined as $\{\mathbf{r}_0\} \equiv \{\mathbf{r}_{0,j} \mid j \in n_0\}$, then it is possible to define a number density and a volume density function as

$$\hat{\rho}_0(\mathbf{r}) = \sum_{j=1}^{n_0} \delta(\mathbf{r} - \mathbf{r}_{0,j})$$

and

$$\hat{\varphi}_0(\mathbf{r}) = v_0 \hat{\rho}_0(\mathbf{r}), \tag{3.1}$$

respectively, where δ is the Dirac delta function, v_0 is the volume occupied by a hole and $\mathbf{r}_{0,j}$ is the position of the centre of hole j.

Similarly, if the set of the centres of the segments of the polymer species is defined as $\{\mathbf{r}\} \equiv \{\mathbf{r}_j \mid j \in nN\}$, then let a number density and volume density be defined

$$\hat{\rho}(\mathbf{r}) = \sum_{j=1}^{nN} \delta(\mathbf{r} - \mathbf{r}_j)$$

and

$$\hat{\varphi}(\mathbf{r}) = v \hat{\rho}(\mathbf{r}), \tag{3.2}$$

where n represents the number of molecules, N represents the number of segments per molecule, and v represents the volume occupied by a segment. It follows from the *free volume partition* assertion that $N_0 = 1$ for the holes.

Each polymer molecule being composed of N segments, it is also possible to define the geometric centre of each molecule by summing the positions of the segments. Since the segments are identical, this also corresponds to the centre of mass of each molecule. Let the set of the centres of mass of the molecules be defined $\{\mathbf{r}^{\mathrm{cm}}\} \equiv \{\mathbf{r}_j^{\mathrm{cm}} \mid j \in n\}$. Each polymer molecule may also be associated with a momentum, defined as the momentum of the centre of mass. Let the set of molecular momenta be defined $\{\mathbf{p}^{\mathrm{cm}}\} \equiv \{\mathbf{p}_j^{\mathrm{cm}} \mid j \in n\}$.

The partition function of a classical continuous system takes the form of an integral over phase space for each independent particle. Therefore, making use of equations 2.7, 3.1, and 3.2, the canonical partition function of a classical continuous system with two species of indistinguishable particles is given by the expression

$$Q = \frac{1}{n! n_0! h^{3n} h^{3n_0}} \int d\{\mathbf{r}^{\mathrm{cm}}\} d\{\mathbf{r}_0\} d\{\mathbf{p}^{\mathrm{cm}}\} d\{\mathbf{p}_0\} e^{-\mathcal{H}(\{\mathbf{r}^{\mathrm{cm}}\},\{\mathbf{r}_0\},\{\mathbf{p}^{\mathrm{cm}}\},\{\mathbf{p}_0\})/k_B T},$$

where $\mathcal{H}$ is the Hamiltonian of the system, T is the temperature, and k_B is Boltzmann's constant. The integral is over the phase space of each molecule and hole in the system.

While the holes represent free volume, the *hole character* assertion that holes behave as segments of a second species has consequences on the form of the partition function. In particular, while each hole is associated with a position, it is not associated with a mass and therefore does not carry a physically real momentum. Nevertheless, their treatment as a second species implies that, just as the molecular segments, holes contribute to both the positional and momentum portions of the phase integral. This contribution is complicated by the *incompressibility* assertion, due to the dependence of hole number on canonical volume. The exact nature of the momentum portion of the integral is fortunately not required for the present derivation. It is, however, assumed that its contribution to the energy is independent of the translational portion and can therefore be factored from the configurational partition function, after Prigogine [98]. This behaves functionally as a normalization factor in order for the partition function to remain dimensionless, as interpreted by Hong and Noolandi [53].

In order to facilitate the derivations to follow, the Hamiltonian's kinetic and potential components are assumed to be independent, as discussed in Section 2.4.2. In addition, the kinetic contributions for the molecules are assumed to be independent, taking the form of a thermal de Broglie wavelength the exact form of which is not important to the present derivation. The potential term is a function only of the set of positions of the molecules. The *short-ranged segment interaction* assertion further implies that the potential is a function of only the positions of the polymer species segments since the holes do not interact. Absorbing the kinetic components of the partition function into factors associated with each species, the partition function reduces to the expression

$$Q = \frac{1}{n! n_0! \Lambda^{3n} \Lambda_0^{3n_0}} \int d\{\mathbf{r}^{\mathrm{cm}}\} d\{\mathbf{r}_0\} e^{-V(\{\mathbf{r}^{\mathrm{cm}}\})/k_B T}, \tag{3.3}$$

where Λ is the thermal de Broglie wavelength of a single polymer molecule, Λ_0 is the previously mentioned normalization factor associated with holes, and V represents the potential term of the Hamiltonian.

The interaction potential between the centres of mass of molecules $V(\{\mathbf{r}^{\mathrm{cm}}\})$ is replaced with an equivalent interaction between segments $U(\{\mathbf{r}\})$. In general, the interaction potential term is very difficult to calculate based on the *short-ranged segment interaction* assertion as it is a sum of the interactions between each particle and an external field (one-body problem), each pair of particles (two-body problem), each combination of three particles (three-body problem), etc. This type of problem is generally referred to as a many-body problem and is beyond the scope of this work. In the absence of an external field, the interaction potential of systems of molecules tends to be dominated by the pairwise interactions [119]. As a necessary simplifying assumption, all interactions other than

the pairwise interactions are ignored.

Assumption 1 (Two-body interactions) *The interaction potential is dominated by two-body interactions. Higher order interactions can be ignored.*

The exact nature of the pair interaction potential is deliberately left ambiguous in the molecular model. While it could be conceivable that anisotropic segment-segment potentials exist somewhere in nature, they are here assumed to be isotropic in keeping with the original SL theory.

Assumption 2 (Isotropic interaction) *Interaction potentials are spherically symmetric.*

The interaction potential thus simplifies to

$$\begin{aligned} U(\{\mathbf{r}\}) &= \sum_{i=1}^{nN}\sum_{j=1}^{i-1} u\left(\left|\mathbf{r}_i - \mathbf{r}_j\right|\right) + O(3 \text{ body and higher}) \\ &\approx \frac{1}{2}\sum_{i=1}^{nN}\sum_{j=1}^{nN} u\left(\left|\mathbf{r}_i - \mathbf{r}_j\right|\right) \\ &= \frac{1}{2}\int d\mathbf{r}\, d\mathbf{r}'\, \hat{\rho}(\mathbf{r}) u\left(\left|\mathbf{r} - \mathbf{r}'\right|\right)\hat{\rho}(\mathbf{r}') \\ &= \frac{1}{2v^2}\int d\mathbf{r}\, d\mathbf{r}'\, \hat{\varphi}(\mathbf{r}) u\left(\left|\mathbf{r} - \mathbf{r}'\right|\right)\hat{\varphi}(\mathbf{r}'), \end{aligned}$$

where $u(r)$ is a scalar function describing the interaction potential between two segments separated by a distance r, the exact nature of which does not need to be specified. It should be noted that approximating the potential in this way has the effect of introducing an unphysical self-interaction term into the potential function $U(\{\mathbf{r}\})$. Since the additional term is linear in n, however, this approximation has no effect on the derivations to follow. Applying this approximation to equation 3.3, the partition function of the system is expressed as

$$Q = \frac{1}{n!n_0!\Lambda^{3n}\Lambda_0^{3n_0}}\int d\{\mathbf{r}^{\text{cm}}\}d\{\mathbf{r}_0\}\exp\left(-\frac{1}{2v^2}\int d\mathbf{r}\, d\mathbf{r}'\, \hat{\varphi}(\mathbf{r})\frac{u\left(\left|\mathbf{r} - \mathbf{r}'\right|\right)}{k_BT}\hat{\varphi}(\mathbf{r}')\right). \tag{3.4}$$

A second assumption, referred to as the random mixture approximation, is here applied to the system. The random mixture approximation imposes the constraint that the volume

fraction of each species is everywhere equal to its spatial average [40]. Integral to this approximation, as the name implies, is the implicit assumption that the system is free to sample all possible positional configurations with equal probability. As a consequence, local volume fraction and density fluctuations are ignored, as are explicit considerations of correlations. Since this approximation has the effect of replacing the many-body problem with an averaged effect, it falls into the category of mean-field approximations, and is akin to the Bragg-Williams approximation for lattice fluids [50]. It is worth noting that a mean field assumption does not equate to a homogeneous mixture. While the random mixture approximation functions as a mean field approximation, alternative mean field approximations that allow for inhomogeneous mixtures are possible. Such approximations are, however, beyond the scope of the present work.

Assumption 3 (Random mixture) *The composition of the mixture is everywhere equal to its spatial average.*

Taking the spatial average of the volume density function given by equations 3.1 and 3.2, the average volume density of the polymers is calculated to be

$$\phi \equiv \frac{1}{V}\int d\mathbf{r}\;\hat{\varphi}(\mathbf{r}) = \frac{v}{V}\sum_{j=1}^{nN}\delta(\mathbf{r}-\mathbf{r}_j) = \frac{nNv}{V} \tag{3.5}$$

and the average volume density of the holes is calculated to be

$$\phi_0 \equiv \frac{1}{V}\int d\mathbf{r}\;\hat{\varphi}_0(\mathbf{r}) = \frac{v_0}{V}\sum_{j=1}^{n_0}\delta(\mathbf{r}-\mathbf{r}_{0,j}) = \frac{n_0 v_0}{V}. \tag{3.6}$$

Under the random mixing approximation, the partition function in equation 3.4 simplifies to

$$Q = \frac{1}{n!n_0!\Lambda^{3n}\Lambda_0^{3n_0}}\exp\left(-\frac{\phi^2}{2v^2}\int d\mathbf{r}\;d\mathbf{r}'\;\frac{u\left(\left|\mathbf{r}-\mathbf{r}'\right|\right)}{k_BT}\right)\int d\{\mathbf{r}^{\mathrm{cm}}\}d\{\mathbf{r}_0\}. \tag{3.7}$$

Taking advantage of the spherical symmetry of the potential $u(r)$, a change of coordinates $\mathbf{r}' \equiv \mathbf{r} + \mathbf{r}''$ allows the double integral to be rephrased as

$$\int d\mathbf{r}d\mathbf{r}'\;u\left(\left|\mathbf{r}-\mathbf{r}'\right|\right) = V\int d\mathbf{r}\;u\left(|\mathbf{r}|\right).$$

In order to yield dimensionless quantities, it is necessary to define a reference volume. The only requirement of this reference volume is that it be independent of all thermodynamic variables. Since, according the the *constant hole volume* assertion, the volume of a hole meets this requirement, it is convenient to define this reference volume to be v_0.

Let the interaction parameter ϵ be defined so that

$$\epsilon \equiv \frac{N^2}{2\alpha^2 v_0} \int d\mathbf{r}\; u(|\mathbf{r}|), \tag{3.8}$$

where

$$\alpha \equiv \frac{Nv}{v_0} \tag{3.9}$$

represents the volume ratio of a molecule to the hole volume. This interaction parameter represents the energy of exchange of a polymer molecule with holes.

Substituting equations 3.8 and 3.9 into equation 3.7, the expression for the partition function of the system becomes

$$Q = \frac{V^n V^{n_0}}{n! n_0! \Lambda^{3n} \Lambda_0^{3n_0}} \exp\left(-\frac{V\epsilon}{k_B T v_0}\phi^2\right), \tag{3.10}$$

The *incompressibility* assertion places a constraint on the number density and volume fractions of each species. Taking into account the relative sizes of the polymer segments and the holes, this requires that the sum of the number density of the *scaled* polymer segments and holes must be the equal number density of the space *as if it were entirely populated with close-packed holes*. This constraint on the number fractions is expressed

$$\hat{\rho}(\mathbf{r})\left(\frac{v}{v_0}\right) + \hat{\rho}_0(\mathbf{r}) = \frac{1}{v_0}.$$

Substituting equations 3.5 and 3.6, the constraint on the volume fractions is thus

$$\hat{\varphi}(\mathbf{r}) + \hat{\varphi}_0(\mathbf{r}) = 1$$

or, under the random mixture assumption,

$$\phi + \phi_0 = 1. \tag{3.11}$$

3.3.2 Helmholtz free energy

The Helmholtz free energy is the thermodynamic potential associated with the canonical ensemble. As discussed in Section 2.3, it has T, V, and n as natural variables. The *incompressibility* assertion places a special constraint on the thermodynamic variables. As a consequence, V, n, and n_0 are not independent variables, which is a feature unique to such hole theories. The Helmholtz free energy is used to derive all thermodynamic properties of the system. The Helmholtz free energy is related to the canonical partition function by the relation

$$F = -k_B T \ln Q.$$

Plugging in the equation 3.10 expression for canonical the partition function and applying Stirling's approximation, the expression for the free energy is

$$\begin{aligned}
\frac{F}{k_B T} &= \frac{V\epsilon}{k_B T v_0}\phi^2 - \ln\left[\frac{V^n V^{n_0}}{n! n_0! \Lambda^{3n} \Lambda_0^{3n_0}}\right] \\
&= \frac{V\epsilon}{k_B T v_0}\phi^2 - \ln\left[\frac{V}{\Lambda^3}\right]^n - \ln\left[\frac{V}{\Lambda_0^3}\right]^{n_0} + \ln(n!) + \ln(n_0!) \\
&\approx \frac{V\epsilon}{k_B T v_0}\phi^2 - n\ln\left[\frac{V}{n\Lambda^3}\right] - n_0 \ln\left[\frac{V}{n_0 \Lambda_0^3}\right] - n - n_0.
\end{aligned}$$

It is worth stating that the application of Stirling's approximation assumes that the system is composed of many particles of each species, despite the fact that the approximation is accurate even for relatively small numbers on the order of ~ 10.

Assumption 4 (Many particle) *The system is composed of many molecules of each species.*

Making use of the definition of the volume fractions of each species outlined in equations 3.5 and 3.6 allows for the free energy, rephrased as

$$\frac{F}{k_B T} = \frac{V\epsilon}{k_B T v_0}\phi^2 + \frac{nVNv}{VNv}\ln\left[\frac{nNv\Lambda^3}{VNv}\right] + \frac{n_0 V v_0}{V v_0}\ln\left[\frac{n_0 v_0 \Lambda_0^3}{V v_0}\right] - \frac{nVNv}{VNv} - \frac{n_0 V v_0}{V v_0},$$

to be expressed as

$$\frac{F}{k_B T} = \frac{V\epsilon}{k_B T v_0}\phi^2 + \frac{V\phi}{Nv}\ln\phi + \frac{V\phi_0}{v_0}\ln\phi_0 - \frac{V\phi}{Nv} - \frac{V\phi_0}{v_0} + \frac{V\phi}{Nv}\ln\left[\frac{\Lambda^3}{Nv}\right] + \frac{V\phi_0}{v_0}\ln\left[\frac{\Lambda_0^3}{v_0}\right].$$

Multiplying though by $\frac{v_0}{V}$ produces an intensive and dimensionless free energy. Terms linear ϕ and ϕ_0 as well as constants do not contribute to the thermodynamics and are ignored. The kinetic terms Λ and Λ_0 require more consideration. For the polymer molecules, the thermal de Broglie wavelength Λ is a function of only temperature and mass [50]. Given that the mass of each molecule is assumed to be invariant, this term will then be equal in all phases that exist at the same temperature. Ignoring this term is only justified in phase equilibrium calculations that feature thermal equilibrium.

Assumption 5 (Thermal equilibrium) *Phases are in thermal equilibrium.*

The term Λ_0, as mentioned, functions as a normalization factor as a consequence of the *hole character* assertion. While the factor does not have a clear physical meaning, it is reasonable given the *hole character* assertion that it should be treated as analogous to the thermal de Broglie wavelength. Such a treatment would imply that Λ_0 is similarly independent of volume. With these simplifications, the reduced Helmholtz free energy is expressed

$$\tilde{f} \equiv \frac{v_0 F}{k_B T V} = \frac{\epsilon}{k_B T}\phi^2 + \frac{\phi}{\alpha}\ln\phi + \phi_0 \ln\phi_0 + \phi_0\left(\ln\left[\frac{\Lambda_0^3}{v_0}\right] - 1\right). \tag{3.12}$$

The role of the normalization factor is best illustrated by deriving the equation of state by applying the relation $P = (\partial F/\partial V)_{T,n}$ to equation 3.12. The observation that $\lim_{\phi_0 \to 1} P \neq 0$ implies that the result is not physical, as the absolute pressure should tend to zero in such a limit. The condition that the residual pressure vanish in the dilute limit leads to the normalization factor $\Lambda_0 = v_0 e$, as suggested by Hong and Noolandi [53]. This leads to a reduced free energy given by

$$\tilde{f} \equiv \frac{v_0 F}{k_B T V} = \frac{\epsilon}{k_B T}\phi^2 + \frac{\phi}{\alpha}\ln\phi + \phi_0 \ln\phi_0. \tag{3.13}$$

3.3.3 Chemical potential

Chemical potential is the thermodynamic generalized force associated with particle number. It is an important quantity to consider in the calculation of diffusive equilibrium. By definition, the chemical potential of the polymer molecules is

$$\mu = \left(\frac{\partial F}{\partial n}\right)_{T,V}.$$

Using the chain rule to relate this expression to the density,

$$\mu = \left(\frac{\partial F}{\partial n}\right)_{T,V} = \left(\frac{\partial F}{\partial \phi}\right)_{T,V}\left(\frac{\partial \phi}{\partial n}\right)_{T,V},$$

becomes, in combination with equation 3.5,

$$\mu = \frac{Nv}{V}\left(\frac{\partial F}{\partial \phi}\right)_{T,V} = \frac{k_B T N v}{v_0}\left(\frac{\partial \tilde{f}}{\partial \phi}\right)_{T,V}.$$

Through the substitution of equation 3.13, the chemical potential of the species s in the pure fluid is expressed

$$\tilde{\mu} \equiv \frac{v_0 \mu}{k_B T N v} = \frac{2\epsilon}{k_B T}\phi + \frac{1}{\alpha}(1 + \ln\phi) - \ln\phi_0 - 1. \tag{3.14}$$

3.3.4 Equation of state

As mentioned in Section 2.3.1, equations of state define an equilibrium surface in the space of the thermodynamic coordinates. The equation of state for the pure fluid is calculated by taking the partial derivative of the Helmholtz free energy with respect to volume. The equation of state $P = P(T, V, n)$ is obtained from

$$P = \left(\frac{\partial F}{\partial V}\right)_{T,n}.$$

In terms of reduced quantities and with the use of equation 3.5, a more convenient form of the relation becomes

$$\frac{v_0 P}{k_B T} = \tilde{f} + V\left(\frac{\partial \tilde{f}}{\partial V}\right)_{T,n} = \tilde{f} + \phi\left(\frac{\partial \tilde{f}}{\partial \phi}\right)_{T,n}.$$

Applying the relation to equation 3.5 finally yields the equation of state

$$\frac{v_0 P}{k_B T} = -\left(1 - \frac{1}{\alpha}\right)\phi - \ln\phi_0 + \frac{\epsilon}{k_B T}\phi^2. \tag{3.15}$$

3.3.5 Critical point

The critical point marks the intersection of the spinodal and binodal curves on the equilibrium surface, as well as marks the boundary of the supercritical region. The critical point is defined as the state that simultaneously satisfies the equations

$$\left(\frac{\partial P}{\partial V}\right)_{T,n} = 0$$

and

$$\left(\frac{\partial^2 P}{\partial V^2}\right)_{T,n} = 0.$$

As a notational convenience, the thermodynamic coordinates held fixed for a partial derivative are only explicitly stated once per equation, with the same implied for all other derivatives in the same line. Using the chain rule as well as equation 3.5 yields the relation

$$\left(\frac{\partial P}{\partial V}\right)_{T,n} = \left(\frac{\partial P}{\partial \phi}\right)\left(\frac{\partial \phi}{\partial V}\right) = -\frac{nNv}{V^2}\left(\frac{\partial P}{\partial \phi}\right) = -\frac{\phi}{V}\left(\frac{\partial P}{\partial \phi}\right).$$

Taking the partial derivative with respect to volume gives the relation

$$\left(\frac{\partial^2 P}{\partial V^2}\right)_{T,n} = \frac{\partial}{\partial V}\left(\frac{\partial P}{\partial \phi}\frac{\partial \phi}{\partial V}\right) = \frac{\partial^2 P}{\partial \phi^2}\left(\frac{\partial \phi}{\partial V}\right)^2 + \frac{\partial P}{\partial \phi}\frac{\partial^2 \phi}{\partial V^2},$$

which yields the relation

$$\left(\frac{\partial^2 P}{\partial V^2}\right)_{T,n} = \frac{\phi^2}{V^2}\left(\frac{\partial^2 P}{\partial \phi^2}\right) + \frac{\phi}{V^2}\left(\frac{\partial P}{\partial \phi}\right).$$

Substitution of the equation of state into the relations yields

$$\frac{v_0 V}{k_B T}\left(\frac{\partial P}{\partial V}\right)_{T,n} = -\frac{2\epsilon}{k_B T}\phi^2 + \left(1 - \frac{1}{\alpha}\right)\phi - \frac{\phi}{1-\phi}$$

and

$$\frac{v_0 V^2}{k_B T}\left(\frac{\partial^2 P}{\partial V^2}\right)_{T,n} = \frac{4\epsilon}{k_B T}\phi^2 + \frac{\phi}{1-\phi}\left(1 + \frac{\phi}{1-\phi}\right) - \left(1 - \frac{1}{\alpha}\right)\phi.$$

Therefore, the critical point is uniquely determined by the simultaneous solution to the equations

$$-\frac{2\epsilon}{k_B T}\phi^2 + \left(1 - \frac{1}{\alpha}\right)\phi - \frac{\phi}{1-\phi} = 0 \tag{3.16}$$

and

$$\frac{4\epsilon}{k_B T}\phi^2 + \frac{\phi}{1-\phi}\left(1 + \frac{\phi}{1-\phi}\right) - \left(1 - \frac{1}{\alpha}\right)\phi = 0. \tag{3.17}$$

3.3.6 Response functions

As a rule, the second derivatives of the thermodynamic potentials, known as the response functions, form the bulk of the experimentally measurable properties of a fluid. The purpose of this section is to derive the response functions from the molecular theory using the Helmholtz free energy. The most common response functions and their definitions are listed in table 2.2. In this section, the thermal expansivity α_V, the isothermal compressibility β_T, the isochoric heat capacity C_V, and the isobaric heat capacity C_P are calculated from the Helmholtz and Gibbs free energies.

By definition, the thermal expansivity is given by the expression

$$\alpha_V = \frac{1}{V}\left(\frac{\partial V}{\partial T}\right)_{P,n} = \frac{1}{V}\left(\frac{\partial T}{\partial V}\right)^{-1}_{P,n} = \frac{1}{V}\left(\frac{\partial T}{\partial \phi}\right)^{-1}_{P,n}\left(\frac{\partial V}{\partial \phi}\right)_{P,n}.$$

In order to proceed, it is necessary to make explicit assumptions about the nature of the interaction parameter ϵ. The following derivation assumes that the interaction parameter contains no entropic component, in line with the original SL derivation.

Assumption 6 (Enthalpic interaction parameter) *Interactions lead purely to a heat of mixing.*

It is worth noting that modifications to the SL theory exist that add a temperature dependence to the interaction parameter ϵ in order to capture the empirically observed weakening of molecular interactions with temperature [55, 78]. These modifications, however, constitute distinct theories and would require separate consideration in a future work. For the equation of state calculated in equation 3.15, implicit differentiation gives a thermal expansivity

$$\alpha_V \equiv \frac{1}{\phi}\left(\frac{v_0 P}{k_B T^2} - \frac{\epsilon\phi^2}{k_B T^2}\right)\left[\frac{1}{\alpha} + \frac{\phi}{1-\phi} + \frac{2\epsilon}{k_B T}\phi\right]^{-1}. \tag{3.18}$$

Isothermal compressibility is defined by

$$\beta_T \equiv \frac{1}{V}\left(\frac{\partial V}{\partial P}\right)_{T,n} = \frac{1}{V}\left(\frac{\partial P}{\partial V}\right)^{-1}_{T,n} = \frac{1}{V}\left(\frac{\partial P}{\partial \phi}\right)^{-1}_{T,n}\left(\frac{\partial V}{\partial \phi}\right)_{T,n}.$$

For the equation of state 3.15, the above relationship yields the isothermal compressibility

$$\beta_T = \frac{v_0}{k_B T \phi}\left[\frac{1}{\alpha} + \frac{\phi}{1-\phi} + \frac{2\epsilon}{k_B T}\phi\right]^{-1}. \tag{3.19}$$

The isochoric and isobaric heat capacities are defined as

$$C_V \equiv T\left(\frac{\partial S}{\partial T}\right)_{V,n}$$

and

$$C_P \equiv T\left(\frac{\partial S}{\partial T}\right)_{P,n},$$

respectively, where S is the extensive thermodynamic quantity known as entropy. The entropy is related to the Helmholtz free energy through the partial derivative

$$S = \left(\frac{\partial F}{\partial T}\right)_{V,n}.$$

Using the more convenient reduced expression for the free energy, the entropy can be found through the relation

$$\frac{v_0 S}{k_B V} = \tilde{f} + T\left(\frac{\partial \tilde{f}}{\partial T}\right)_{V,n}.$$

Further differentiation produces the relation

$$\frac{v_0 C_V}{k_B V} = \frac{v_0 T}{k_B V}\left(\frac{\partial S}{\partial T}\right)_{V,n} = 2T\left(\frac{\partial \tilde{f}}{\partial T}\right)_{V,n} + T^2\left(\frac{\partial^2 \tilde{f}}{\partial T^2}\right)_{V,n}$$

Finally, substituting the reduced Helmholtz free energy of equation 3.13 leads to the isochoric heat capacity of zero with

$$\frac{v_0 C_V}{k_B V} = 0.$$

The isobaric heat capacity is more naturally calculated from the Gibbs free energy, which can in turn be calculated from the Helmholtz free energy through Legendre transformation. The transformation from one potential to the other is achieved through $G = F + PV$. The Gibbs free energy is found to be

$$\tilde{g} = \frac{G}{k_B T \alpha n} = \frac{\epsilon}{k_B T}\phi + \frac{1}{\alpha}\ln\phi - \phi\ln\phi_0 + \frac{v_0 P}{k_B T \phi} \tag{3.20}$$

For the purpose of verification, the entropy calculated from the Gibbs free energy is found to match that calculated from the Helmholtz free energy. The isobaric heat capacity is related to the reduced Gibbs free energy by the equation

$$\frac{C_P}{k_B \alpha n} = 2T\left(\frac{\partial \tilde{g}}{\partial T}\right)_{P,n} + T^2\left(\frac{\partial^2 \tilde{g}}{\partial T^2}\right)_{P,n}$$

Substitution of the Gibbs free energy of equation 3.20 into the relation similarly leads to a zero isobaric heat capacity where

$$\frac{C_P}{k_B \alpha n} = 0.$$

This zero isochoric and isobaric heat capacity result is not surprising given both quantities' dependence on internal degrees of freedom. Since the molecular theory was designed in a way that lacks this feature, the heat capacities should not be expected to yield accurate predictions. Indeed, in their pure fluid paper, Sanchez and Lacombe similarly come to this conclusion [104].

3.4 Description of the multicomponent fluid model

Many of the molecular model assertions presented in Section 3.2 readily lend themselves to expansion to multicomponent mixtures. In some cases, however, multiple modes of expansion may exist. For this reason, it is worth making the changes explicit. Each model assertion expands as follows:

1. The *segment excluded volume* assertion expands to include i species of molecules. Each molecule of a given species is composed of N_i segments of volume v_i. In practice, different species need not have the same number of segments per molecule or segment volume.

2. The *preserved close-packed volume* assertion does not require modification. The close-packed volume occupied by a molecule characterizes a given species.

3. The *short-ranged segment interaction* assertion expands to include both intraspecies and interspecies interactions. Intramolecular interactions characterize a given species. Intermolecular interactions characterize a given binary mixture.

4. The *free volume partition* assertion does not require modification.

5. The *hole character* assertion is unaffected by the expansion.

6. The *incompressibility* assertion expands easily to include many species.

Two of the model assertions, the *free volume partition* and *constant hole volume*, are problematic when taken together. If the free volume is divided into equal segments of volume v_0 that are constant and characteristic of a given polymer species, then it cannot limit to different values for each of the pure fluids. In their multicomponent mixture paper, Sanchez and Lacombe chose to replace the assertion with a variant as mentioned in Section 2.5.3. In the off-lattice construction, this is equivalent to replacing the *constant hole volume* with:

7a (Mixing rule) The volume of a hole v_0 is a function only of the hole volumes of the constituents and the composition of the mixture.

In mathematical form, mixing rules are equivalent to the hole volume becoming a function of the form

$$v_0 = v_0(\{v_0^{(i)}\}, \{n_i \mid \forall\ i \in S\}), \tag{3.21}$$

where $v_0^{(i)}$ refers to the volume of a hole in the pure fluid phase of species i and S refers to the number of species in the mixture, excluding holes. Table 2.5 lists common mixing rules from the literature. These mixing rules are arbitrary [105].

In the thermodynamic derivations to follow, it is found that the application of mixing rules create artefacts that lead to a theory inconsistent with the principles of statistical mechanics and thermodynamics. The present work instead chooses to expand the *constant hole volume* assertion with one that is more in line with the spirit of the pure fluid model. The assertion is taken to be:

7b (Constant hole volume) The volume of a hole v_0 is constant and a characteristic of a given saturated mixture. Changes in free volume correspond solely to changes in the number of holes.

Validation of this assertion and a physical interpretation of holes is discussed in Chapter 5.

3.5 Statistical thermodynamics of multicomponent fluids

3.5.1 Partition function based on the canonical ensemble

The fluid model presented in Section 3.2 is now expanded to multiple species of particles. Let the system be composed of S species i. Each i species polymer molecule is composed of N_i segments. Let n_i be the number of polymer molecules of species i. For clarity, sums and products over all species with the superscript "0" include holes and those without the superscript "0" exclude holes. Sums with the superscript n_iN_i are sums over all the segments of species i.

Just as in Section 3.3.1, functions describing the number and volume density of each species should be defined. Let $\{\mathbf{r}_i\} \equiv \{\mathbf{r}_{i,j} \mid j \in n_iN_i\}$ be the set of polymer segment positions of species i and $\{\mathbf{r}_i^{\mathrm{cm}}\} \equiv \{\mathbf{r}_{i,j}^{\mathrm{cm}} \mid j \in n_i\}$ be the molecular centre of mass positions. The number and volume density of each species is given by

$$\hat{\rho}_i(\mathbf{r}) = \sum_j^{n_iN_i} \delta(\mathbf{r} - \mathbf{r}_{i,j})$$

and

$$\hat{\varphi}_i(\mathbf{r}) = v_i\hat{\rho}_i(\mathbf{r}), \tag{3.22}$$

respectively. Taking the spatial average of the volume density function in equation 3.22 as per the *random mixture* assumption leads to the expression

$$\phi_i = \frac{n_iN_iv_i}{V}. \tag{3.23}$$

The number and volume density definitions for the holes remain unchanged.

The partition function of a system of many species of indistinguishable particles is given by

$$Q = \frac{1}{\prod_i^0 n_i!\Lambda_i^{3n_i}} \int \prod_i^0 d\{\mathbf{r}_i\} e^{-U(\{\mathbf{r}_i\})/k_BT}.$$

The expression for the interaction potential is once again simplified using the *two-body interactions* and *isotropic interaction* assumptions. The total interaction potential is therefore simplified to

$$\begin{aligned} U(\{\mathbf{r}_1\},...,\{\mathbf{r}_S\}) &\approx \frac{1}{2}\sum_i \sum_j \sum_k^{n_i N_i} \sum_l^{n_j N_j} u'_{ij}\left(\left|\mathbf{r}_{i,k}-\mathbf{r}_{j,l}\right|\right) \\ &= \frac{1}{2}\sum_i \sum_j \int d\mathbf{r}\, d\mathbf{r}'\, \hat{\rho}_i(\mathbf{r}) u'_{ij}\left(\left|\mathbf{r}-\mathbf{r}'\right|\right)\hat{\rho}_j(\mathbf{r}') \\ &= \sum_i \sum_j \frac{1}{2v_i v_j}\int d\mathbf{r}\, d\mathbf{r}'\, \hat{\varphi}_i(\mathbf{r}) u'_{ij}\left(\left|\mathbf{r}-\mathbf{r}'\right|\right)\hat{\varphi}_j(\mathbf{r}'), \end{aligned}$$

where $u'_{ij}(r)$ is a scalar function describing the interaction potential between a segment of species i and a segment of species j separated by a distance r. Each of the interactions is symmetric and thus obeys

$$u'_{ij}(r) = u'_{ji}(r)\ \forall\ r.$$

Assumption 7 (Symmetric interaction) *All intermolecular interactions are symmetric.*

Applying the *random mixture* assumption, the partition function becomes

$$Q = \frac{\int \prod_i^0 d\{\mathbf{r}_i\}}{\prod_i^0 n_i! \Lambda_i^{3n_i}} \prod_i \prod_j \exp\left(-\frac{\phi_i\phi_j}{2v_i v_j}\int d\mathbf{r} d\mathbf{r}' \frac{u'_{ij}\left(\left|\mathbf{r}-\mathbf{r}'\right|\right)}{k_B T}\right).$$

Each of the potentials u'_{ij} can be simplified using

$$\int d\mathbf{r} d\mathbf{r}'\, u'_{ij}\left(\left|\mathbf{r}-\mathbf{r}'\right|\right) = V\int d\mathbf{r}\, u'_{ij}\left(|\mathbf{r}|\right).$$

Taking into account the relative sizes of the polymer segments and holes, the *incompressibility* assertion is expressed as the constraint

$$\sum_i^0 \phi_i = 1 \tag{3.24}$$

In many theories, including the original lattice-based SL theory, many important quantities are ratios as a matter of necessity. This is especially true in a lattice construction, where the quantities of importance to the statistics are *relative* volumes, rather than absolute volumes. It is not surprising then that lattice fluid models, by necessity, fix the reference volume to that of a single lattice site. Indeed, as the SL lattice statistics assumed that lattice sites were either occupied or unoccupied, the volume of a hole and the volume of a lattice site were linked, but not inextricably so.

The present off-lattice construction allows more flexible consideration of reference volumes. Let the reference volume v_r be defined as an arbitrary reference volume. *The only requirement of this volume is that it be independent of all thermodynamic variables.* This is done as a matter of convenience for the derivations to follow.

Assumption 8 (Constant reference volume) *The reference volume is independent of all thermodynamic variables.*

The pure fluid theory of Section 3.3 uses the volume of a hole as a reference volume. The *constant hole volume* assertion made this an appropriate choice. It is clear, though, that the *mixing rule* assertion and equation 3.21 disqualify the use of hole volume as a reference volume, except in the case that the hole volume is constant.

For the derivations that follow, all of the quantities derived that make use of a reference volume appear twice: once with the reference volume v_r and again with the reference volume v_0. This is done for several reasons. The first is to explicitly illustrate that the theory containing mixing rules creates artefacts in the theory. The second is to simultaneously create a multicomponent mixture theory without mixing rules, using the hole volumes as reference volumes. The third is that, in the absence of mixing rules, some parameters defined in the pure fluid require translation into the mixture theory, which would be confusing if defined only in terms of disparate reference volumes.

Let the interaction parameters be defined

$$\epsilon_{ij,r} \equiv \frac{N_i N_j}{2\alpha_{i,r}\alpha_{j,r} v_r} \int d\mathbf{r}\; u_{ij,r}(|\mathbf{r}|) \tag{3.25}$$

or, if the hole volume satisfies the reference volume condition

$$\epsilon_{ij} \equiv \frac{N_i N_j}{2\alpha_i \alpha_j v_0} \int d\mathbf{r}\; u'_{ij}(|\mathbf{r}|), \tag{3.26}$$

where

$$\alpha_{i,r} = \frac{N_i v_i}{v_r} \tag{3.27}$$

represents the ratio of the close-packed molecule volume of molecule i relative to the reference volume and

$$\alpha_i = \frac{N_i v_i}{v_0} \tag{3.28}$$

represents the ratio with respect to the hole volume. The prime superscript is defined in order to differentiate the interaction potential function defined here from that of the pure fluid in Section 3.3.1. The relationship between the parameters of multicomponent fluids and their respective pure fluids is discussed further in Section 3.8.

Comparison of their definitions reveals that the interaction parameters obey the relation $\epsilon_{ij,r} = \epsilon_{ij}/\alpha_{0,r}$. Since $\alpha_{0,r}$ is assumed to be position-independent, the two interaction functions $u_{ij,r}$ and u'_{ij} are related by

$$u_{ij,r}(r) = \alpha_{0,r} u'_{ij}(r) \;\forall\; r.$$

Using definitions in equations 3.25 and 3.27, the expression for the partition function then becomes

$$Q = \frac{\prod_i^0 V^{n_i}}{\prod_i^0 n_i! \Lambda_i^{3n_i}} \prod_i \prod_j \exp\left(-\frac{V\epsilon_{ij,r}}{k_B T v_r}\phi_i\phi_j\right). \tag{3.29}$$

3.5.2 Helmholtz free energy

As in Section 3.3.2, the relation $F = -k_B T \ln Q$ applied to equation 3.29 is used to calculate the Helmholtz free energy. The complete expression of the free energy is therefore

$$\frac{F}{k_B T} = \sum_i \sum_j \frac{V\epsilon_{ij,r}}{k_B T v_r}\phi_i\phi_j + \sum_i \frac{V\phi_i}{N_i v_i}\ln\phi_i - \sum_i \frac{V\phi_i}{N_i v_i} + \frac{V\phi_0}{v_0}\ln\phi_0 - \frac{V\phi_0}{v_0} + \sum_i \frac{V\phi_i}{N_i v_i}\ln\left[\frac{\Lambda_i^3}{n_i v_i}\right] + \frac{V\phi_0}{v_0}\ln\left[\frac{\Lambda_0^3}{v_0}\right].$$

Several terms in the free energy do not contribute to the thermodynamics and are ignored. The results are not affected by terms that are constant or linear in n_i, which are dropped. In addition, the *thermal equilibrium* assumption allows the thermal de Broglie wavelengths Λ_i to be similarly dropped. Terms linear in n_0 cannot be ignored due to its dependence on $\{n_i\}$ and V from the incompressibility constraint. As discussed in Section 3.3.2, requiring $\lim_{\phi_0 \to 1} P = 0$ implies the normalization factor $\Lambda_0^3 = v_0 e$, as proposed by Hong and Noolandi [53].

Multiplying through by $\frac{v_r}{V}$ creates an intensive, dimensionless expression. The free energy is therefore expressed

$$\tilde{f} \equiv \frac{v_r F}{k_B T V} = \sum_i \sum_j \frac{\epsilon_{ij,r}}{k_B T} \phi_i \phi_j + \sum_i \frac{\phi_i}{\alpha_{i,r}} \ln \phi_i + \frac{\phi_0}{\alpha_{0,r}} \ln \phi_0. \tag{3.30}$$

If the hole volume v_0 is used as reference volume through equations 3.26 and 3.28, with the normalization factor set to $\Lambda_0^3 = v_0 e$, then the free energy reduces to the expression

$$\tilde{f} \equiv \frac{v_0 F}{k_B T V} = \sum_i \sum_j \frac{\epsilon_{ij}}{k_B T} \phi_i \phi_j + \sum_i \frac{\phi_i}{\alpha_i} \ln \phi_i + \phi_0 \ln \phi_0. \tag{3.31}$$

3.5.3 Chemical potential

The chemical potential of species i in the multicomponent mixture can be calculated using the definition

$$\mu_i = \left(\frac{\partial F}{\partial n_i} \right)_{T,V,\{n_{j \neq i}\}},$$

which yields the equation

$$\mu_i = \frac{k_B T N_i v_i}{v_r} \left(\frac{\partial \tilde{f}}{\partial \phi_i} \right)_{T,V,\{n_{j \neq i}\}}.$$

Applying this definition to the Helmholtz free energy produces the chemical potential

$$\tilde{\mu}_i \equiv \frac{v_r \mu_i}{k_B T N_i v_i} = 2 \sum_j \frac{\epsilon_{ij,r}}{k_B T} \phi_j + \frac{1}{\alpha_{i,r}} (\ln \phi_i + 1) - \frac{1}{\alpha_{0,r}} \ln \phi_0 - \frac{1}{\alpha_{0,r}} + \tilde{\mu}_{0,i}, \tag{3.32}$$

where

$$\tilde{\mu}_{0,i} \equiv \frac{v_r \mu_{0,i}}{k_B T N_i v_i} = -\frac{\phi_0}{\alpha_{0,r} v_0} \left(\frac{\partial v_0}{\partial \phi_i} \right)_{T,V,\{n_{j \neq i}\}}. \tag{3.33}$$

If the hole volume v_0 is constant then the chemical potential simplifies to the expression

$$\tilde{\mu}_i \equiv \frac{v_0 \mu_i}{k_B T N_i v_i} = 2 \sum_j \frac{\epsilon_{ij}}{k_B T} \phi_j + \frac{1}{\alpha_i} (\ln \phi_i + 1) - \ln \phi_0 - 1. \tag{3.34}$$

3.5.4 Equation of state

Based on the canonical ensemble

The pressure P is derived from the Helmholtz free energy using the relation

$$P = -\left(\frac{\partial F}{\partial V}\right)_{T,\{n_i\}}.$$

It follows that the relation can be rephrased as

$$\frac{v_r P}{k_B T} = -\tilde{f} - V\left(\frac{\partial \tilde{f}}{\partial V}\right)_{T,\{n_i\}}.$$

Making use of the fact that $\tilde{f}(\{\phi_i(V)\})$, the partial derivative with respect to volume becomes

$$\left(\frac{\partial \tilde{f}}{\partial V}\right)_{T,\{n_i\}} = \sum_i \left(\frac{\partial \tilde{f}}{\partial \phi_i}\right)\left(\frac{\partial \phi_i}{\partial V}\right) = -\frac{\phi_i}{V}\sum_i \left(\frac{\partial \tilde{f}}{\partial \phi_i}\right).$$

The above identities reduce the pressure equation to

$$\frac{v_r P}{k_B T} = -\tilde{f} + \phi_i \sum_i \left(\frac{\partial \tilde{f}}{\partial \phi_i}\right)_{T,\{n_i\}}.$$

Substituting the free energy leads to the equation of state

$$\frac{v_r P}{k_B T} = \sum_i \sum_j \frac{\epsilon_{ij,r}}{k_B T}\phi_i \phi_j - \sum_i \left(\frac{1}{\alpha_{0,r}} - \frac{1}{\alpha_{i,r}}\right)\phi_i - \frac{1}{\alpha_{0,r}}\ln \phi_0. \tag{3.35}$$

Based on the grand canonical ensemble

The grand canonical ensemble is described by the grand potential Φ_G. The Helmholtz free energy is related to the grand potential by the Legendre transformation

$$\Phi_G = F - \sum_i n_i \mu_i$$

which, through the substitution of equation 3.5, produces

$$\Phi_G = F - \sum_i \frac{V \phi_i}{N_i v_i}\mu_i.$$

Multiplying through by $\frac{v_r}{k_B T V}$ to achieve an intensive, dimensionless free energy, the transformation is phrased as

$$\frac{v_r \Phi_G}{k_B T V} = \tilde{f} - \sum_i \phi_i \tilde{\mu}_i.$$

Making use of the property $\Phi_G = -PV$, the equation of state is found through the substitution of equations 3.30, 3.32 and 3.33 to become

$$\frac{v_r P}{k_B T} = -\tilde{f} + \sum_i \phi_i \tilde{\mu}_i \left(= -\tilde{f} + \sum_i \phi_i \left(\frac{\partial \tilde{f}}{\partial \phi_i} \right)_{T,V,\{n_{j \neq i}\}} \right).$$

The equation of state derived from the grand canonical ensemble finally becomes

$$\frac{v_r P}{k_B T} = \sum_i \sum_j \frac{\epsilon_{ij,r}}{k_B T} \phi_i \phi_j - \sum_i \left(\frac{1}{\alpha_{0,r}} - \frac{1}{\alpha_{i,r}} \right) \phi_i - \frac{1}{\alpha_{0,r}} \ln \phi_0 + \frac{\phi_0}{\alpha_{0,r} v_0} \ln \phi_0 \sum_i \phi_i \frac{\partial v_0}{\partial \phi_i}. \quad (3.36)$$

Implications

Through equations 3.35 and 3.36, it is clear that the equations of state derived from the canonical and grand canonical ensembles do not match. This problem can be viewed in two ways: from a statistical mechanical point of view and from a thermodynamic point of view. Ensemble equivalence in statistical mechanics holds that, in the limit of the *many particle* assumption, thermodynamic quantities derived from the same molecular model using different ensembles, in this case canonical and grand canonical, should be identical under identical thermodynamic conditions. In thermodynamics, the equilibrium surface of a system should not depend on which thermodynamic potential, in this case the Helmholtz or grand potential, is employed to describe it, as discussed in Section 2.3.1.

Since disagreement with either statistical mechanics or thermodynamics principles implies the falsification of the theory as mentioned in Section 3.1, this implies that the statistical thermodynamical model is only valid under the condition

$$\frac{\phi_0}{v_0} \ln \phi_0 \sum_i \phi_i \frac{\partial v_0}{\partial \phi_i} = 0. \quad (3.37)$$

This condition is further examined in Section 3.7.

3.6 Contact with the SL-EOS

3.6.1 Pure fluids

Despite differences in their underlying assertions necessitated by the differences between on-lattice and off-lattice constructions, the SL model and the present construction produce equivalent statistical thermodynamic theories. This can be shown by examining the relationships between the quantities in both models.

In the original SL theory, the reduced density $\tilde{\rho}$ was defined as the ratio of the density of the system to a maximal close-packed density [104]. This is akin to a ratio of the volume occupied by polymer species to the total volume of the system, an equivalence also noted in SL [104]. This observation establishes an equivalence between the reduced density $\tilde{\rho}$ and the volume fraction ϕ, defining

$$\tilde{\rho} = \frac{\rho}{\rho^*} \equiv \phi,$$

where the characteristic density is given by

$$\rho^* \equiv \frac{M}{Nv}. \tag{3.38}$$

Further, the number of lattice sites occupied by a molecule r is equivalent to the relative volume of a molecule with respect to a hole, thus defining

$$r \equiv \alpha.$$

The interaction parameter ϵ is defined similarly to that of the SL theory ϵ^*. Contact is made through the equation

$$\frac{1}{\tilde{T}} = \frac{T^*}{T} \equiv -\frac{\epsilon}{k_B T},$$

which implies that

$$T^* = -\frac{\epsilon}{k_B}. \tag{3.39}$$

Finally, the pressure scaling parameter is related to the temperature scaling parameter through the usual definition

$$P^* = \frac{k_B T^*}{v_0} = -\frac{\epsilon}{v_0}, \tag{3.40}$$

used by SL [104].

Substituting these relations into the equation of state defined by equation 3.15, one arrives at the equation

$$\tilde{P} + \tilde{\rho}^2 + \tilde{T}\left[\ln(1-\tilde{\rho}) + \left(1 - \frac{1}{r}\right)\tilde{\rho}\right] = 0,$$

which matches the SL-EOS in equation 2.9 [104].

3.6.2 Multicomponent fluids

Making contact with the multicomponent SL-EOS requires the assumption that the hole volume v_0 be taken as reference volume, even if mixing rules are considered.

Just as in the pure fluid, the reduced density is defined to be the ratio of the total density to the close-packed fluid density, or the occupied volume to the total volume. This establishes the reduced density $\tilde{\rho}$ to be the sum of the reduced densities of the constituents, or

$$\tilde{\rho} \equiv \sum_i \phi_i.$$

In their 1978 paper, Sanchez and Lacombe established an interaction mixing rule in order to maintain a consistent energy density between pure fluids and the mixture [105]. This was done through a weighted average of pressure parameters P^*. Using a similar argument, the SL temperature and pressure parameters can be related to the interaction parameters ϵ_{ij} by defining

$$\epsilon^* \equiv \frac{\sum_i \sum_j \epsilon_{ij}\phi_i\phi_j}{\left(\sum_i \phi_i\right)^2}.$$

Similarly, the mixture average number of lattice sites occupied by a molecule, r, should be related to the volume fractions α_i through the same weighted average employed by Sanchez and Lacombe [66, 105] using the definition

$$\frac{1}{r} = \frac{\sum_i \frac{\phi_i}{\alpha_i}}{\sum_i \phi_i}.$$

Substituting these definitions into the multicomponent equation of state given by equation 3.35 also produces the SL-EOS given by equation 2.9.

3.7 Mixing rules and thermodynamic inconsistency

Determining the success of a statistical thermodynamical model is a difficult matter, one that is beyond the scope of this work. On the other hand, determining if a theory is unsuccessful need not be as difficult, but requires discussion of expectations. In other words, a thermophysical model should meet certain criteria in order to be considered viable.

Chief among the requirements of a model is that the assertions should not lead to a contradiction with the set of physical laws. In the hierarchy of inconsistencies, such contradictions are considered most severe. For example, the model should not be incompatible with conservation of energy, regardless of its success in agreement with experimental observations.

Next, the model should not lead to a contradiction with firmly established theories, unless the aim is specifically to supplant or invalidate them. Such an exception is similarly beyond the scope of this work. For example, it is required that a statistical thermodynamical model be compatible with the fundamental thermodynamic relation. This is particularly true since such theories make use of the principles of thermodynamics to calculate physical properties. Indeed, the present theory makes use of the principles of thermodynamics presented in Section 2.3.1 in order to determine material properties and phase equilibria. As a consequence, contradiction with these same principles is impermissible. The implications of Section 3.5.4 are therefore examined with the goal of imposing these thermodynamic principles.

A necessary caveat is that a theory is only expected to meet the criteria of relevance within the bounds of its limitations. For example, if a model is developed to describe only systems where interactions are of prime importance, then it need not be compatible with the ideal gas since this regime is outside of the bounds within which the model was designed to operate.

In order for the theory to be internally consistent, the multicomponent fluid theory should not contradict the pure fluid theory. This requirement puts a constraint on the mixing rules. Since the pure fluid theory, through the *constant hole volume* assertion, requires that the volume of a hole is constant, then the same should be true of the pure fluid limits of the multicomponent fluid. This is expressed as the set of conditions

$$v_0(\{n_i \mid n_i = 0 \ \forall \ i \neq j\}) = v_0^{(j)}.$$

Combining these conditions, equation 3.23 and the observation that N_i, v_i and V are finite

and non-zero, implies that

$$v_0(\{\phi_i \mid \phi_i = 0 \ \forall \ i \neq j\}) = v_0^{(j)}. \tag{3.41}$$

These requirements form the boundary conditions of the differential equation 3.37

$$\frac{\phi_0}{v_0} \ln \phi_0 \sum_i \phi_i \frac{\partial v_0}{\partial \phi_i} = 0.$$

Since the hole volume is assumed to be finite, there are three situations that satisfy this equation.

- (Flory-Huggins limit) The equation is satisfied in the limit $\phi_0 \to 0$. This limit is useful if compressibility of the polymeric fluid is not a key issue [40].
- (Constant hole volume) The equation is satisfied when $\frac{\partial v_0}{\partial \phi_i} = 0 \ \forall \ i$. In other words, when the volume of a hole is constant with respect to composition. This situation will be discussed in further detail in Chapter 5.
- (Mixing rule condition) The equation is satisfied when the mixing rule satisfies the first-order homogeneous partial differential equation $\sum_i \phi_i \frac{\partial v_0}{\partial \phi_i} = 0$ with the set of boundary conditions $v_0(\{\phi_i \mid \phi_i = 0 \ \forall \ i \neq j\}) = v_0^{(j)}$.

In the mixing rule condition case, it is more useful to examine the Cauchy problem than it is to calculate the solution. For clarity, this work will focus only on the binary mixture, with the knowledge that the analysis readily scales to larger mixtures. For the binary mixture, the differential equation becomes

$$\phi_1 \frac{\partial v_0}{\partial \phi_1} + \phi_2 \frac{\partial v_0}{\partial \phi_2} = 0. \tag{3.42}$$

Re-parametrizing so that $v_0(\phi_1, \phi_2) = v_0(\phi_1(t), \phi_2(t))$, the derivative with respect to t becomes by definition

$$\frac{dv_0}{dt} = \frac{\partial v_0}{\partial \phi_1}\frac{d\phi_1}{dt} + \frac{\partial v_0}{\partial \phi_2}\frac{d\phi_2}{dt} = 0. \tag{3.43}$$

Comparison of equations 3.42 and 3.43 implies that

$$\frac{d\phi_1}{dt} = \phi_1$$

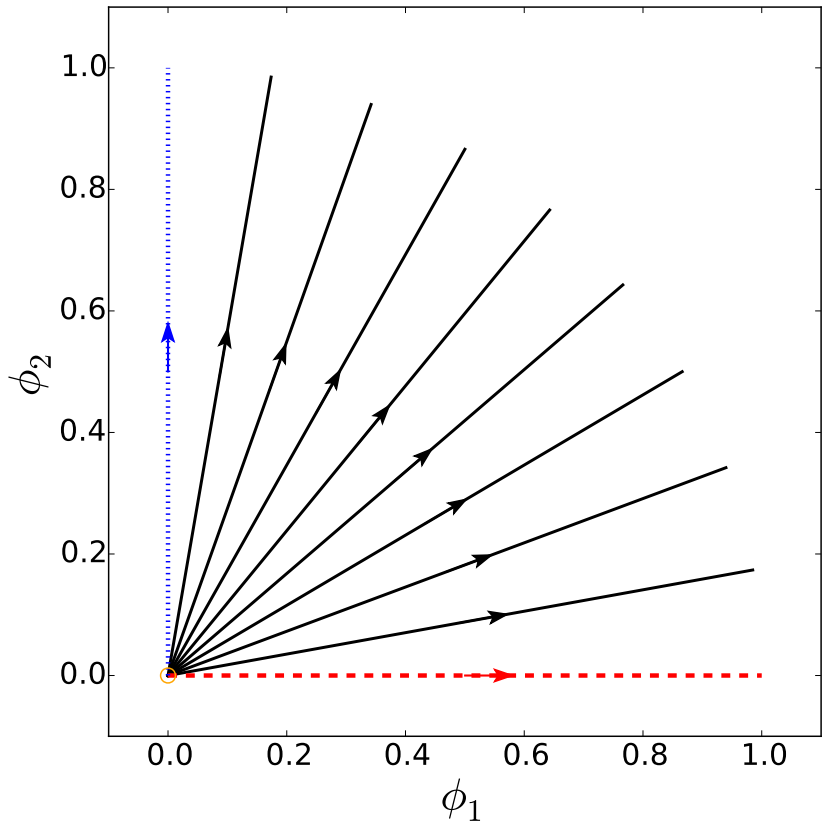

Figure 3.1 The characteristic curves of the first-order homogeneous differential equation given by equation 3.42. The boundary conditions, defined along the ϕ_1 (red, dashed) and ϕ_2 (blue, dotted) axes. Since the characteristics each have two boundary conditions specified at the origin (orange, circle), the boundary value problem is overdetermined except in the trivial case that $v_0^{(1)} = v_0^{(2)}$.

and

$$\frac{d\phi_2}{dt} = \phi_2.$$

These equations are in turn used to plot the characteristic curves of the differential equation, illustrated by figure 3.1. The figure shows the characteristic curves of the differential equation originate from the same point.

The boundary conditions given by equation 3.41 are shown in figure 3.1, and correspond to the lines of constant hole volume along the ϕ_1 and ϕ_2 axes of $v_0^{(1)}$ and $v_0^{(2)}$, respectively. Since all characteristic curves originate from the point $(\phi_1, \phi_2) = (0, 0)$ and the boundary conditions overlap at that point, the boundary value problem is thus overdetermined,

except in the trivial case that $v_0^{(1)} = v_0^{(2)}$.

Since there are no meaningful solutions to the mixing rule condition, it is concluded that mixing rules on the hole volume contradict the thermodynamic principles outlined in Section 2.3.1. This implies that, in order to be thermodynamically consistent, the SL theory for multicomponent mixtures should be used in either the Flory-Huggins limit or with a constant hole volume. Since many polymer fluid mixtures feature compressibility, with volume changes upon mixing of particular interest to polymer foaming, a constant hole volume in the mixture is assumed.

While a constant hole volume allows for a *thermodynamically* consistent theory, it does not allow for an *internally* consistent theory since a constant hole volume in the mixture precludes the ability of the mixture theory to limit correctly to describe the pure fluids in each of the pure fluid limits.

It is possible, however, that there exist cases that do not require the theory to limit correctly. In the case of saturated polymer-solvent mixtures, one could use a constant hole volume along the line of saturation. Indeed, limiting cases along the line of saturation are not required. Following the saturation curve towards the pure solvent limit would imply the unphysical circumstance of polymer vapour within a solvent liquid, while following the saturation curve towards the pure polymer result in the solidification of the polymer before all solvent is excluded. The constant hole volume assumption, like many of the statistical mechanical approximations discussed in Section 2.4.2, requires *a posteriori* validation through comparison to experiment.

Nevertheless, some inconsistency is inevitable since comparison of any two phases with different hole volumes cannot be performed consistently due to the presence of the hole volume in the chemical potentials, first reported by Neau [88]. One would hope that, given sufficiently similar hole volumes in the phases being compared, the effects of this inconsistency would be minimal. This can only be determined through *a posteriori* comparison of hole volumes in each phase.

3.8 Relationship between pure fluid and multicomponent fluid parameters

In the SL theory, both intermolecular interactions and segment volumes are subject to mixing rules. For reference, the SL lattice-based mixing rules are described in Appendix A. In the absence of mixing rules, it is necessary to ensure the cohesiveness of the energy

density, as Sanchez and Lacombe do [105]. In other words, it is necessary to ensure that the energy density of the system does not change depending on how the system is partitioned. Given that the hole volume is used as reference volume, this is an important consideration.

To this end, a requirement is added that the change in energy on the exchange of a polymer molecule with holes must be independent of the size of the hole. In the derivations to follow, the superscript (p) refers to the value of the quantity in the pure fluid and the superscript (m) refers to the value of the quantity in the mixture. This leads to the requirement that

$$\epsilon_{ii}^{(p)} = \epsilon_{ii}^{(m)},$$

where $\epsilon_{ii}^{(p)}$ refers to ϵ of pure component i. This implies that all pure interactions parameters remain consistent in the mixture. It follows that

$$\int d\mathbf{r}\; u_{ii}(|\mathbf{r}|) = \frac{v_0^{(m)}}{v_0^{(p)}} \int d\mathbf{r}\; u_{ii}^{\prime}(|\mathbf{r}|),$$

where the function u_{ii} refers to the function u of pure component i. Since the volume of a hole is independent of position, the relationship between the potentials becomes

$$u_{ii}(r) = \frac{v_0^{(m)}}{v_0^{(p)}} u_{ii}^{\prime}(r) \;\forall\; r.$$

A further consequence of this transformation is that if $v_r^{(p)} = v_r^{(m)}$, then

$$u_{ii,r}^{(p)}(r) = u_{ii,r}^{(m)}(r) \;\forall\; r,$$

or rather $\epsilon_{ii,r}^{(p)} = \epsilon_{ii,r}^{(m)}$ as expected.

It is also necessary to translate the volume ratio α in equation 3.9 into the mixture. From the *preserved close-packed volume* assertion, Nv in the pure fluid is equal to $N_i v_i$ in the mixture. From equations 3.9 and 3.28, this can be used to establish the relationship

$$\alpha_i^{(m)} = \frac{v_0^{(p)}}{v_0^{(m)}} \alpha_i^{(p)}, \tag{3.44}$$

where $\alpha_i^{(p)}$ refers to α of pure component i.

3.9 Parameter estimation

In order to make predictions about the fluid properties, the theory requires the input of experimental data to estimate the molecular or characteristic parameters. In order to estimate these parameters, it is necessary to define a scalar objective function as well as an algorithm for optimizing the objective function [35, 83, 126].

The objective function is a scalar quantity that acts as a measure of the goodness of fit between experimental data and corresponding values predicted by the theory. The experimental data can take the form of thermodynamic properties or functions of thermodynamic properties.

Since the theory defines an equilibrium surface in the thermodynamic coordinate space, it is important to define which thermodynamic variables in the set of coordinates are dependent and independent quantities. The number of independent thermodynamic variables in phase equilibrium calculations can be determined using the Gibbs phase rule [64]. In the present work, however, additional constraints on the system due to the typically fixed composition of the solvent-rich phase reduce the number of independent thermodynamic variables. The number of independent variables is given by the equation

$$f = S + 2 - \gamma - \delta, \tag{3.45}$$

where S is the number of species in the mixture and γ is the number of phases in coexistence, and δ is the number of *additional* constraints on the system. The number of dependent variables is given by the equation $d = \gamma + \delta$. The Gibbs phase rule is recovered when no additional constraints on the system exist, or $\delta = 0$. In saturated polymer-solvent mixtures, additional constraints often take the form of a set of fixed molar ratios in a given phase. For pure fluids, two cases are considered: fluids in a single phase and fluids in a liquid-vapour coexistence phase. In a single phase system, composed of a single species with no additional constraints, the phase rule given by equation 3.45 indicates that there are $f = 2$ independent variables and 1 dependent variable. In a two-phase system, composed of a single species with no additional constraints, there are $f = 1$ independent and 2 dependent variables. For multicomponent fluids, the present work considers saturated polymer-solvent mixtures in two cases: binary polymer-solvent mixtures and ternary polymer-co-solvent mixtures. In a binary mixture, composed of two species in two phases with no additional constraints, the phase rule indicates that there are $f = 2$ independent variables and 2 dependent variables. In a ternary mixture, composed of three species in two phases with an additional constraint imposed by a fixed molar ratio in the solvent-rich phase, the phase rule indicates that there are $f = 2$ independent and 3 dependent variables.

Let the thermodynamic variables be divided into independent $\{I_j\}$ and dependent $\{D_j\}$ variables. The objective function should take the form

$$\mathrm{OF}_n(\{\sigma_j\},\{D_j^0\}) = \sum_k \sum_i w_k \left| \frac{D_k^0(\{I_j\}_i) - D_k(\{\sigma_j\},\{I_j\}_i)}{D_k^0(\{I_j\}_i)} \right|^n ,$$

where the superscript "0" indicates experimentally measured quantities and $\{\sigma_i\}$ represents the set of parameters to be estimated. The factor w_k represents an optional weighting function to adjust the relative importance of each data point to the sum. Setting $w_k = 1$ gives the same relative importance to each data point. The weighting function is discussed further in Section 4.1.2. This view suggests that in order to provide the best possible fit over the entire equilibrium surface, the objective function should include data obtained for a variety of points over a span of all independent variables in order to reduce ambiguity of parameters. Ambiguity caused by a limited data set is illustrated through a simple contrived example in Appendix B.

Rather than being thermodynamic variables, the observables are generally functions of the thermodynamic variables. The observables should then have the form

$$A_k = A_k(\{I_j\};\{D_j(I_j)\}).$$

This implies that in general, the objective function should have the form

$$\mathrm{OF}_n(\{\sigma_j\},\{A_j^0\}) = \sum_k \sum_i w_k \left| \frac{A_k^0(\{I_j\}_i) - A_k(\{\sigma_j\},\{I_j\}_i)}{A_k^0(\{I_j\}_i)} \right|^n . \tag{3.46}$$

The choice of power n of the objective function is related to the importance placed on outlying data. Typically, a value $n = 2$ is chosen, which allows for a least-squares fitting approach. In this case, the objective function is referred to as the sum of squares (SSQ), where $\mathrm{SSQ}_A = \mathrm{OF}_2(\{\sigma_j\},\{A_j^0\})$.

For the pure fluid systems, the thermodynamic coordinates are P, T, and ρ, with the same quantities forming the measurable properties. The set of parameters $\{\sigma_i\}$ is either taken to be the set of characteristic parameters $\{P^*, T^*, \rho^*\}$ or the set of molecular parameters $\{\epsilon, v_0, \alpha\}$. With T, and ρ chosen as independent variables, P then becomes the dependent variable on the equilibrium surface. The objective function used to estimate pure fluid parameters is

$$\mathrm{SSQ}_P = \sum_i^{\mathrm{sp}} w_P \left(\frac{P_i^0(T,\rho) - P(P^*,T^*,\rho^*,T,\rho)}{P_i^0(T,\rho)} \right)^2 + \sum_i^{\mathrm{coex}} w_P \left(\frac{P_i^0(T) - P(P^*,T^*,\rho^*,T)}{P_i^0(T)} \right)^2 , \tag{3.47}$$

where "sp" refers to the single-phase region and "coex" refers to the coexistence curve on the equilibrium surface. Often in the literature, T, and P are chosen as independent variables, which is associated with the objective function

$$\mathrm{SSQ}_\rho = \sum_i^{\mathrm{sp}} w_\rho \left(\frac{\rho_i^0(T,P) - \rho(P^*,T^*,\rho^*,T,P)}{\rho_i^0(T,P)} \right)^2 + \sum_i^{\mathrm{vap}} w_\rho \left(\frac{\rho_i^0(T) - \rho(P^*,T^*,\rho^*,T)}{\rho_i^0(T)} \right)^2 + \sum_i^{\mathrm{liq}} w_\rho \left(\frac{\rho_i^0(T) - \rho(P^*,T^*,\rho^*,T)}{\rho_i^0(T)} \right)^2, \quad (3.48)$$

where "vap" indicates vapour and "liq" indicates liquid.

For multicomponent systems, it is assumed in the present work that the composition of the solvent-rich is fully constrained and that the system is in a two-phase solvent-rich-polymer-rich equilibrium. This configuration is further discussed in Section 3.10. The thermodynamic coordinates are P, T, and $\{\mu_i \mid i \in S\}$. The set of parameters $\{\sigma_i\}$ is taken to be the the set $\{\{\epsilon_{ij}\}, v_0\}$ corresponding to the set of binary interaction parameters $\{\epsilon_{ij}\}$ and the mixture hole volume v_0. The pure fluid parameters in the mixture are generally constrained to be equal to those of the constituent pure fluids, estimated from pure fluid experimental data, although this is discussed further in Section 5.1.4. With variables P and T chosen to be independent variables, then $\{\mu_i \mid i \in S\}$ are dependent variables at equilibrium. For such mixtures, the common observable property is total solvent solubility, leading to the objective function

$$SSQ_\chi = \sum_i \left(\frac{\chi_i^0(P,T) - \chi_i(\{\epsilon_{ij}\}, v_0, P, T)}{\chi_i^0(P,T)}. \right)^2. \quad (3.49)$$

Once an objective function is chosen, it only remains to apply an optimization algorithm in order to determine parameters that best fit the data. There exist diverse methods to perform this optimization [1, 77]. A variation on the Newton method known as the Levenberg-Marquardt algorithm is used in the present work [83].

3.10 Saturated fluid mixtures

3.10.1 Equilibrium condition

Saturation is defined as the state in which a maximal concentration of one species or set of species has been achieved in a polymer mixture. Typically in polymer foaming, such

calculations are performed on polymer-solvent mixtures. Calculation of the composition of such mixtures is equivalent to determination of the composition of a polymer-solvent mixture under the constraint that it is in coexistence with one or more solvent-rich phases. This is tantamount to assuming that these solvent-rich phases are in thermal, mechanical, and diffusive equilibrium with the mixture phase. Thus, let an initially pure polymer phase having Q species of polymers and known composition be denoted (p). Let C solvent rich phases, denoted (c), of known composition be composed of R species of solvents. Let the solvent-rich phases be in coexistence with a polymer-solvent mixture phase (m), composed of all R solvents as well as all Q species of polymers for a total number of species $S = Q + R$. It is assumed that, due to the large size of their molecules, that the solvent-rich phases will contain no polymer molecules at equilibrium.

Assumption 9 (Large polymer) *Polymer molecules do not diffuse into solvent-rich phases due to their large size, therefore solvent-rich phases contain no polymer at equilibrium.*

Equilibrium is then defined as the set conditions

$$P^{(c)} = P^{(m)}, \tag{3.50}$$

$$T^{(c)} = T^{(m)}, \tag{3.51}$$

and

$$\{\mu_i^{(c)} = \mu_i^{(m)} \ \forall \ i \in R\} \tag{3.52}$$

for all $c \in C$.

In the polymer-solvent systems to which the theory is applied in Chapter 5, the system is defined using two-phase coexistence. A solvent-rich phase of fixed composition is assumed to be in thermal, mechanical, and diffusive equilibrium with a polymer-solvent mixture phase defined through equations 3.50, 3.51, and 3.52, respectively. The procedure is outlined for a system containing only one polymer species, but is easily expanded assuming the initial composition of the polymer system is known.

Composition can be uniquely determined by calculating the set of volume fractions ϕ_i in the mixture phase. The temperature and pressure of the system are treated as independent variables. Since the volume fractions of all species are unknown in both solvent-rich and mixture phases, this means that there are a total of $2R+1$ unknowns. These are determined by simultaneously solving the set or R equations 3.52, the equation of state in equation 3.31 for both phases, as well as the constraints on the composition of the solvent-rich phase.

3.10.2 Solvent solubility

Once the composition of the mixture phase is established, the solubility of the ith species in a multi-species mixture is calculated using the definition

$$\chi_i \equiv \frac{n_i M_i}{\sum_j n_j M_j},$$

where n_i is once again the number of molecules of species i and M_i is the molecular weight of species i. This quantity therefore represents the mass fraction of species i in the saturated mixture. Since expressions derived in the previous sections are given in terms of volume fraction rather than number fraction, it is useful to derive this relation in terms of ϕ_i instead. Using equation 3.5, the solubility becomes

$$\chi_i = \frac{M_i \phi_i V / v_i}{\sum_j M_j \phi_j V / N_j v_j},$$

which, combined with equation 3.28, finally reduces to the general equation

$$\chi_i = \frac{M_i \phi_i / \alpha_i}{\sum_j M_j \phi_j / \alpha_j}. \tag{3.53}$$

For mixtures with multiple solvent species, the solubility is defined as the total mass of solvent present in the polymer solvent mixture. The solubility is therefore defined as the sum of the solubilities of the individual solvent species, given by the equation

$$\chi_s = \sum_i^{\text{solvents}} \chi_i. \tag{3.54}$$

3.10.3 Volume swelling

In a saturated polymer mixture, the swelling ratio is defined as the ratio of the volume of the saturated mixture (m) to the volume of the polymer-rich phase (p) when the number of molecules of each polymer species $n_k = n_k^{(p)} = n_k^{(m)}$, is held constant between the two phases. In practice, this ratio is expressed as

$$S_W = \frac{V(T, P, t_{eq})}{V(T, P, t_{ini})} = \frac{V(T, P, t_{eq})}{m_{sample} v(T, P)},$$

where $V(T, P, t_{eq})$ is defined as the volume of the saturated mixture at equilibrium at a given temperature T, pressure P and equilibrium time t_{eq}, and $V(T, P, t_{ini})$ is the volume of the polymer-rich sample. To simplify the notation, let the set $\{k\}$ denote the indices of only the polymer species, the set $\{j\}$ the indices of only the solvent species, and $\{i\} = \{j\} \cup \{k\}$ the set of all species in the mixture. The sums over these indices is assumed to be the sum over their respective sets. Therefore, the swelling ratio is given by the expression

$$S_W = \frac{n_0^{(m)} v_0^{(m)} + \sum_i n_i^{(m)} N_i v_i}{n_0^{(p)} v_0^{(p)} + \sum_k n_k^{(p)} N_k v_k},$$

where care is taken to note that the number and volume of holes as well as the number of solvent molecules are in general not consistent between the mixture and the pure fluid phases, denoted with (m) and (p), respectively. It is also worth noting that the number of molecules of species k in the initial and final systems is identical, but for all other species the number of molecules is not consistent. Once again, since the expressions derived in previous sections are derived with respect to the volume fractions ϕ_i, it is useful to express the swelling in the same way. Dividing numerator and denominator by the sum of the volume of polymer in both phases, the swelling expression becomes

$$S_W = \frac{1 + \frac{n_0^{(m)} v_0^{(m)}}{\sum_k n_k N_k v_k} + \frac{\sum_j n_j^{(m)} N_j v_j}{\sum_k n_k N_k v_k}}{1 + \frac{n_0^{(p)} v_0^{(p)}}{\sum_k n_k N_k v_k}}.$$

The definition of equation 3.23 as well as the incompressibility constraint given by equation 3.24 allows the swelling ratio to be expressed as

$$S_W = \frac{1 + \left(1 - \sum_i \phi_i^{(m)}\right) / \sum_k \phi_k^{(m)} + \sum_j \phi_j^{(m)} / \sum_k \phi_k^{(m)}}{1 + \left(1 - \sum_k \phi_k^{(p)}\right) / \sum_k \phi_k^{(p)}}.$$

Incompressibility therefore implies that the swelling equation must reduce to

$$S_W = \frac{\sum_k \phi_k^{(p)}}{\sum_k \phi_k^{(m)}}. \tag{3.55}$$

It is equally possible to derive the above result by relating the swelling ratio to intensive quantities rather than extensive ones. Using the density ρ rather than the volume V, the swelling ratio becomes

$$S_W = \frac{\rho^{(p)}}{\rho^{(m)} \sum_k m_k},$$

where m_k is the mass fraction of species k. Such a definition, when related once again to the volume fractions ϕ_i identically yields equation 3.55.

Chapter 4

Application to pure fluids

4.1 Pure fluid parameter estimation applied to CO_2

It has been noted that correlation of pure fluid properties from pure component parameters with experiment has a direct effect on the predictive power of the mixture theory [5, 45, 97]. For this reason, a discussion of the pure component theory and characteristic parameters is warranted before moving on to considerations of polymeric mixtures.

The present work uses CO_2 as prototype to discuss general parameter estimation procedures. There are several reasons for this choice. The low critical point makes CO_2 a useful material for supercritical fluid extraction [16, 114]. Its abundance and relatively low environmental impact make it desireable for use as a blowing agent [9, 17, 108, 109, 118, 138]. Following application to CO_2, the pure fluid parameter estimation considerations are applied to further materials in Section 4.2.

4.1.1 Pure fluid parameters

Pure fluids in the present theory are fully characterized by a set of three parameters in addition to the molecular weight M. These parameters can either take the form of the molecular model quantities (ϵ, v_0, and α), referred to in the present work as the set of molecular parameters, or thermodynamic quantities (P^*, T^*, and ρ^*), referred to in the present work as the characteristic parameters. The molecular and characteristic parameters are related through equations 3.38, 3.39, and 3.40.

It is conventional wisdom in the literature that no constant set of SL parameters is capable of describing the properties of a fluid over a large range of pressures and temperatures. Instead, it is common practice to derive a set of parameters only for the temperature and pressure range under consideration. Despite their importance, no universally accepted practices for parameter estimation or universally accepted limits to the thermodynamic ranges that can be represented by a constant set of parameters exists in the literature. As a result, a great number parameter sets exist in the literature for CO_2 alone, many applying to overlapping thermodynamic ranges [4, 12, 20, 34, 36, 45, 58, 63, 87, 95, 135, 138]. A selection of these literature parameters, as well as the pressure and temperature ranges from which they were derived, is found in table 4.1.

4.1.2 Experimental PVT data

While a great variety of parameter estimation procedures have been proposed, including several for CO_2 alone, all are based on the comparison of theoretically derived properties with the corresponding experimental observation, as discussed in Section 3.9. Whatever fitting procedure is employed, it should be verified that only properties that are expected to correlate with experiment are included in the estimation. This should be done with the limitations discussed in Section 3.2 in mind. The observable properties to be used in fitting are dictated in part by the nature of the material at hand. For example, liquid-vapour equilibrium data is included for CO_2, but is not available for polymeric materials due to their low volatility [104]. A full list of the sources of experimental data for CO_2 used in the present work is found in table 4.1.

The quality of experimental data should be considered in parameter estimation procedures. This quality of information is typically included with experimental data through the use of error estimations, typically given as bounds on the error. These error bounds are used to appropriately weight the experimental data, entering the least-squares objective functions through the weighting factors w_k in equation 3.46. Many of the sources of experimental data considered in the present work do not include error bounds. With the absence of error bounds, there is then no basis for the weighting of experimental data. Further, the experimental data used in the present work shows a high level of consistency [114], further implying that no relative weighting is required.

Group	Year	P^* (MPa)	T^* (K)	ρ^* (g/cm^3)	P (MPa)	T (K)	Method	Data source (Ref.)	$SSQ_P(10^{-4})$
Kilpatrick [58]	1986	719.51	280.0	1.618	0.51 – 7.4	216.6 – 304	—	7	241.1
Kiszka [63]	1988	574.5	305.0	1.510	10.1 – 16.2	313 – 333	Piezometer	3	58.64
Pope [95]	1991	659.63	283.0	1.62	0.1	304	—	133	245.1
Wang [135]	1991	720.3	†	1.580	< 8	313 – 333	Piezometer	3	424.7
Hariharan [45]	1993	418.07	316.0	1.369	0.58	219.26	Piezometer	11	213.5
Garg [36]	1994	464.2	328.1	1.426	< 26	323 – 373	Piezometer	86	14.57
Xiong [138]	1995	420.0	340.9	1.392	20 – 60	360 – 420	Viscometer	138	6.083
Doghieri [20]	1996	630.0	300.0	1.515	8 – 50	270 – 360	—	124	68.12
Nalawade [87]	2006	427.7	338.7	1.4055	< 30	333 – 420	Buoyancy	114	6.101
Funami [34]	2007	369.1	341.2	1.2530	< 40	394.4 – 522.9	Buoyancy	34	94.87
Cao [12]	2010	453.53	327.0	1.46	13 – 28	318 – 368	—	89	18.78
Arce [4]	2009	585.61	301.23	1.53253	< 7.4	216.6 – 304.0	—	4	76.94
This work	**2016**	**419.9**	**341.8**	**1.397**	**< 66.57**	**216.6 - 1100.0**	—	—	**4.968**

Table 4.1 List of pure component CO_2 SL parameter sets with corresponding pressure and temperature ranges, the experimental method used, where available, and the reference number for the source of the experimental data. The deviation between theory and experiment is also given (SSQ_P) using equation 3.47. All experimental data was derived from pure component samples. †The temperature scaling parameter of Wang et al. is given by the expression $T^* = 208.9 + 0.459T - 7.56 \times 10^{-4}T^2$.

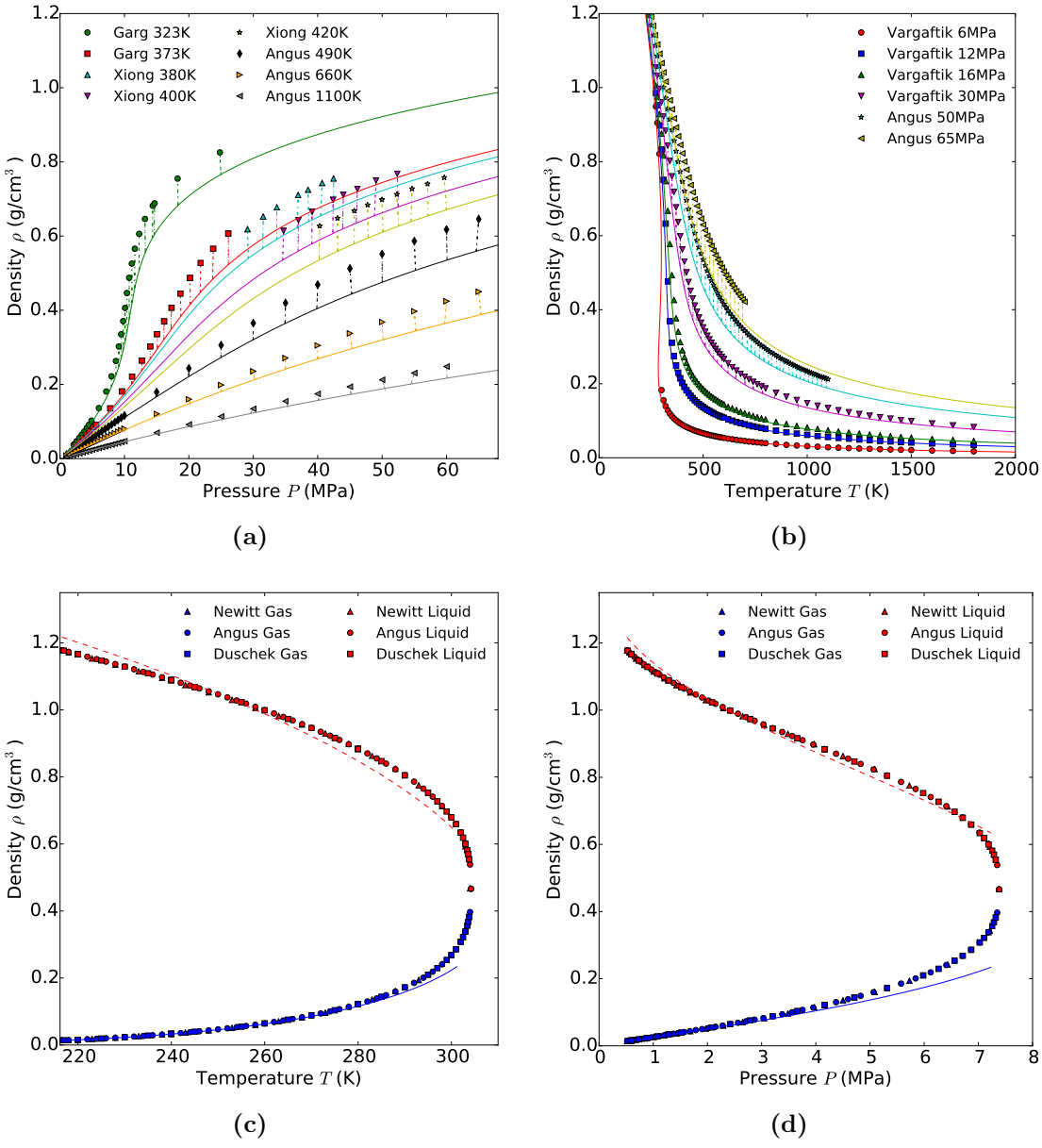

Figure 4.1 A comparison of (a) density-pressure isotherm, (b) density-temperature isobar, (c) saturated liquid-vapour density-temperature curve, and (d) density-pressure curve obtained using the Kilpatrick and Chang [58] parameters with the ones obtained experimentally. Lines represent predicted density while filled shapes represent experiment. Dashed lines are added to link experimental data with the corresponding theoretical curve for clarity. The legends indicate the experimental sources [127].

Group	T_c (K)	P_c (MPa)
Kilpatrick [58]	309.7	8.66
Kiszka [63]	316.2	9.08
Pope [95]	305.0	8.89
Wang [135]	310.4	8.38
Hariharan [45]	303.9	8.73
Garg [36]	318.1	9.42
Xiong [138]	319.0	9.64
Doghieri [20]	320.1	8.85
Nalawade [87]	318.5	9.66
Funami [34]	316.8	8.69
Cao [12]	312.8	9.65
Arce [4]	313.7	9.09
This work	319.2	9.70

Table 4.2 List of CO_2 critical temperatures and pressures predicted by the SL parameters of each group. The experimentally measured critical point is 304.2K at 7.38MPa [3, 16].

4.1.3 Comparison of literature parameter sets

The variability of parameter sets in the literature is in part the result of different parameter estimation practices. For example, Pottiger and Laurence [97] note that the fitting procedure employed by Zoller [141] favours a fit to the zero-pressure isotherms at the expense of agreement at high pressures. Kilpatrick and Chang [58] determine parameters from experimental vapour-pressure data, consequently limiting the fit to the pressure and temperature range between the triple-point and the critical point. In yet another approach, Hariharan et al. [45] determine parameters from the critical temperature as well as the liquid density, vapour density, and heat of vapourization at a single arbitrarily chosen point on the coexistence curve. For Xiong and Kiran [138], while the fitting procedure employed is not explicitly described, the source of the experimental data is stated to be PVT data over the temperature and pressure range given in table 4.1. One of the most common methods for parameter estimation is the use of nonlinear least-squares fitting, as discussed in Section 3.9.

Regardless of method, it is common practice to determine SL parameters only for the thermodynamic range being considered for a given application. For this reason, many

of the parameter sets in the literature for CO_2 were determined from data in a limited thermodynamic range. While this practice may not be detrimental in linear least-squares fitting procedures, provided sufficient numbers of data points, nonlinear fitting requires additional vigilance [125, 126]. In particular, great care should be taken when extrapolating the results of nonlinear least squares fits, since features outside of the range from which parameters were determined may be poorly described [125, 126]. Through the use of Monte-Carlo techniques applied to chemical kinetic models, Vidaurre et al. [125] find that uncertainty caused by incomplete data sets has a significant effect on the robustness of the resulting parameters. A simplified contrived example of this nonlinear regression pitfall is found in Appendix B. While the issue of limited data sets is not unique to this group in particular, the parameter set of Kilpatrick and Chang [58], estimated from the pressure range of $0.51 - 7.4$ MPa and the temperature range from $216.6 - 304$ K, is used here for the purpose of illustration. Figure 4.1 compares theoretically predicted densities (lines) with experimental density (points) for CO_2 using the Kilpatrick and Chang set of parameters. The density isotherms and isobars are shown in figures 4.1a and 4.1b, and liquid-vapour coexistence curves are shown in figures 4.1c and 4.1d. Since the parameters were determined from vapour-pressure data, it is not surprising that the predicted vapour-liquid coexistence density curves of figures 4.1c and 4.1d agree well with experiment over their entire range. More importantly, it is clear from the single-phase density curves of figures 4.1a and 4.1b that density correlates well to experiment only within the considered thermodynamic range, diverging from experiment when extrapolated.

Even though the SL theory has the capacity to predict the critical point of a fluid, the use of the mean field *random mixture* assumption implies that one would not expect accurate predictions, as discussed in Section 2.4.2. A list of critical temperatures T_c and pressures P_c predicted from the literature parameter sets is found in table 4.2. In nearly all cases, the theory predicts a critical point higher than the accepted experimentally determined values 304.2 K and 7.38 MPa. The exceptions to this observation seem to be the parameter sets proposed by Kilpatrick and Chang [58], Pope et al. [95], and Hariharan et al. [45], which predict the critical temperature with greater accuracy. This is to be expected for the Hariharan et al. parameters, as the critical temperature is used directly in the parameter estimation procedure [45]. This can also be explained for the Kilpatrick and Chang parameters, since the parameter estimation includes data near the critical point. The case of Pope et al. is not as clear, however, since confusion exists over the exact nature of the estimation procedure [45]. In all three cases, the parameters do not accurately predict the critical pressure, with the accurate estimation of the critical temperature coming at the expense of good agreement with experiment elsewhere. It should be noted that modifications to the SL-EOS do exist in the literature that allow for more accurate pre-

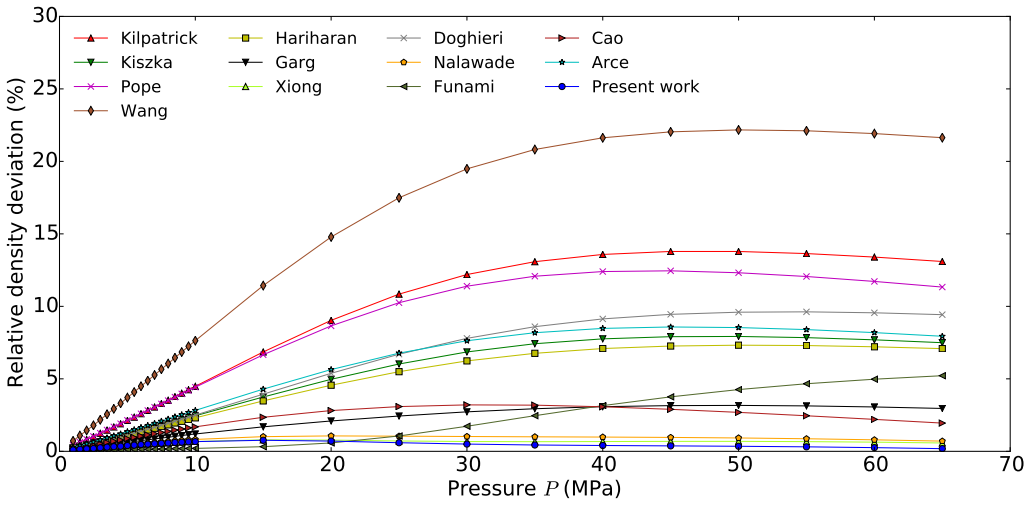

Figure 4.2 A comparison of relative density deviations between experiment and theory as functions of pressure at a temperature of 490 K for all sets of characteristic parameters given in table 4.1. The legend indicates the source for each parameter set [127].

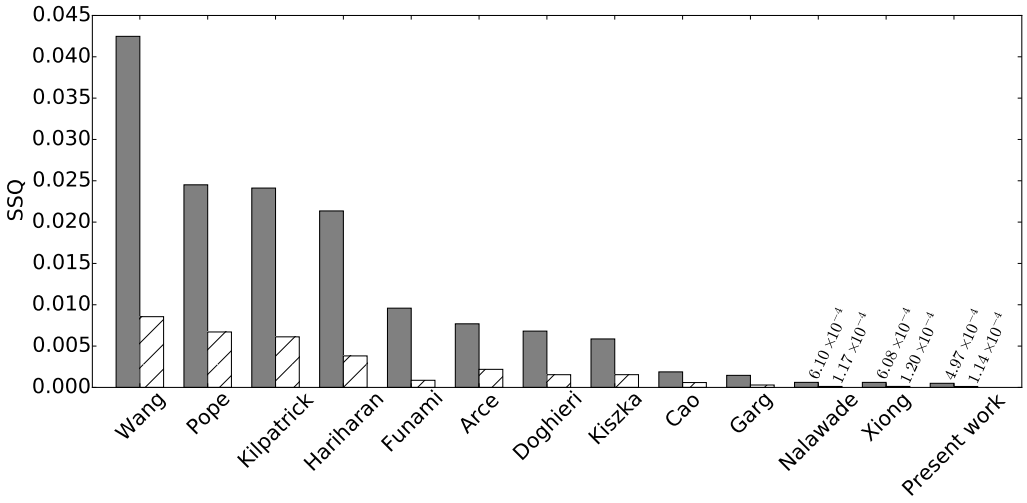

Figure 4.3 A comparison of the sum of the squares of the fractional deviation predicted by each set of SL parameters from experiment using the (filled) pressure-based measure given by equation 3.47 and the more standard (hashed) density-based measure given by equation 3.48 for all data points. The parameter sets that fit the data well are given in table 4.3 [127].

diction of critical temperature [37, 65, 93]. These necessitate, however, the abandonment of the connection between the parameters and the underlying molecular model.

4.1.4 Goodness of fit measure

A plot of the relative density deviation from experiment for each parameter set at 490 K is found in figure 4.2. Given that the nonlinear least-squares measure is minimized in order to achieve a fit, it is then the natural choice to be the measure of agreement with experimental data, known as "goodness of fit". Given that temperature and pressure are more easily controlled in a laboratory setting, and thus natural choices for independent variables, SSQ_ρ given by equation 3.48 has been a common choice for this measure. In order to minimize computational effort, as discussed in Section 3.9, the SSQ_P measure of equation 3.47 is instead used in the present work. Figure 4.3 shows both SSQ_ρ and SSQ_P for each parameter set over nearly the entire set of experimental data. Data within 15 K and 1.5 MPa of both the experimentally calculated and theoretically predicted critical points are excluded, as discussed in Section 3.9.

Comparison of figure 4.3 with table 4.1 shows that two groups, Xiong and Kiran [138] and Nalawade et al. [87], not only provide the best agreement with experiment as measured by goodness of fit, but also arrive at a similar sets of parameters. This conclusion is further indicated by the relative deviation shown in figure 4.2, which shows that these two groups have among the lowest density deviation overall. Moreover, it is clear that while there are minor differences between the two choices of goodness of fit measure, this conclusion remains unchanged regardless of whether SSQ_ρ or SSQ_P is chosen. This is taken to be justification for the choice of SSQ_P for goodness of fit.

Scrutiny of figure 4.3 and table 4.1 seems to imply that there is a correlation between the goodness of fit and the scope of the thermodynamic data used to obtain the parameters, with better agreement for parameters calculated using larger ranges. The exception to this observation is the parameter set found by Kilpatrick and Chang, which can be explained by the proximity of much of their experimental data to the critical point. Since PVT data in this region is not expected to correlate well to experiment, its inclusion is likely to worsen the resulting fit [127].

4.1.5 Parameter estimation procedure

The observations and conclusions made in Section 4.1.4 are used in the present section to propose a set of best practice parameter estimation procedures. These procedures are used

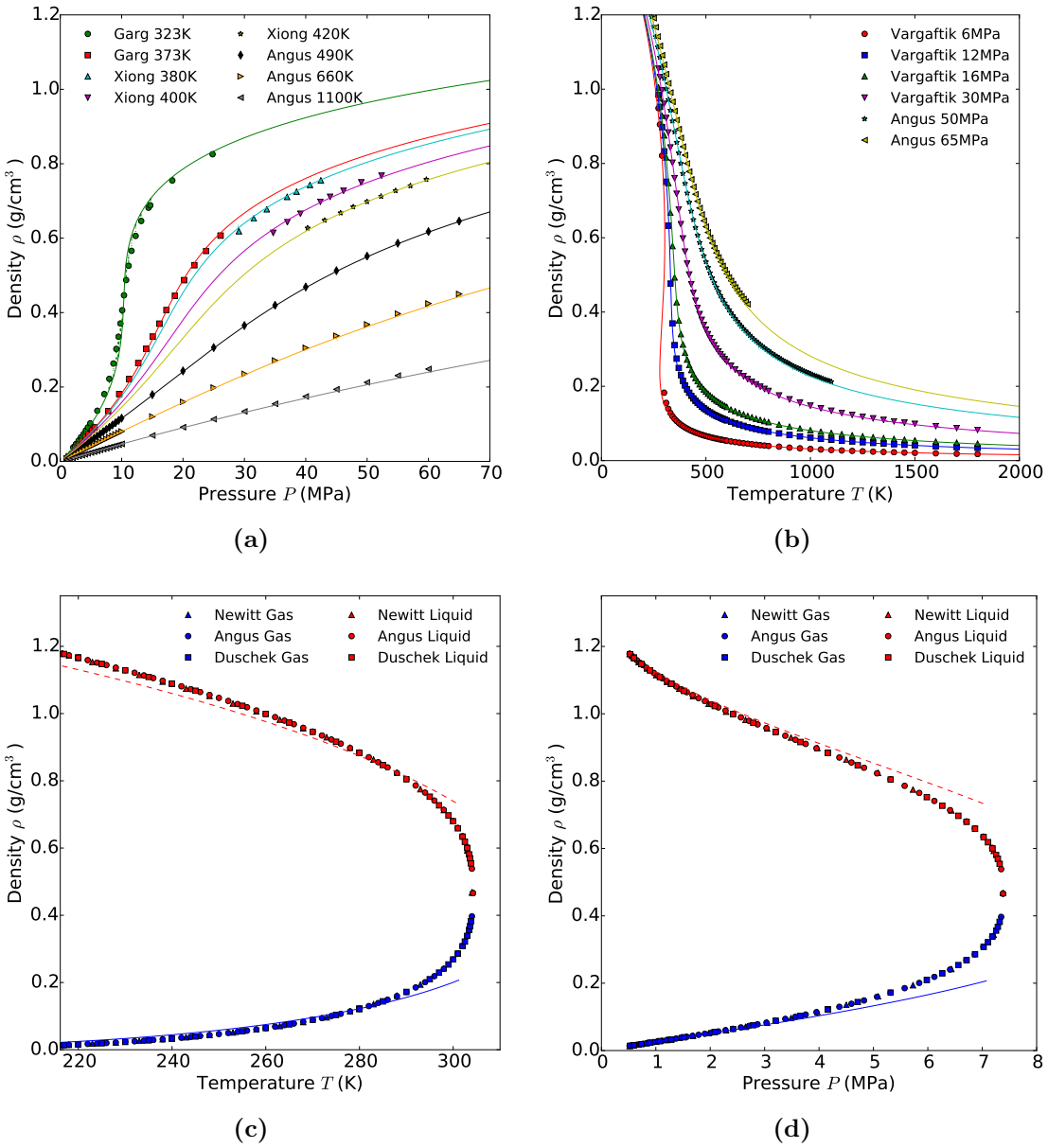

Figure 4.4 A comparison of (a) density-pressure isotherm, (b) density-temperature isobar, (c) saturated liquid-vapour density-temperature curve, and (d) density-pressure curve obtained using the parameters calculated in this work with the ones obtained experimentally. Lines represent predicted density while filled shapes represent experiment. The legends indicate the experimental sources [127].

Group	P^* (MPa)	T^* (K)	ρ^* (g/cm^3)	SSQ_P (10^{-4})
Xiong [138]	420.0	340.9	1.392	6.083
Nalawade [87]	427.7	338.7	1.4055	6.101
This work	**419.9**	**341.8**	**1.397**	**4.968**

Table 4.3 Sanchez-Lacombe pure fluid parameters for carbon dioxide that fit the experimentally determined thermodynamic data. Parameter choices that fit the entire range of data reasonably well fall roughly within ±8 MPa, ±3 K, and ±0.007 cm^3/g of each other but, due to the non-linear nature of the equation of state, not all parameter combinations that fall within these bounds will fit well.

to determine a set of parameters for CO_2, which are then contemplated in line with the literature parameters of the previous section.

Since parameters are estimated through comparison to experiment, it is necessary to establish how these properties are to be chosen. Internal degrees of freedom are deliberately not considered in the present theory, as discussed in Section 3.2. Therefore one would not expect the theory to correlate well to any thermodynamic property that depends on these degrees of freedom. More precisely, the present theory considers only the configurational partition function in the calculation of thermodynamic properties, strongly implying that only PVT and related experimental data should be included in the procedure. As previously discussed, inclusion of properties not well correlated may decrease the accuracy of the resulting parameters. Experimental data in the present work is composed of PVT data from the single-phase region of the equilibrium surface including the supercritical regime, saturated vapour pressure data, as well as liquid and vapour density data at coexistence taken from the literature [3, 22, 23, 36, 124, 138]. As previously discussed, the breakdown of the *random mixture* assumption near the critical point implies that this region does not correlate well to experiment. Data points over within 15 K and 1.5 MPa of both the experimentally determined and theoretically predicted critical points are excluded from consideration.

As previously discussed, particular care should be taken when estimating parameters using nonlinear regressions. Least square methods are famously sensitive to outliers, particularly in fits with limited numbers of data points [112]. In addition, the results of the optimization may also represent a local, rather than a global minimum [8, 125, 126], meriting caution during interpretation. The parameters in the present work are regressed from 556 data points over a temperature range of $216.58 - 1800$ K and a pressure range of $0.5 - 66.57$ MPa. A nonlinear least-squares parameter estimation procedure is employed, using a Levenberg-Marquardt algorithm to optimize the objective function given by equa-

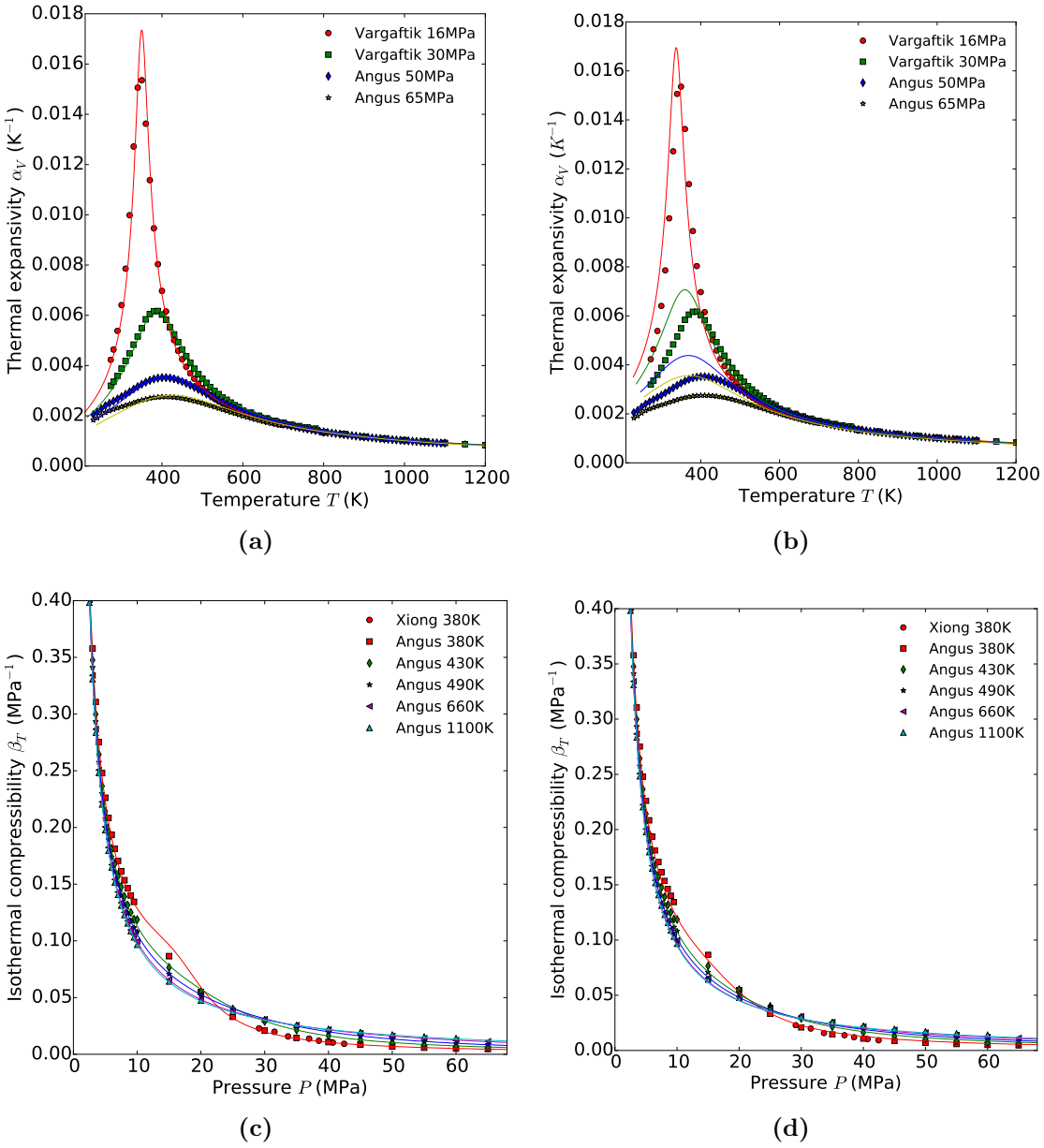

Figure 4.5 Thermal expansivity α_V as a function of temperature for a selection of pressures using (a) the characteristic parameters presented in this work, and (b) the characteristic parameters of Kilpatrick and Chang [58]. Isothermal compressibillity β_T as a function of pressure for a selection of temperatures using (c) the characteristic parameters presented in this work, and (d) the characteristic parameters of Kilpatrick and Chang. Symbols are experimental data from the sources indicated in the legends, and the solid lines are calculated from the SL-EOS [127].

tion 3.47.

This procedure results in the set of characteristic parameters P^* = 419.9 MPa, T^* = 341.8 K, ρ^* = 1.397 g/cm^3, agreeing closely those of Xiong and Kiran and Nalawade et al., with all parameter sets falling roughly within ±8 MPa, ±3 K, and ±0.007 g/cm^3. Table 4.3 compares the parameter sets that fit the data well, as well as their goodness of fit. In order to provide further validation of the present procedure, it is prudent to verify the correlation qualitatively. This helps to ensure that the resulting parameters are not the result of a local minimum, should one exist. Figures 4.4 compares the single phase region density curves (4.4a and 4.4b) and the liquid-vapour coexistence curves (4.4c and 4.4d) with experiment. The theoretical density curves agree very well with experiment over the entire temperature and pressure range, in contradiction of the conventional wisdom, except near the critical point where the theory is expected to diverge from experiment. The agreement of the present parameters with those of Xiong and Kiran and Nalawade et al., the comparatively small goodness of fit measures of the same in table 4.3, as well as the qualitative agreement with experiment in figure 4.4 are together taken as validation of the presently considered parameter estimation procedure.

4.1.6 Correlation with experiment

Deiters and de Reuck prescribe a set of considerations that should be taken by authors publishing a new equation of state [19]. Their remarks are motivated by the desire to have new equations of state considered not just for the often narrow application for which they where derived, but rather for all relevant applications [19]. To this end, Deiters and de Reuck recommend that authors discuss the limits of applicability, the quantities expected to correlate with experiment, the predictions that can be made, as well as other considerations [19]. While not strictly a new equation of state, the present theory merits such a discussion. To avoid excessive repetition, this section makes explicit only those considerations that have not already been addressed.

It has already been mentioned that quantities directly related to PVT properties are expected to correlate well with experiment. This implies that thermal expansivity α_V and isothermal compressibility β_T are expected to be predicted by the theory with some accuracy. Figure 4.5 compares the thermal expansivity and isothermal compressibility predicted by the theory with experiment. The predictions made using the parameters of the present work, figures 4.5a and 4.5c, agree with experiment better than those made by Kilpatrick and Chang, figures 4.5b and 4.5d. The cause of the small overshoot and bump generated by the present parameters in the thermal expansivity and isothermal

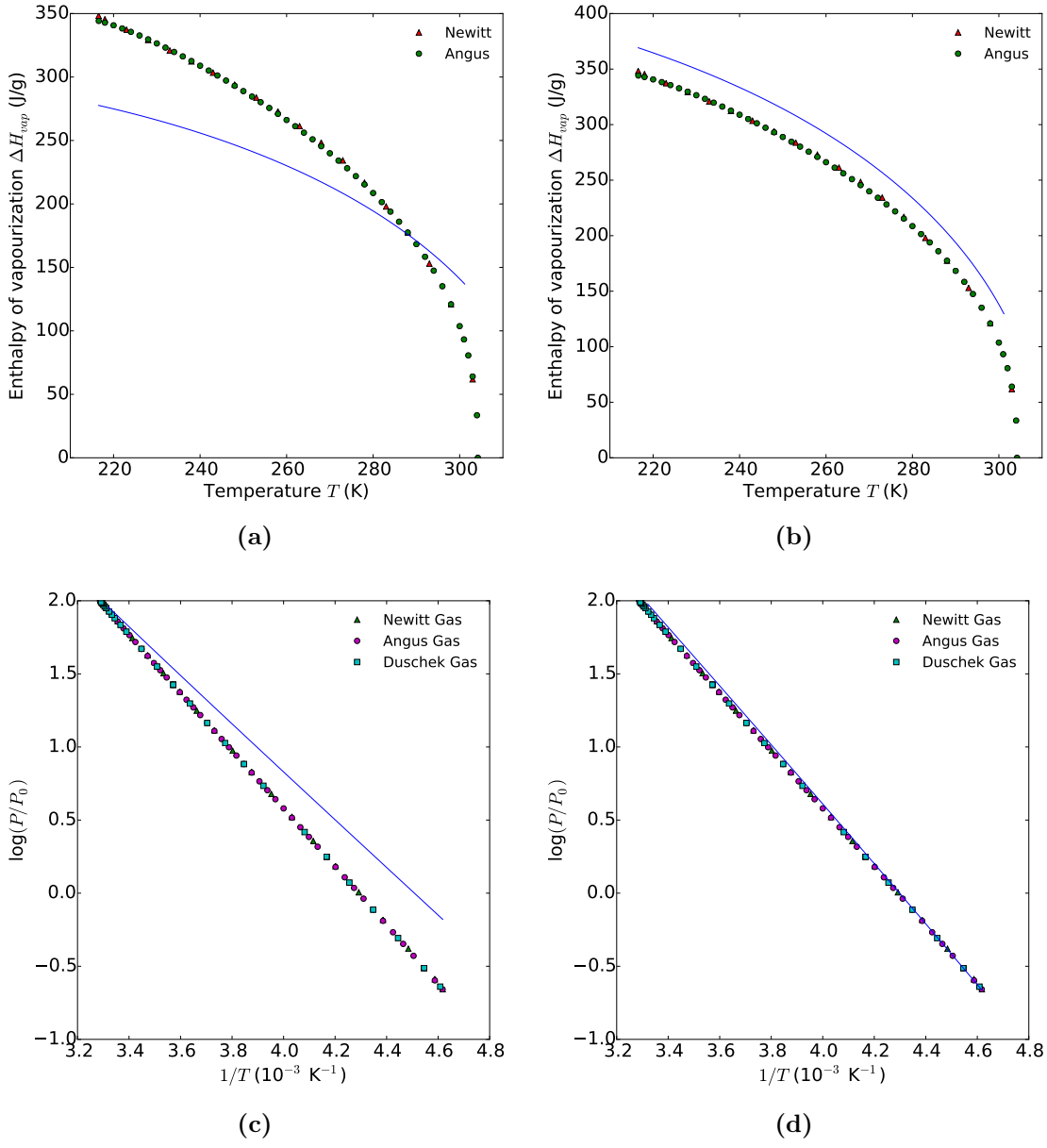

Figure 4.6 Enthalpy of vapourization as a function of temperature using (a) the characteristic parameters presented in this work, and (b) the characteristic parameters of Kilpatrick and Chang [58]. Logarithm of vapour pressure as a function of inverse temperature using (c) the characteristic parameters presented in this work, and (d) the characteristic parameters of Kilpatrick and Chang. Symbols are experimental data from the sources indicated in the legends, and the solid lines are fits using the SL-EOS [127].

compressibility, respectively, is not presently clear [127]. Figure 4.6 shows the plots of enthalpy of vapourization and the logarithm of vapour-pressure compared with experiment [127]. In this case, the Kilpatrick and Chang parameters perform better than those of the present work. This can be attributed to the proximity of the critical point, since these quantities are only defined in the narrow temperature and pressure range between the triple and critical points. The excellent performance of the Kilpatrick and Chang parameters on the vapour pressure curve is not surprising since they were regressed using this property over this range.

Since the model deliberately does not consider internal degrees of freedom, as previously mentioned, thermodynamic properties related to these degrees of freedom would not be expected to correlate well. This implies that both isochoric and isobaric heat capacities c_V and c_P, as well as the Joule-Thomson inversion curve are not expected to be predicted by the theory with any accuracy. In addition, while the majority of materials considered in the present work correlate extremely well to experimental PVT data, there are some notable exceptions. Both LDPE and N_2 do not achieve the same level of success as the other pure fluids. In both cases, the regressions produce quantitatively satisfactory correlations with experiment, but fail to accurately reproduce the experimentally observed PVT curves. The reason for the relatively poorer fits for these materials is not presently known.

Figure 4.7 shows the comparison of the second virial coefficient B predicted by the theory with those determined experimentally. The curve calculated from the present parameters perform better than those of Kilpatrick and Chang overall. The present predictions do, however, deviate as expected approaching the critical point.

4.2 Characteristic parameters of other fluids

Given its success for CO_2, the parameter estimation procedure proposed in 4.1.5 is applied to other fluids. Table 4.4 lists the characteristic parameters for dimethyl ether (DME), low-density polyethylene (LDPE), nitrogen gas (N_2), polylactide (PLA), linear polypropylene (LPP), branched polypropylene (BPP), and polysterene (PS) as well as the sources of experimental data.

Since many residual equation of state effects are absorbed into the hole volume, it is not immediately clear *a priori* whether closely related polymer species can be represented by a single parameter set, or rather if different sets of parameters are indicated. This must be determined *a posteriori* by comparison with experiment. For example, linear and branched polypropylene are composed of the same repeating chemical units, albeit with

Pure fluid	P^* (MPa)	T^* (K)	ρ^* (g/cm^3)	P (MPa)	T (K)	Data source (ref.)
CO_2	419.9	341.8	1.397	0.5 – 66.57	216.58 – 1800.0	refer to 127
DME	313.8	450.0	0.8146	0.01 – 164.8	423.0 – 543.0	136
LDPE	407.5	586.6	0.9271	0.01 – 0.927	393.0 – 453.0	46
N_2	178.5	103.7	1.128	0.01 – 1000.0	135.0 – 650.0	3,115
PLA	598.4	617.3	1.347	0.1 – 200.0	453.4 – 493.3	111
BPP	356.4	656.0	0.8950	0.5 – 65.0	453.0 – 493.0	72
LPP	316.2	662.8	0.8685	0.5 – 65.0	453.0 – 493.0	72
PS	421.8	687.8	1.118	0.01 – 200.0	402.65 – 524.45	142

Table 4.4 A list of the pure fluid characteristic parameters determined from experimental PVT data. The sources of the experimental data are indicated in the last column.

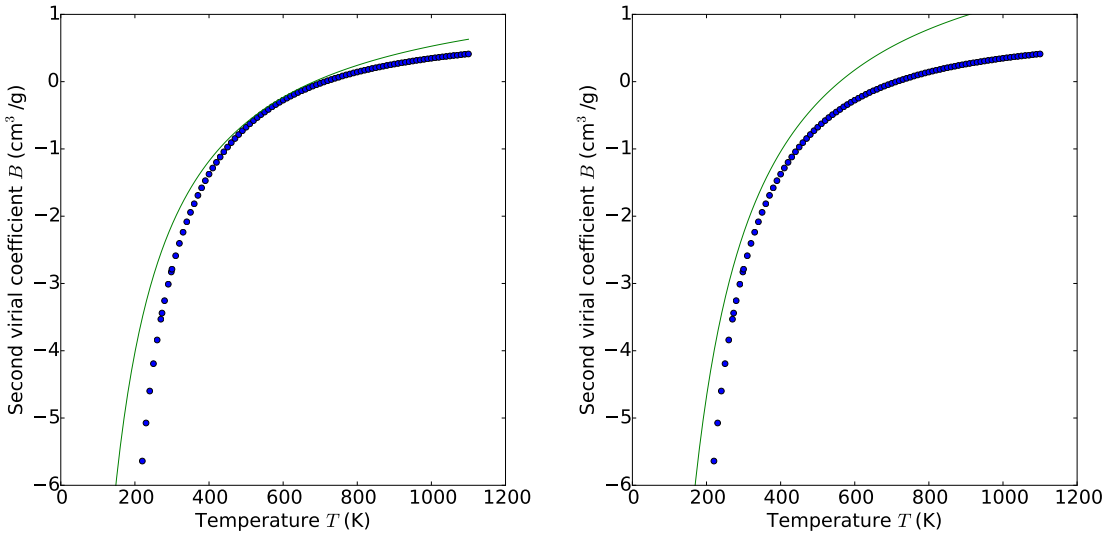

Figure 4.7 Second virial coefficient as a function of temperature using (a) the characteristic parameters presented in this work, and (b) the characteristic parameters of Kilpatrick and Chang [58]. Symbols are experimental results compiled by Angus et al. [3], and the solid lines are fits using the SL expression for B [127].

different network properties. A comparison of experimentally derived PVT data [72] for the two species shows slight differences in their equilibrium properties, as shown in figure 4.8. Indeed, a single pure fluid parameter set for both fluids fails to yield satisfactory results. Instead, two different parameter sets, one for LPP and one for BPP, were determined independently from the pure fluid PVT data of each species, the molecular parameters of which are found in table 4.5. A comparison of the interaction energies ϵ of the two species shows remarkable agreement ($\sim 1\%$). The close-packed specific volumes of the pure fluids also agree very closely ($\sim 3\%$). The difference in density behaviour observed in figures 4.8 may then be attributed to the differences in hole volume, which are much larger ($\sim 14\%$). The figure shows that the two parameter sets agree well with experiment.

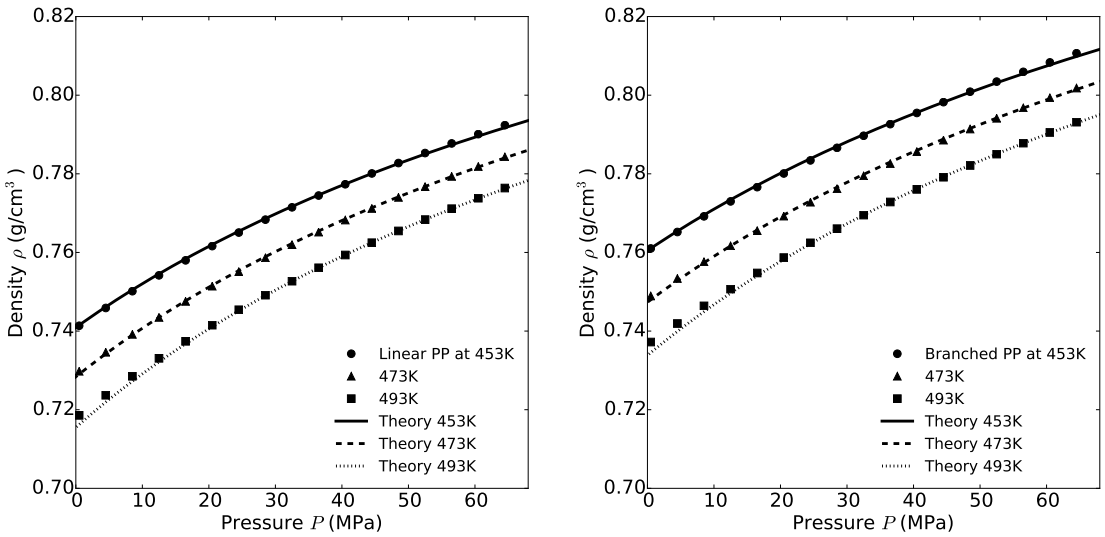

Figure 4.8 A comparison of experimental and theoretical density isotherms for (a) linear polypropylene (LPP) and (b) branched polypropylene (BPP). Points are experimental data and lines are fits based on the present theory as denoted by the legends. Points were obtained from an empirical density equation derived from experiment [72].

Fluid	ϵ (10^{-21} J)	v_0 (10^{-24} cm^3)	Nv/M (cm^3/g)
BPP	9.057	25.41	1.117
LPP	9.151 (1.03%)	28.94 (13.9%)	1.151 (3.04%)

Table 4.5 The independently derived pure fluid molecular parameters for both linear polypropylene (LPP) and branched polypropylene (BPP) calculated by fitting the present theory to experimental PVT data. The data was obtained from separate empirical equations derived from experimental data of the two materials [72]. Percentages indicate the deviation of the LPP parameters from those of BPP.

Chapter 5

Application to saturated polymer-solvent mixtures

5.1 Saturated binary polymer-solvent mixtures

The purpose of this section is to apply the polymeric mixture theory outlined in Section 3.5 to polymeric mixtures that include one or more solvent species. In keeping with the use of the term in Chapters 2 and 3, a solvent molecule in a polymeric mixture is taken to be one that is much smaller in size than the surrounding macromolecules. Mixtures of this type are of particular importance to the polymer foaming industry, as discussed in Section 2.2. The mixtures considered in this section are taken to be in two-phase coexistence, with a solvent-rich phase containing no polymer in thermal, mechanical, and diffusive equilibrium with a polymer-solvent mixture phase, as considered in Section 3.10.

5.1.1 Characteristic mixture parameters

The binary interactions $\{\epsilon_{ij}\}$ where $i \neq j$ are characteristic of the mixture, ideally being derived from experimental data obtained from each binary i/j mixture. For convenience, the present work characterizes binary interactions using a dimensionless parameter defined as the ratio of the binary interaction energy to the geometric mean of the corresponding pair of pure fluid interaction energies [128] given by the equation

$$\zeta_{ij} \equiv \frac{\epsilon_{ij}}{\left(\epsilon_{ii}\epsilon_{jj}\right)^{\frac{1}{2}}}. \tag{5.1}$$

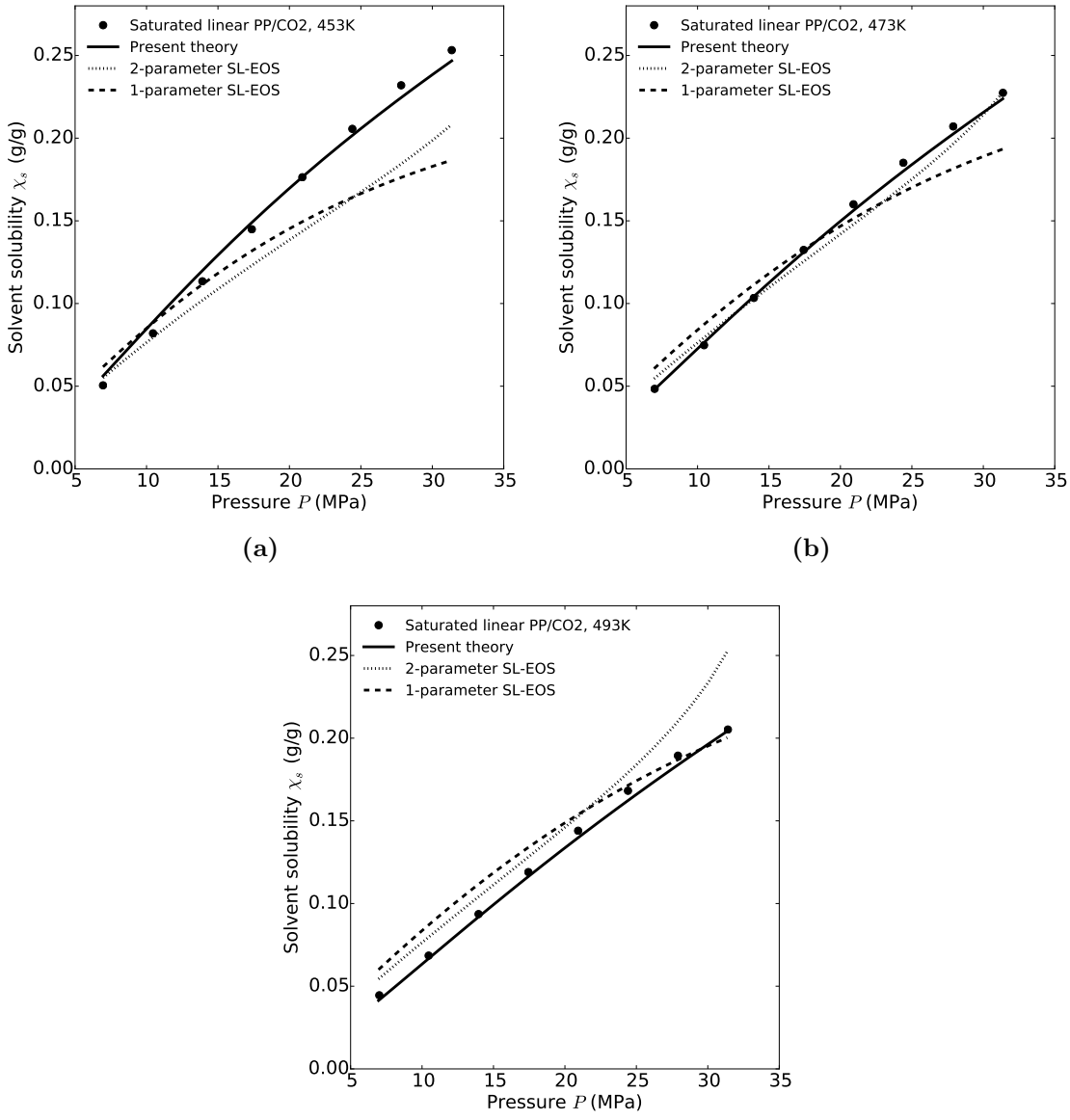

Figure 5.1 Solubility data for linear PP-CO2 mixtures at saturation at temperature (a) 453 K (b) 473 K and (c) 493 K. Points are experimental data and lines are various theoretical fits denoted by the legends [128].

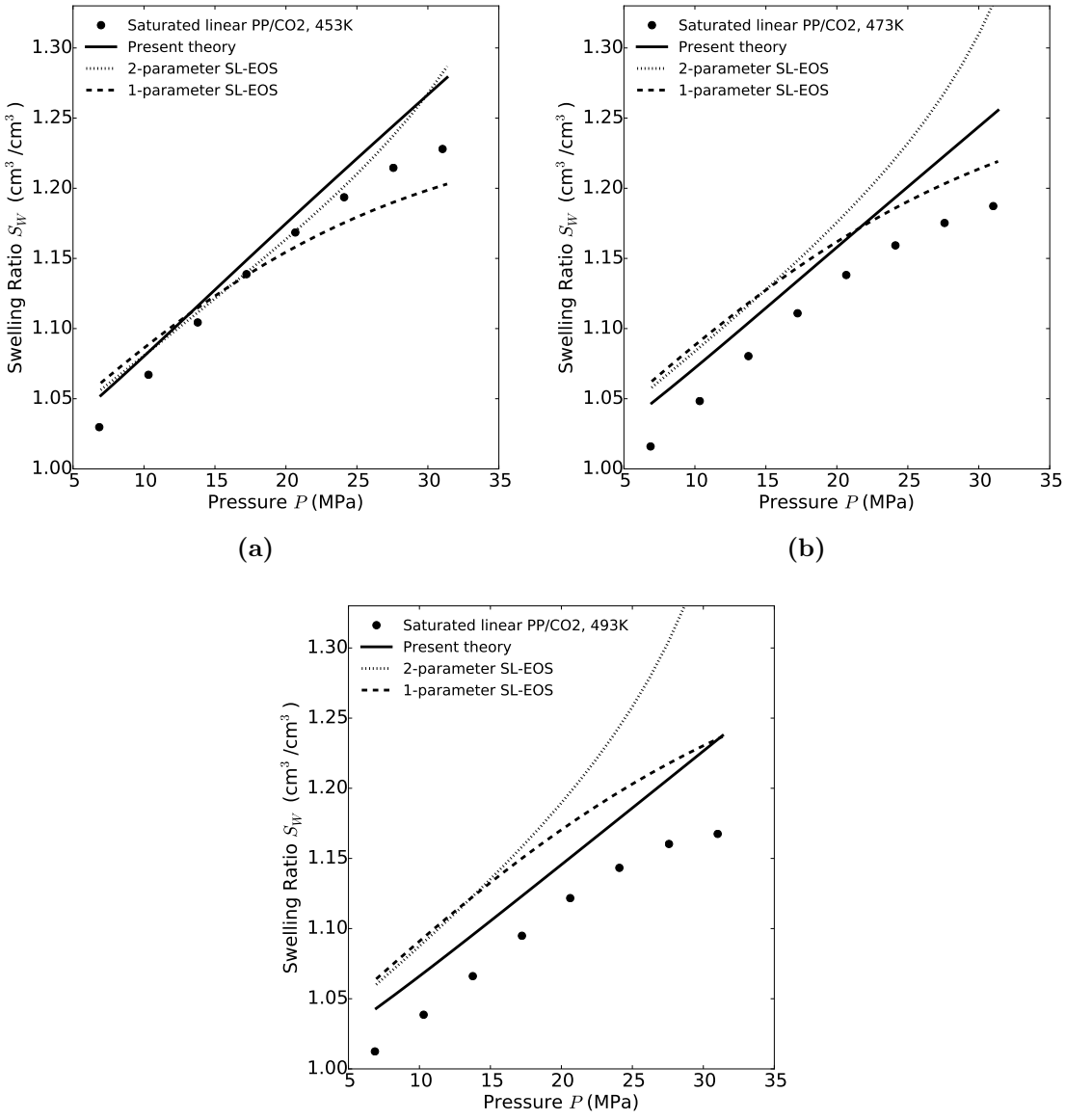

Figure 5.2 Swelling data for linear PP-CO2 mixtures at saturation at temperature (a) 453 K (b) 473 K and (c) 493 K. Points are experimental data and lines are various theoretical fits denoted by the legends [128].

Mixtures are fully characterized by the set of pure fluid interactions $\{\epsilon_{ii}\}$ and relative volumes $\{\alpha_i\}$, properly translated into the mixture as per Section 3.8, as well as the set of binary interaction parameters $\{\zeta_{ij}\}$ and the mixture hole volume v_0. It should be noted that since the pure fluid hole volumes do not enter into the mixture theory, the full set of three pure component characteristic parameters contains extraneous information. Therefore, the pure components can equivalently contribute the sets $\{T_i^*\}$ and $\{\rho_i^*\}$ to the mixture, with the redundant set of parameters $\{P_i^*\}$ being discarded. The mixture hole volume is assumed to be constant and unique to each saturated mixture, as discussed in Section 3.7.

5.1.2 Experimental data and parameter estimation

In the polymer foaming industry, observable polymer-solvent mixture data often takes the form of solubility, given by equation 3.53, and volume swelling, given by equation 3.55. For a mixture containing multiple solvent species, the solubility is defined as the sum of the individual solvent solubilities. In this way, the solubility of a mixture containing multiple solvents is the total mass fraction of solvent in the saturated mixture. Mixture parameters ζ_{ij} and v_0 are regressed from experimental solubility data using the least-squares measure given by equation 3.49. Just as in the pure fluid case, a Levenberg-Marquardt algorithm is used to determine the set of parameters that best fits the experimental observation [83].

5.1.3 Binary LPP/CO_2 and BPP/CO_2 mixtures

Figures 5.1 - 5.4 compare the solubility and swelling predictions made by the present theory, a 1-parameter SL theory, and a 2-parameter SL theory with experiment for saturated LPP/CO_2 and BPP/CO_2 mixtures [128]. Experimental solubility and swelling data was taken from Hasan et al. [47]. Parameters were regressed from experimental solubility data only. Regressions using only swelling data as well as regressions compromising between fits to solubility data and swelling data were performed, but were found to offer no improvement in agreement with experiment. The 1-parameter SL theory refers to the SL-EOS with only one mixture parameter found in the energetic mixing rule, with the volumetric mixing rule taken to be the linear mixing rule outlined in the 1978 formulation found in table 2.5 [105]. The 2-parameter SL theory replaces the volumetric mixing rule with the one proposed by Poser and Sanchez [96].

The mixture parameters are regressed using a constant set of parameters over all temperatures and pressures. The resulting mixture parameters are found in table 5.1. The solubility predictions made using the present theory, seen in figures 5.1 and 5.3 as a solid

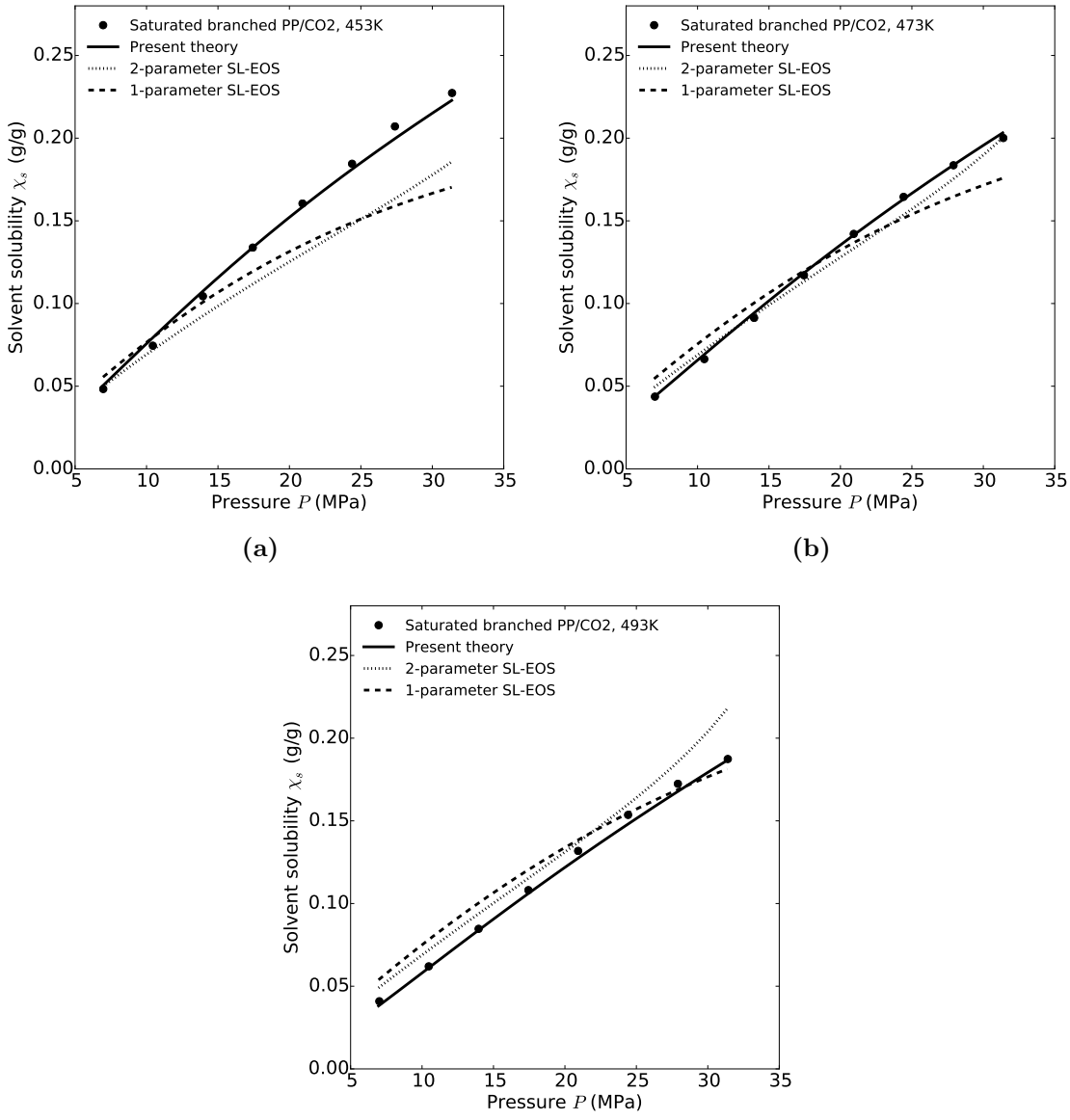

Figure 5.3 Solubility data for branched PP-CO2 mixtures at saturation at temperature (a) 453 K (b) 473 K and (c) 493 K. Points are experimental data and lines are various theoretical fits denoted by the legends [128].

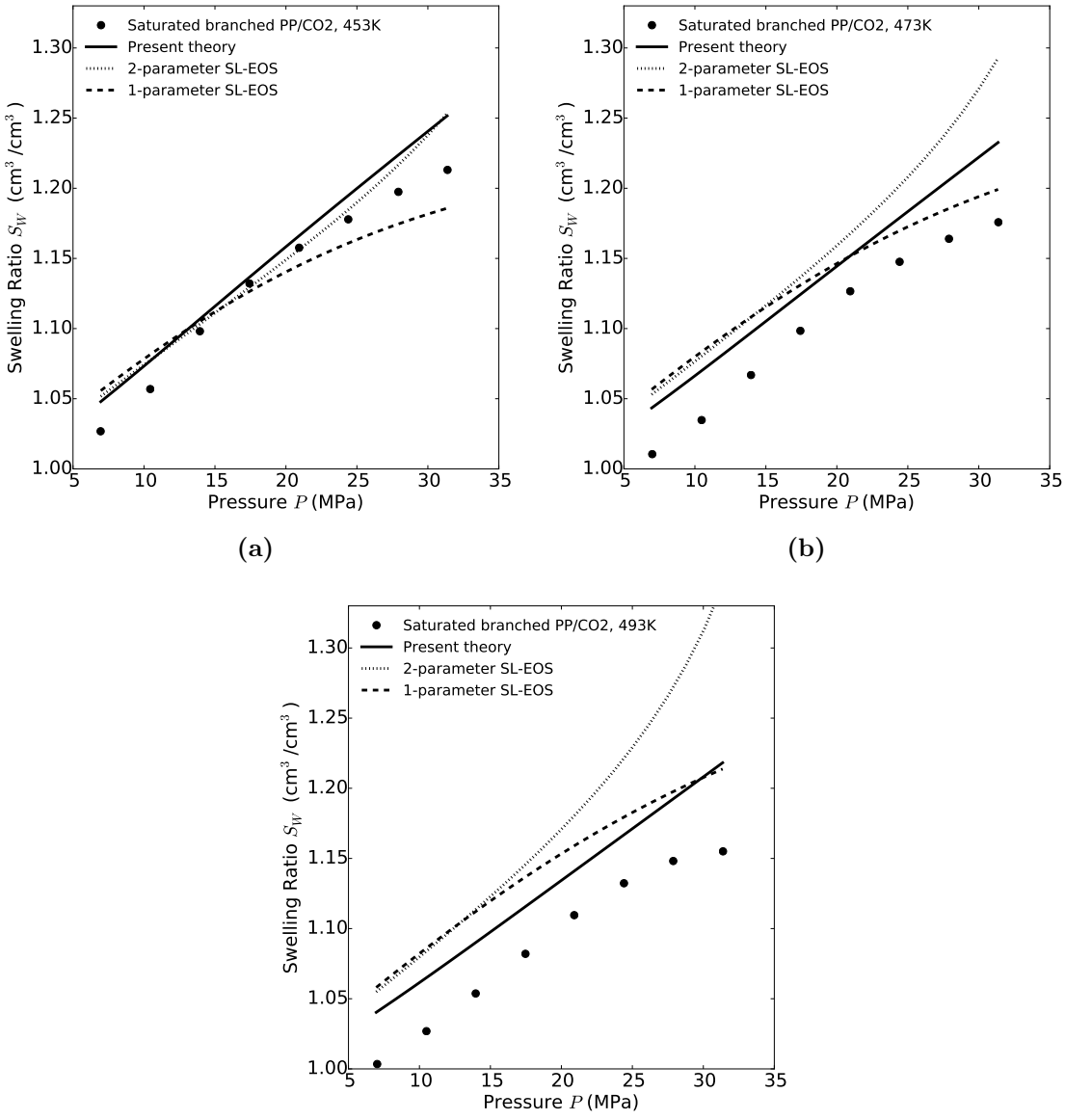

Figure 5.4 Swelling data for branched PP-CO2 mixtures at saturation at temperature (a) 453 K (b) 473 K and (c) 493 K. Points are experimental data and lines are various theoretical fits denoted by the legends [128].

MIXTURE	ζ	v_0 (10^{-24} cm^3)	ζ_{2SL}	δ_{2SL}	ζ_{1SL}
LPP/CO_2	1.110	8.436	0.7244	0.1858	0.7571
BPP/CO_2	1.091	8.646	0.7398	0.1728	0.7709

Table 5.1 Mixture parameters for the present method (ζ, v_0), the two parameter SL-EOS (ζ_{2SL},δ_{2SL}), and one-parameter SL-EOS (ζ_{1SL}).

line, agree with experiment much better at all temperatures than either the 1- or 2- parameter SL theory for both linear- and branched- PP, represented by the broken lines.

As discussed in Section 3.7, comparison of the hole volume in the mixture and the hole volume in the solvent phase is needed to justify the inconsistent comparison of two phases with different hole volumes. The volume of a hole in the pure CO_2 fluid $v_0^{CO_2} = 1.124\times10^{-23}$ cm^3 is relatively similar to the hole volume in the LPP/CO_2 mixture $v_0^{mix} = 8.436 \times 10^{-24}$ cm^3. The same is true for the BPP/CO_2 mixture, with hole volume $v_0^{mix} = 8.646\times10^{-24}$ cm^3. This serves to justify the equilibrium calculation between the two phases for both mixtures. The surprisingly good agreement of the present constant hole volume approach, coupled with the unsatisfactory fits provided by the volumetric mixing-rule-based theories, would suggest that the inconsistencies introduced by mixing rules are not similarly justifiable.

While solubility calculations rely only on equilibrium calculations performed between the solvent-rich phase and the mixture phase, swelling calculations involve consideration of three phases. Given that swelling calculations consider the pure polymer phase in addition to those in diffusive equilibrium, one would expect the inconsistency issue to be amplified for this property. Indeed, the comparison of predicted and experimental swelling found in figures 5.2 and 5.4 show considerably less agreement for the present theory, again represented by the solid line. The present theory with constant hole volume, more importantly, fails to capture the slight concavity of the experimental swelling curve [128]. Nevertheless, despite the consistent overestimate of the swelling, the present theory provides better than order-of-magnitude quantitative predictions [128].

On the other hand, the volumetric mixing-rule-based theories, represented by the broken lines, provide much less satisfactory predictions. Since these theories limit to the correct hole volumes for the pure fluids, the poor performance is presumably then the result of the inherent inconsistencies discussed in Section 3.7. Surprisingly, the 1-parameter SL theory performs competitively with that of the 2-parameter SL theory, providing better predictions in some cases. This would seem to imply that the correction to the linear mixing rules proposed by Poser and Sanchez is not appropriate in this case [128].

Mixture	ζ	v_0 (10^{-24} cm^3)	T^*_{PP}
LPP/CO_2	1.039 (6%)	7.745 (8%)	470.4 (29%)
BPP/CO_2	1.115 (2%)	7.719 (11%)	639.3 (3%)

Table 5.2 Mixture parameters for the present method (ζ, v_0) assuming the parameter T^*_{PP} is also unknown and is regressed from the mixture. Percentages in parenthesis indicate changes in values with respect to tables 4.4 and 5.5 where T^*_{PP} was known from pure component data.

5.1.4 Regression of pure parameters from the mixture

It should be possible to regress pure fluid parameters from the mixture. The purpose of this is twofold. Successful regression of a known set of pure fluid and mixture parameters provides additional validation of the present theory. As well, successful regression indicates that predictions could be made from a mixture for which the parameters of one of the pure components is not known.

In Section 5.1.1, it is mentioned that only two of the three pure parameters translate into mixture considerations in the present theory, since the volume of a hole in the pure fluid does not appear in the mixture. While this observation is true for general materials, special circumstances apply to large polymeric molecules. In polymer-solvent mixtures, the relative polymer volume appears only in factors of the form $\left(1 - \frac{1}{\alpha}\right)$, which approaches unity for molecules of macromolecular size. This implies that, for polymeric materials in such mixtures, only one pure component parameter is contributed to the mixture: only the characteristic parameter T^* or the molecular parameter ϵ_{ii}.

Figure 5.5 shows the fit produced by a regression of T^*_{PP}, ζ, and v_0 for both linear and branched PP at a single temperature of 453 K. The plot shows excellent agreement of the resulting fit with experiment. Table 5.2 shows the regressed parameters T^*_{PP}, ζ, and v_0 as well as their deviation with respect to the known values in the form of a percent. While some of this deviation is due to the inclusion of fewer data points, most is due to the removal of the additional constraint that the fit should agree with the pure fluid data [128]. In spite of the large deviation in T^*_{PP}, oddly found to deviate 29% for linear PP and 3% for branched PP, successful predictions can be made with these parameters. Figure 5.5 shows the comparison of predicted to experimental data using the parameters regressed in table 5.2 at 453 K, 473 K, and 493 K. The plots show excellent agreement with experiment for both linear and branched PP.

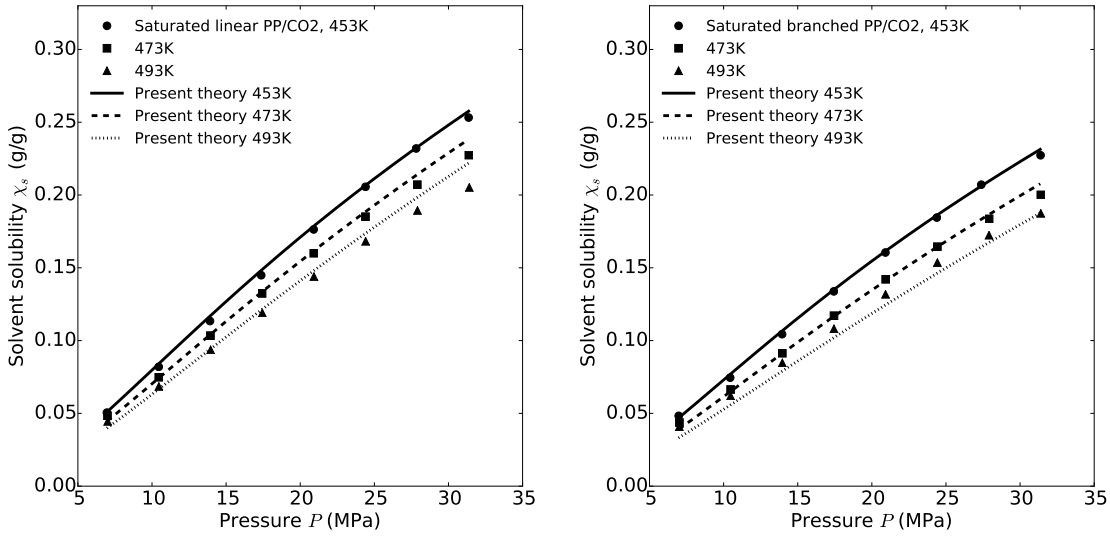

Figure 5.5 Solubility data for (a) linear and (b) branched PP-CO_2 mixtures at saturation at temperatures of 453 K, 473 K and 493 K as denoted by the legends. Points are experimental data and lines are theoretical fits for parameters ζ, v_0 and T^*_{PP} regressed at 453 K [128].

5.1.5 Binary PLA/CO_2 and LDPE/CO_2 mixtures

The same parameter estimation procedure as the one used for PP/CO_2 mixtures is applied to both PLA/CO_2 and LDPE/CO_2 saturated mixtures. The resulting fits are compared to experimental solubility and swelling for PLA/CO_2 in figures 5.6a and 5.6b and LDPE/CO_2 in figures 5.6c and 5.6d, respectively. Experimental data is obtained from Mahmood et al. [81] for PLA/CO_2 and Hasan [46] for LDPE/CO_2. As before, parameters are assumed to be constant over all temperatures and pressures. Pure fluid characteristic parameters for both PLA and LDPE are regressed from pure PVT data, with the parameters and the sources of data found in table 4.4. While both figures show that the predicted solubility produces good agreement with experiment, they encounter varied success in terms of swelling.

Despite good agreement overall, comparing figures 5.6a and 5.6c one notices a slight difference in the quality of the two predictions. While both predictions fall within the correct range, the PLA/CO_2 solubility predictions produce a better fit to the overall trend than those of LDPE/CO_2 [129]. The difference in the quality of the fits is likely not attributable to the difference in hole volumes between mixture and solvent. On the contrary, the hole volume disparity is greater for PLA than it is for LDPE. If this disparity were

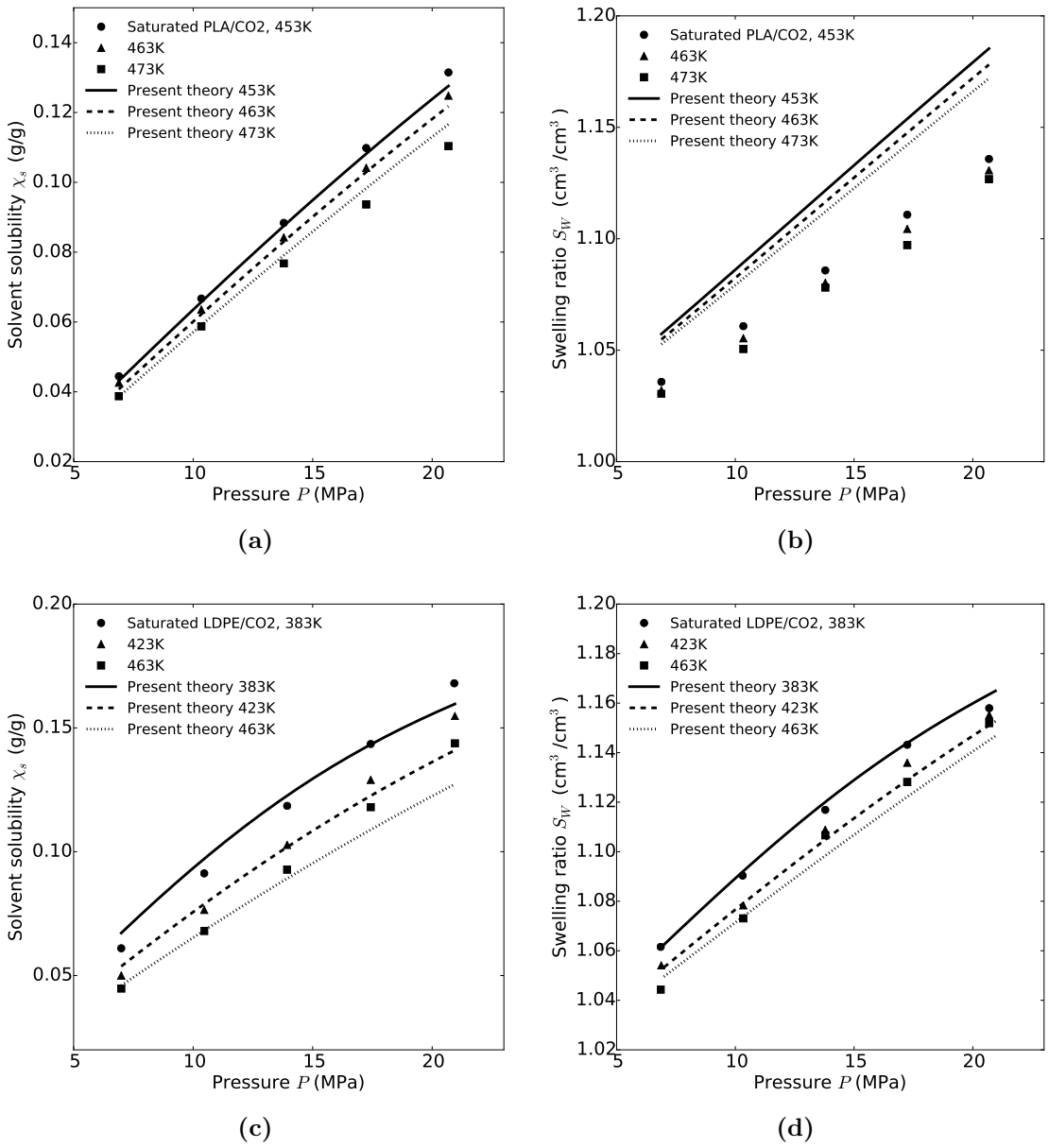

Figure 5.6 A comparison of experimental and theoretical (a) solubility and (b) swelling for saturated binary PLA/CO_2 mixtures at various temperatures. A comparison of experimental and theoretical (c) solubility and (d) swelling for saturated binary LDPE/CO_2 mixtures at various temperatures. Points are experimental data and lines are fits based on the present theory as denoted by the legends [129].

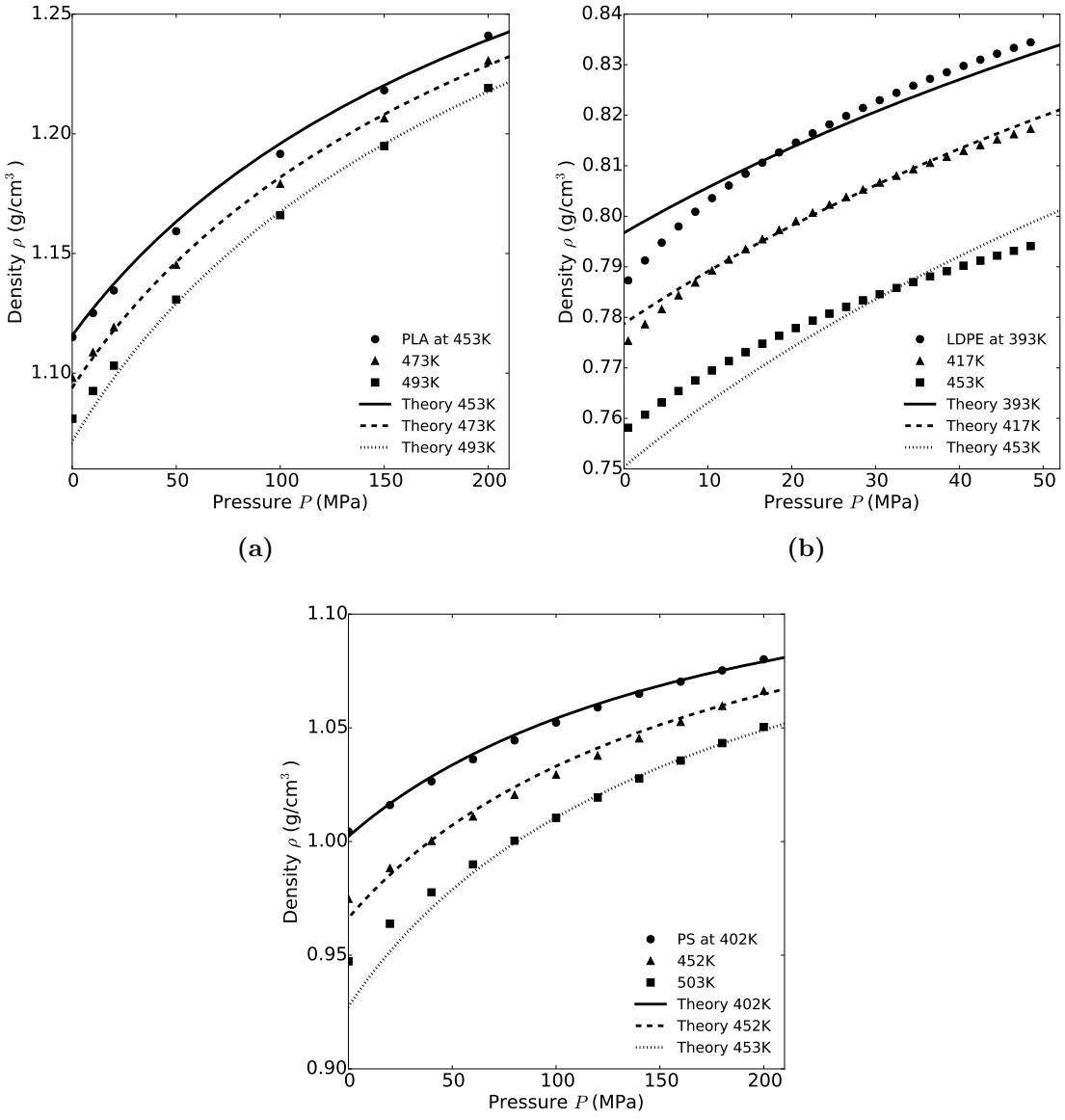

Figure 5.7 A comparison of experimental and theoretical density isotherms for (a) PLA, (b) LDPE, and (b) PS. Points are experimental data and lines are fits based on the present theory as denoted by the legends [129].

Fluid	v_0 (10^{-24}cm^3)
CO_2	11.24
PLA	14.24 (26.70%)
PLA/CO_2	9.883 (12.07%)
LDPE	19.87 (76.78%)
LDPE/CO_2	10.48 (8.30%)

Table 5.3 A comparison of the CO_2 hole volume to those of pure PLA and LDPE as well as saturated binary PLA/CO_2 and PLA/CO_2 mixtures.

solely responsible, one would expect a worse fit for linear and branched PP/CO_2 mixtures, which exhibit even larger differences. The hole volume disparity between pure polymer and mixture is also greatest between PP and PP/CO_2 for both linear and branched cases, seeming to confirm the irrelevance of this disparity to solubility calculations for saturated fluids, as postulated in Section 3.7.

A possible explanation is evident when cross referencing with figure 5.7, which compares the pure fluid PVT predictions made by the present theory with experiment for both PLA and LDPE. The sources of the experimental data are Sato et al. [111] for PLA and Hasan [46], with the resulting parameters found in table 4.4. The figure shows much better agreement for the PLA parameters than it does for the LDPE parameters. This is consistent with the observations by Bashir et al. [5] that the quality of the predictive power of the pure component parameters has a profound effect on the predictions made in the mixture.

Figures 5.6b and 5.6d compare swelling prediction for PLA/CO_2 and LDPE/CO_2 mixtures. While showing expectedly poor results for swelling of PLA mixtures, these figures seem to produce better than expected swelling for LDPE mixtures, despite the fact that swelling is not considered in the parameter estimation procedure. This result is all the more surprising since, as illustrated by table 5.3, the hole volume of PLA is much closer to that of CO_2 ($\sim$ 27%) than that of LDPE ($\sim$ 77%). Given the relative hole volume disparities, one would expect the swelling predictions made by PLA to perform better. This result remains so far unexplained [129].

5.2 Interpretation of the function of holes

The good agreement of the present theory with experiment provides validation for the constant hole volume assumption discussed in Section 3.7. It is possible to interpret this surprising success in terms of correlations. The holes, while not physically real, are artificially adjusted take on some "residual" PVT effects not directly considered in the molecular model. Specifically, the holes represent, in the molecular model, the spaces left behind in the material as segments move, in line with the more dynamical interpretation of holes in the free volume theories [33]. In this picture, if the segments were to move in correlated ways, then the tuning of the hole volume may reflect this [128]. It is therefore conceivable that, while the mean field assumption of the theory does not allow for physically real correlations, the holes function akin to an averaged correlation, if only in a rudimentary way [128]. This interpretation is consistent with the observations made about the pure fluid parameters found in Section 4.2.

Of course, correlations are not independent of temperature and pressure, with correlations increasing in importance in proximity to the critical point. Nonetheless, excluding data to a sufficient distance from the critical point, one would hope that these correlations could be represented by a single constant hole volume characteristic of a given pure fluid or mixture [128].

This interpretation of the function of holes does not hold in all regimes. In the dilute limit, where the system would be composed predominantly of holes, this interpretation is not justified [128]. It should be noted, however, that the SL-EOS with mixing rules is similarly not expected to hold in this regime: examination of the figure 3.1 shows that the hole volume is expected to take on multiple values at this single point.

A list of the hole volumes characteristic of the pure fluids and mixtures considered in the present work is found in table 5.4. Examination of the table reveals several possible patterns. For the pure fluids, the hole volumes associated with macromolecules tend to be larger than those of solvents [129]. In binary mixtures, the hole volume seems to be dominated by that of the solvent. In ternary systems that contain two species of solvent, the hole volume of the mixture appears to lie between those of the two solvents [129]. These observations could be used to greatly simplify the parameter estimation procedure if the hole volumes of the constituent species are compared beforehand.

It is worth noting that these observed patterns are not strictly adhered to, appearing to have their exceptions. Contrary to the observation that solvent hole volumes tend to be smaller than those of polymers, the hole volume associated with the solvent DME is larger than that of the polymer PLA and comparable to that of LDPE [129]. As well, it

	Fluid	v_0 (10^{-24}cm^3)
Pure fluid	CO_2	11.24
	DME	19.80
	LDPE	19.87
	N_2	8.021
	PLA	14.24
	BPP	25.41
	LPP	28.94
	PS	22.51
Binary mixture	LDPE/CO_2	10.48
	PLA/CO_2	9.883
	BPP/CO_2	8.646
	LPP/CO_2	8.436
	PS/CO_2	9.900
	PS/N_2	8.769
Ternary mixture	PS/CO_2+DME	16.74
	PS/CO_2+N_2	8.628

Table 5.4 A list of the hole volumes characteristic of each of the pure, binary mixture, and ternary mixture fluids.

is conceivable that for all mixtures, the hole volume of the mixture is dominated by the smallest hole volume among those of the pure components, with the hole volume of the ternary PS/CO_2+DME mixture as an exception [129]. Analysis of a larger set of pure fluids and mixtures would be needed to reduce the ambiguity in these patterns.

5.3 Temperature dependence of solubility

For the majority of polymer-solvent mixture studied to date, the solubility of the mixture decreases with temperature if pressure is held fixed [79, 110]. It has been noted, however, that for mixtures containing solvent molecules with a low critical point such as N_2, this temperature dependence is reversed [46]. As mentioned in Chapter 2, one of the purposes of statistical mechanics is to relate such behaviours to molecular considerations. The present

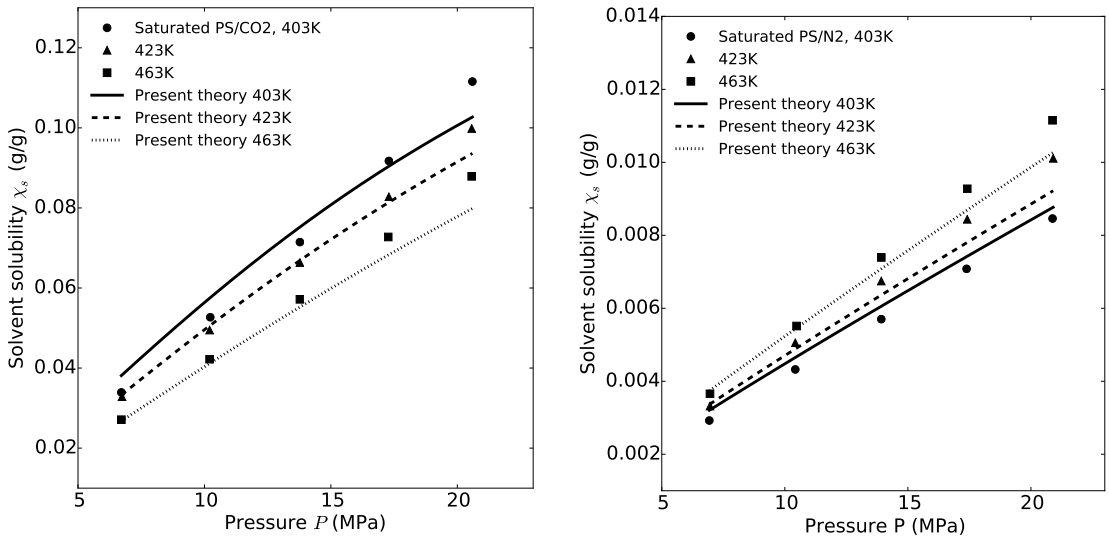

Figure 5.8 A comparison of experimental and theoretical solubility at various temperatures for saturated (a) PS/CO_2 and saturated (b) PS/N_2 mixtures. Points are experimental data and lines are fits based on the present theory as denoted by the legends [129].

section explores this possibility.

5.3.1 Binary PS/CO_2 and PS/N_2 mixtures

The reversed temperature dependence can be investigated using binary PS/CO_2 and PS/N_2 mixtures, since the critical temperature of CO_2 (304.2 K) is much higher than that of N_2 (126.2 K). Indeed, examination of figure 5.8 illustrates the reversed temperature dependence of the solubility. As before, predicted solubilities are represented by solid lines, while experimental data is represented by points. Experimental data is taken from Hasan [46].

The solubility of N_2 is much lower than that of CO_2, implying that CO_2 has a much greater affinity for PS. While the experimental solubility data for the PS/CO_2 mixture in figure 5.8a features a typical temperature dependence decreasing with temperature, the PS/N_2 in figure 5.8b features the reverse. Surprisingly, the theoretically predicted solubilities reproduce this behaviour, implying that whatever molecular considerations are responsible for this behaviour are included in the current model [129]. As such, it should be possible to trace this behaviour back to the source molecular features.

Binary mixture	ζ	v_0 (10^{-24} cm^3)	P (MPa)	T (K)	Data source
$LDPE/CO_2$	0.9680	10.48	7.0 – 21.0	383.0–463.0	46
PLA/CO_2	1.046	9.883	6.9 – 20.7	453.0–473.0	79
BPP/CO_2	1.091	8.646	7.0 – 31.4	453.0–493.0	46
LPP/CO_2	1.110	8.436	7.0 – 31.4	453.0–493.0	46
PS/CO_2	1.021	9.900	6.7 – 20.6	403.0–463.0	46
PS/N_2	1.346	8.769	6.9 – 20.9	403.0–463.0	46

Table 5.5 A list of the binary mixture parameters for each pair of mixture components and their corresponding sources of experimental data.

The temperature dependence of solubility as a function of a given parameter can be investigated by numerically calculating the partial derivative of solubility with respect to temperature in the neighbourhood of a thermodynamic state. The temperature dependence of the solubility is therefore given by $\left(\frac{\partial \chi_s}{\partial T}\right)$. Figure 5.9 plots the temperature dependence of solubility for a PS/N_2 mixture near 10 MPa and 423 K as a function of the mixture parameters ζ and v_0 in the neighbourhood of their actual values. Figure 5.9b shows that the temperature dependence does not change sign over the entire considered domain of v_0. On the contrary, figure 5.9b shows that as the strength of the binary interaction parameter is increased, the temperature dependence changes sign from positive to negative at a critical value. This result strongly suggests that the observed phenomenon is somehow related to the relative strength of the binary interaction. Future consideration might be given to calculating this temperature dependence exactly.

5.4 Saturated ternary polymer-co-solvent mixtures

5.4.1 System and experimental data

Ternary polymer-co-solvent mixtures involve the coexistence of a polymer-solvent mixture with a solvent-rich phase composed to two distinct solvent species. Typically, the solvent-rich phase contains a fixed composition. These mixtures have been of recent interest to polymer foaming applications due to recent postulation that such systems may increase the solubility of low-solubility solvents [80, 81]. Since these mixtures typically involve a

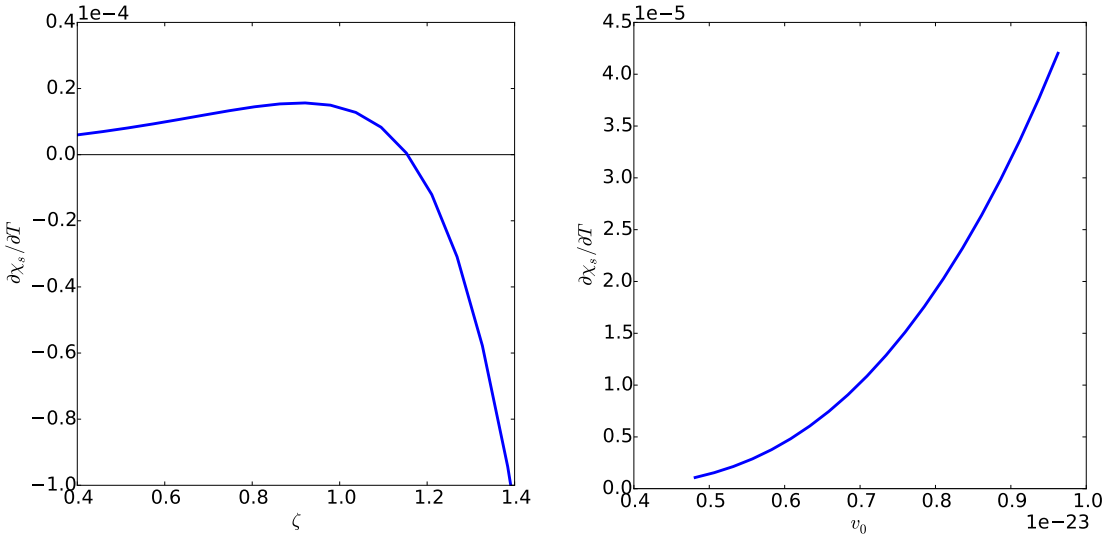

(a) **(b)**

Figure 5.9 Theoretically predicted partial derivatives of the solubility of a PS/N_2 mixture near 10 MPa and 423 K calculated as a function of the mixture parameter (a) ζ and (b) v_0.

solvent species of primary interest and a solvent species as used as plasticizer, these are referred to as solvent and co-solvent, respectively.

As mentioned in Section 3.10, solubility in higher order mixtures refers to the *total* mass fraction of solvent that can be dissolved into a saturated mixture. Referring to the solubility of a given species is taken to mean the mass fraction of that species alone. The solubility of such mixtures is then the sum of the solubilities of the individual solvents, as given by equation 3.54. The definition of swelling, as given by equation 3.55 does not require modification.

5.4.2 Ternary PS/CO_2+DME

Figure 5.10 shows the results of fitting the present theory to a ternary PS/CO_2+DME mixture. Pure fluid parameters are regressed from pure PVT data, with parameters and data sources found in table 4.4. Mixture parameters, which are regressed only from solubility data, are assumed to be constant for all temperatures and pressures. Experimental data was obtained from Mahmood et al. [80, 81]. Since extrapolation should be used with caution for nonlinear fitting, the parameter estimation includes as much of the equilibrium

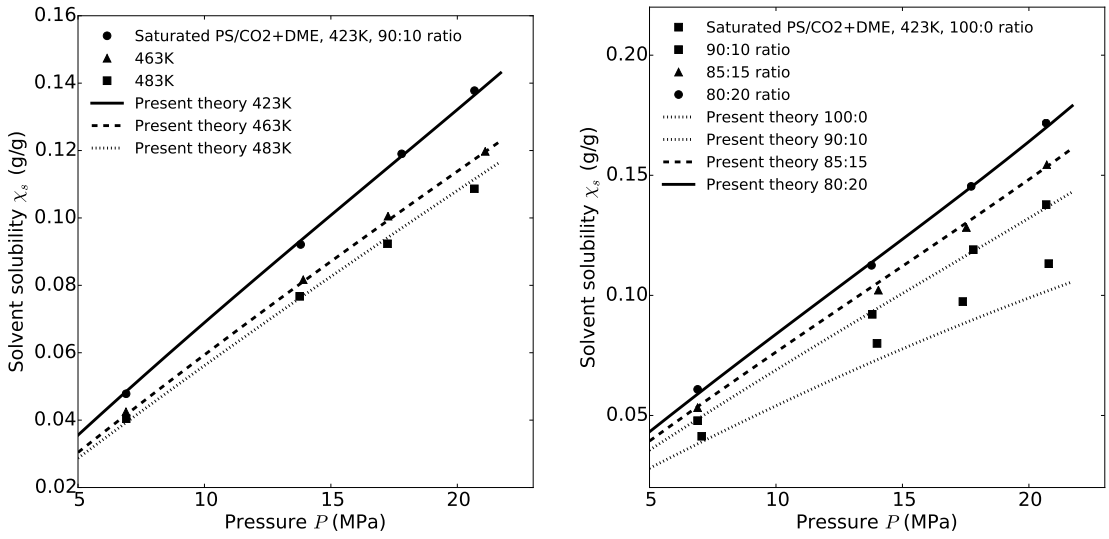

Figure 5.10 A comparison of experimental and theoretical gas solubility for saturated ternary PS/CO_2+DME mixtures at various (a) temperatures and (b) solvent ratios. A plot of theoretical CO_2 solubility (c) at various solvent ratios. Points are experimental data and lines are fits based on the present theory as denoted by the legends [129].

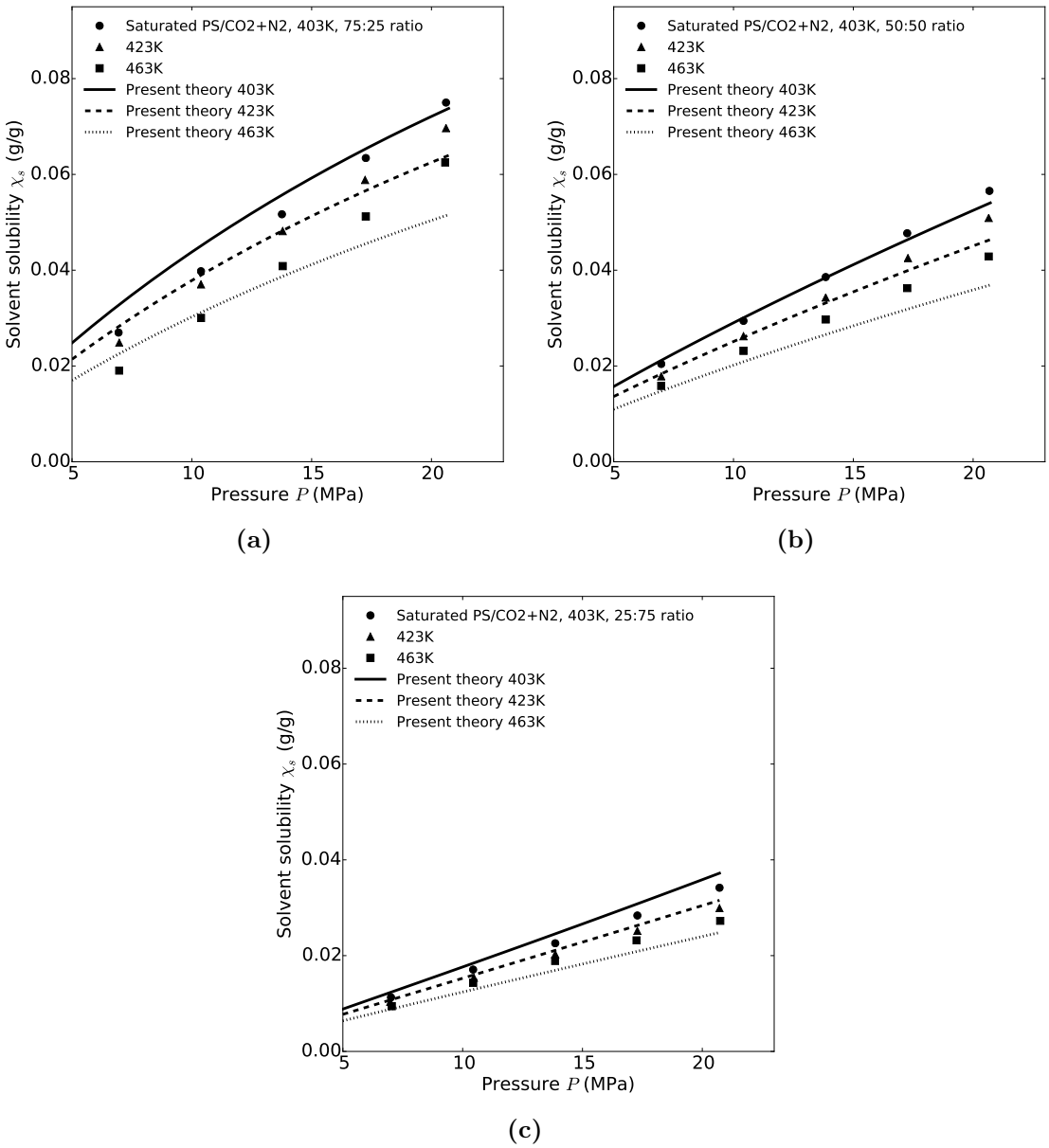

Figure 5.11 A comparison of experimental and theoretical solubility for saturated PS/CO_2+N_2 mixtures at various temperatures for CO_2:N_2 solvent ratios of (a) 75:25, (b) 50:50, and (c) 25:75. Points are experimental data and lines are fits based on the present theory as denoted by the legends [129].

surface as possible for a variety of solvent composition ratios, temperatures, and pressures.

In figure 5.10a, the predicted solubilities at a constant solvent:co-solvent ratio of 90:10 at 423 K, 463 K, and 483 K are compared with experiment. At all three temperatures, the present theory exhibits excellent agreement with experiment. Figure 5.10b compares theory with experiment at a fixed temperature of 423 K for CO_2:DME ratios of 100:0, 90:10, 85:15, and 80:20. While the agreement is excellent for the 90:10, 85:15, and 80:20 ratios, the 100:0 ratio appears to deviate from experiment, underestimating solubility significantly. This is likely attributable to the incorrect limiting of the hole volume at that ratio to the one regressed from the binary PS/CO_2 mixture found in Section 5.3.1 [129]. Table 5.4 shows a disparity between the hole volume of the binary mixture (9.900×10^{-24} cm^3) and that of the ternary mixture (1.562×10^{-23} cm^3). Since the theoretical predictions for the ternary mixture agree with experiment quite well even at the high ratio of 90:10, this would seem to indicate that there exists a fairly sharp transition between the two fluid characters [129].

It has been deduced from other equations of state that the presence of DME in the mixture increases the solubility of CO_2 [81]. Due to present technical limitations, while the total solubility of the solvents can be experimentally observed, it is not possible to measure the solubility of the constituent solvents independently. Since it is not possible to independently verify the predictions of individual solvent solubility with experiment, verification is instead inferred from agreement with total solubility [81]. The solubility of CO_2 in the ternary mixture is plotted in figure 5.10c for CO_2:DME ratios of 100:0, 90:10, 85:15, and 80:20. The trend shows decreasing solubility of CO_2 as the concentration of DME is increased. Figures 5.10a and 5.10c together seem to imply that the increase in availability of DME induces the replacement of CO_2 with a solvent with greater affinity for PS [129].

5.5 Critical solvent ratio

5.5.1 Ternary PS/CO_2+N_2 mixtures

In section 5.3.1, the temperature dependence of solubility in saturated PS/N_2 mixtures was found to be the reverse of that in PS/CO_2. In the present section, ternary mixtures of PS/CO_2+N_2 are considered. Figures 5.11a, 5.11b, and 5.11c compare theoretically predicted solvent solubilities at 403 K, 423 K, and 463 K to experiment for CO_2:N_2 ratios of 75:25, 50:50, and 25:75, respectively. Experimental data is taken from Hasan [46].

Together, the figures illustrate a trend of decreasing solubility with increasing concentration of N_2, as expected. It is apparent that as the concentration of N_2 is increased, the separation of solubility isotherms seems to decrease in tandem. Indeed, referring to figure 5.8b, it is evident that, as the ratio of CO_2:N_2 decreases towards 0:100, the temperature dependence of solubility will eventually reverse. This seems to imply that there exists a critical CO_2:N_2 ratio at which the temperature dependence of solubility would vanish, with CO_2 dominating the temperature dependence above this ratio and N_2 dominating the temperature dependence below [129]. Given the difficulty in calculating the temperature derivatives of solubility analytically, it may be possible to calculate this critical ratio numerically instead. This problem may merit future consideration, as it may imply that it is possible to tailor the temperature-dependence of solubility by tuning the solvent ratios. This may benefit applications such as those that require highly stable solubility even under thermal fluctuation, for example.

5.6 Manipulation of the model

The present work outlines the SL molecular model for the purpose of making predictions of phase equilibria for polymer-solvent mixtures relevant to polymer foaming, as discussed in Section 1.2. It is conceivable, however, that the present theory could be expanded to include additional model features to make predictions of other phenomena, provided that the limitations of the resulting theory are correctly anticipated. For example, Condo et al. [15] endeavour to expand the lattice-fluid to include additional molecular considerations for the purpose of predicting glass transition phenomena. Indeed, one of the purposes of statistical mechanics discussed in Section 2.4 is tracing physical phenomena to their molecular sources through the manipulation of model features.

The present work provides a framework in Chapter 3 through which model features could be manipulated. If such manipulation were to be undertaken, it is important to verify the thermodynamic consistency of the theory with each change. As discussed in Section 2.4.3, adherence to the first-power homogeneous form of thermodynamic potentials is required in statistical thermodynamic theories that make use of the same to derive results. Therefore, a consistency verification similar to the one performed in Sections 3.5.4 and 3.7 should be imposed on semi-empirical systems that include features that do not have a physical basis, such as holes.

The following procedure is proposed, which is a direct expansion of the one performed in Section 3.5.4. Once a thermodynamic potential is derived using statistical mechanical

methods, the complete set of thermodynamic potentials should be calculated through Legendre transformation, as outlined in Section 2.3.1. From each potential, the full set of equations of state should be calculated and compared, with validation of the proposed changes following from the consistency of the equations of state. This procedure may result in additional constraints on features of the theory that do not have a physical basis, such as holes. It may also result in the discarding of the considered feature, such as mixing rules.

Chapter 6

Conclusions

The present work details an off-lattice derivation of the SL-EOS for pure fluids as well as multicomponent mixtures. In doing so, a methodology for tracking assumptions and ensuring the consistency of semi-empirical theories is established. In addition, a physical interpretation of holes in the SL-EOS is proposed. These considerations allow for the application of a variant of the SL-EOS to be applied to phase equilibrium calculations for the saturated polymer-solvent mixtures relevant to polymer foaming. To this end, an additional methodology for determining solubility and swelling in polymer-solvent mixtures is outlined.

The present work was undertaken to achieve three primary aims. In satisfaction of the first aim of determining whether the poor performance of the SL-EOS is due to fundamental features or ancillary considerations, such performance is traced to several sources. One of these sources is found to be sub-optimal implementation. Investigation of the parameter estimation practices in the literature identifies a best practice procedure. The present work challenges the accepted notion that a single set of parameters is incapable of agreement with experiment over large thermodynamic ranges by identifying such parameters for CO_2. Employment of a nonlinear least-squares fit procedure over a large thermodynamic range, excluding data in the neighbourhood of any critical points, is found to significantly improve correlation to experiment. More generally, a methodology for carefully tracking fundamental model assertions and simplifying assumptions is proposed to ensure that the theory is not inappropriately applied to regimes where it is not expected to correlate to experiment. An additional source for the poor performance is found to be a thermodynamic inconsistency introduced by mixing rules. It is shown in the present work that no matter their form, the introduction of mixing rules to a theory that includes holes and features incompressibility leads to incompatibility with the principles of thermodynamics. Given

the use of the same principles to derive material properties, this inconsistency is entirely impermissible. It is found that this inconsistency cannot be corrected through the use of fugacities, as was previously thought.

In satisfaction of its second aim of a successful variant of the SL-EOS for application to polymer foaming, the present work contrives a variant of the theory that replaces the mixing rules with a constant hole volume. This approach is found to provide an effective method for calculating solubility in saturated polymer-solvent mixtures. As opposed to mixing rule variants, the present theory is thermodynamically consistent in a given phase, lacking instead internal consistency typically necessary for phase equilibrium calculation due to the inability of the hole volume to limit correctly to the pure fluids. This inconsistency is found to be permissible in solubility calculations, provided that the hole volumes describing the solvent-rich phase and the mixture are not too dissimilar. Such a determination is made *a posteriori*, with validation of this approach made through agreement with experiment. This is found to be significantly better than both one- and two- parameter mixing rule approaches, indicating that while the constant hole volume is justifiable in the considered mixtures, the application of mixing rules is not. In light of its success, a physical significance is proposed for holes. Holes are postulated to be manifestations of averaged molecular correlations, otherwise ignored in such mean field theories. The success in calculating solubility indicates that the theory can successfully be applied to the mixtures relevant to polymer foaming.

It is important, on the other hand, to note the limitations and areas of caution. The application of a mean field assumption means that properties calculated wherever correlations are important to the results, for example the critical point or glass transition, are not expected to be accurate. In addition, as a direct result of its original aims, the theory does not presently allow for the calculation of quantities that are based on internal degrees of freedom, such as heat capacities. As previously stated, the lack of internal consistency means that phase equilibrium calculations are not possible if the hole volumes of different phases are too different, the bounds of which are not presently known.

Of the quantities originally stated to be measures of success, the present theory falls shy only of its goal of accurately predicting swelling. Despite better than order-of-magnitude predictions of swelling, the predictions fail to reproduce the shape of the trends observed in experiment. This is likely the result of consideration the polymer-rich phase in addition to those necessary for the phase equilibrium calculation. While mixture hole volume tends to be strongly influenced by the solvent phase, helping to ensure the success of phase equilibrium calculations, the additional consideration of the polymer-rich phase includes fluids with typically larger hole volume disparities. Nonetheless, excellent correlation of the theory with PVT behaviour for pure fluids, first-order phase transitions, as well as

solubility indicate that the theory is overall successful.

Finally, in order to satisfy its third aim, the present work proposes a methodology for ensuring the fundamental thermodynamic consistency of a semi-empirical statistical thermodynamic theory that contains features without physical basis by verifying that the free energies obey the first-power homogeneous form of a thermodynamic potential. This is done by applying the Legendre transformations to the free energy derived from the molecular theory and verifying the consistency of the resulting equations of state. In the paradigm of statistical mechanics, this is tantamount to imposing ensemble equivalence as a constraint on the theory.

Given the successful satisfaction of its aims, much future work is warranted. A few paths for future of investigation merit particular mention. The present theory takes the form of a regular solution, with interactions leading purely to a heat of mixing. The constant hole volume variant could be extended to allow for the inclusion of an entropic term in the interactions. It is possible that such a modification may improve the correlation to experiment, although care should be taken that the consistency requirement is fulfilled. In addition, while only binary polymer-solvent and ternary polymer-co-solvent systems are considered presently, the theory is readily scalable to other systems, including co-polymer-solvent and higher-order mixtures. The present observation that the hole volumes of polymer-solvent mixtures are dominated by the hole volume of the solvent species leads to hope for successful application of the theory to these systems in spite of the additional complexity. Finally, a more thorough investigation into the source of the atypical temperature dependence seen in low critical point materials may prove useful. One might hope, should this phenomenon be related to relative interaction strengths of the pure components, that it would allow for the tailoring of temperature dependence in the solubility through tuning of the solvent composition.

In spite of its shortcomings in terms of swelling prediction, the present theory is shown to be a useful tool. In addition to its success in its original goals, the theory is found to be capable of making accurate predictions for mixtures where one of the pure components is not known by regressing both the unknown pure fluid parameters and mixture parameters from experimental solubility data. While such a regression may not produce accurate predictions of known pure component parameters, the resulting predictions of solubility provided excellent agreement with experiment. Such an approach could be applied to exotic polymer-solvent mixtures. The present theory has also been shown capable of tracing some unusual phenomena to their molecular sources. The reversed temperature dependence of solubility observed in mixtures featuring a solvent with a low critical point is attributed to the weaker polymer-solvent interactions exhibited by these fluids, although not yet conclusively. The manipulation of the theory by incremental adjustment in this way

indicates that the SL-EOS with constant hole volume has potential for new exploration.

Since applicability of the SL-EOS to successfully describe homogeneous mixtures is requisite for the application of Hong-Noolandi Self-Consistent Field Theory to inhomogeneous systems, the success of the present theory gains a larger significance. The successful application of the constant hole volume SL theory to saturated polymer-solvent mixtures is indicative of the potential for the successful application of HN-SCFT to inhomogeneous polymeric mixtures, such as polymeric foams.

References

[1] S. J. Ahn. *Least Squares Orthogonal Distance Fitting of Curves and Surfaces in Space*, volume 1070. Springer Berlin Heidelberg, Berlin, Heidelberg, 2004.

[2] S. J. Alesaadi and F. Sabzi. Hydrogen storage in a series of Zn-based MOFs studied by Sanchez-Lacombe equation of state. *Int. J. Hydrogen Energy*, 40(4):1651–1656, 2015.

[3] S. Angus, B. Armstrong, and K. M. de Rueck. *International Thermodynamic Tables of the Fluid State 3: Carbon Dioxide*. Pergamon Press, Oxford, 1976.

[4] P. F. Arce and M. Aznar. Modeling of thermodynamic behavior of PVT properties and cloud point temperatures of polymer blends and polymer blend+carbon dioxide systems using non-cubic equations of state. *Fluid Phase Equilib.*, 286(1):17–27, 2009.

[5] M. A. Bashir, M. Al-haj Ali, V. Kanellopoulos, J. Seppälä, E. Kokko, and S. Vijay. The effect of pure component characteristic parameters on Sanchez-Lacombe equation-of-state predictive capabilities. *Macromol. React. Eng.*, 7(5):193–204, 2013.

[6] J. J. Binney, N. J. Dowrick, A. J. Fisher, and M. E. J. Newman. *The Theory of Critical Phenomena: An Introduction to the Renormalization Group*. Oxford University Press, New York, 1 edition, 1992.

[7] A. Bondi. *Physical Properties of Molecular Crystals, Liquids, and Glasses*. Wiley, New York, 1968.

[8] A. Bonilla-Petriciolet. On the capabilities and limitations of harmony search for parameter estimation in vapor-liquid equilibrium modeling. *Fluid Phase Equilib.*, 332:7–20, 2012.

[9] C. Boyère, C. Jérôme, and A. Debuigne. Input of supercritical carbon dioxide to polymer synthesis: An overview. *Eur. Polym. J.*, 61:45–63, 2014.

[10] H. B. Callen. *Thermodynamics and an Introduction to Thermostatistics*. John Wiley & Sons, New York, 1985.

[11] L. N. Canjar and F. S. Manning. *Thermodynamic Properties and Reduced Correlations for Gases*. Gulf Publishing Company, Houston, 1967.

[12] G.-P. Cao, T. Liu, and G. W. Roberts. Predicting the effect of dissolved carbon dioxide on the glass transition temperature of poly(acrylic acid). *J. Appl. Polym. Sci.*, 115(4):2136–2143, 2010.

[13] J. Cardy. *Scaling and Renormalization in Statistical Physics*. Cambridge University Press, Cambridge, 1996.

[14] M. H. Cohen and D. Turnbull. Molecular transport in liquids and glasses. *J. Chem. Phys.*, 31(5):1164–1169, 1959.

[15] P. D. Condo, I. C. Sanchez, C. G. Panayiotou, and K. P. Johnston. Glass transition behavior including retrograde vitrification of polymers with compressed fluid diluents. *Macromolecules*, 25(23):6119–6127, 1992.

[16] A. I. Cooper. Polymer synthesis and processing using supercritical carbon dioxide. *J. Mater. Chem.*, 10(2):207–234, 2000.

[17] S. Costeux. CO_2-blown nanocellular foams. *J. Appl. Polym. Sci.*, 131(23):1–16, 2014.

[18] David. *Introduction to Modern Statistical Mechanics*. Oxford University Press, Oxford, 1987.

[19] U. K. Deiters and K. M. de Reuck. Guidelines for publication of equations of state - I. Pure fluids. *Fluid Phase Equilib.*, 161:205–219, 1999.

[20] F. Doghieri and G. C. Sarti. Nonequilibrium lattice fluids: A predictive model for the solubility in glassy polymers. *Macromolecules*, 29(24):7885–7896, 1996.

[21] X. X. Duan, Y. C. Li, and C. J. Gao. Constraining the lattice fluid dark energy from SNe Ia, BAO and OHD. *Sci. China: Phys., Mech. Astron.*, 56(6):1220–1226, 2013.

[22] W. Duschek, R. Kleinrahm, and W. Wagner. Measurement and correlation of the (pressure, density, temperature) relation of carbon dioxide I. The homogeneous gas and liquid regions in the temperature range from 217 k to 340 k at pressures up to 9 mpa. *J. Chem. Thermodyn.*, 22(9):827–840, 1990.

[23] W. Duschek, R. Kleinrahm, and W. Wagner. Measurement and correlation of the (pressure, density, temperature) relation of carbon dioxide II. Saturated-liquid and saturated-vapour densities and the vapour pressure along the entire coexistence curve. *J. Chem. Thermodyn.*, 22(9):841–864, 1990.

[24] S. F. Edwards. The statistical mechanics of polymers with excluded volume. *Proc. Phys. Soc.*, 85(4):613–624, 1965.

[25] U. Eisele. *Introduction to Polymer Physics*. Springer-Verlag, Berlin, 1990.

[26] P. J. Flory. Thermodynamics of heterogeneous polymers and their solutions. *J. Chem. Phys.*, 12(11):425–438, 1944.

[27] P. J. Flory. *Principles of Polymer Chemistry*. Cornell University Press, Ithica, 1953.

[28] P. J. Flory, R. A. Orwoll, and A. Vrij. Statistical thermodynamics of chain molecule liquids. I. An equation of state for normal paraffin hydrocarbons. *J. Am. Chem. Soc.*, 86(17):3507–3514, 1964.

[29] P. J. Flory, R. A. Orwoll, and A. Vrij. Statistical thermodynamics of chain molecule liquids. II. Liquid mixtures of normal paraffin hydrocarbons. *J. Am. Chem. Soc.*, 86 (17):3515–3520, 1964.

[30] T. G. Fox and P. J. Flory. Second-order transition temperatures and related properties of polystyrene. I. Influence of molecular weight. *J. Appl. Phys.*, 21(6):581–591, 1950.

[31] K. F. Freed. Functional integrals and polymer statistics. In I. Prigogene and S. A. Rice, editors, *Advances in Chemical Physics*, volume 22, chapter 1. John Wiley and Sons, Inc., Hoboken, 1972.

[32] H. Fujita. Free diffusion in a two-component system in which there is a volume change on mixing. *J. Am. Chem. Soc.*, 83(13):2862–2865, 1961.

[33] H. Fujita. Notes on free volume theories. *Polym. J.*, 23(12):1499–1506, 1991.

[34] E. Funami, K. Taki, and M. Ohshima. Density measurement of polymer/CO_2 single-phase solution at high temperature and pressure using a gravimetric method. *J. Appl. Polym. Sci.*, 105(5):3060–3068, 2007.

[35] P. Gans. *Data Fitting in the Chemical Sciences*. John Wiley & Sons, Chichester, 1992.

[36] A. Garg, E. Gulari, and C. W. Manke. Thermodynamics of polymer melts swollen with supercritical gases. *Macromolecules*, 27(20):5643–5653, 1994.

[37] K. Gauter and A. Heidemann. A proposal for parametrizing the Sanchez-Lacombe equation of state. *Ind. Eng. Chem. Res.*, 39:1115–1117, 2000.

[38] J. Gross and G. Sadowski. Application of perturbation theory to a hard-chain reference fluid: an equation of state for square-well chains. *Fluid Phase Equilib.*, 168(2): 183–199, 2000.

[39] J. Gross and G. Sadowski. Perturbed-Chain SAFT: An equation of state based on a perturbation theory for chain molecules. *Ind. Eng. Chem. Res.*, 40(4):1244–1260, 2001.

[40] Y. Guerrieri, K. V. Pontes, G. M. N. Costa, and M. Embiruçu. A survey of equations of state for polymers. In A. De Souza Gomes, editor, *Polymerization*. InTech, 2012.

[41] E. A. Guggenheim. Statistical thermodynamics of mixtures with non-zero energies of mixing. *Proc. R. Soc. London, Ser. A*, 1944.

[42] E. A. Guggenheim. *Thermodynamics: An Advanced Treatment for Chemists and Physicists*. Elsevier, Amsterdam, 1949.

[43] E. A. Guggenheim. *Mixtures*. Oxford University Press, London, 1952.

[44] E. A. Guggenheim. *Applications of Statistical Thermodynamics*. Oxford University Press, London, 1966.

[45] R. Hariharan, B. D. Freeman, R. G. Carbonell, and G. C. Sarti. Equation of state predictions of sorption isotherms in polymeric materials. *J. Appl. Polym. Sci.*, 50 (10):1781–1795, 1993.

[46] M. M. Hasan. *A Systematic Study of Solubility of Physical Blowing Agents and Their Blends in Polymers and Their Nanocomposites*. Ph.D. thesis, University of Toronto, 2013.

[47] M. M. Hasan, Y. G. Li, G. Li, C. B. Park, and P. Chen. Determination of solubilities of CO_2 in linear and branched polypropylene using a magnetic suspension balance and a PVT apparatus. *J. Chem. Eng. Data*, 55(11):4885–4895, 2010.

[48] E. Helfand and A. M. Sapse. Theory of unsymmetric polymer-polymer interfaces. *J. Chem. Phys.*, 62(4):1327–1331, 1975.

[49] E. Helfand and A. M. Sapse. Theory of concentrated polymer solution-solvent interface. *J. Polym. Sci., Part C: Polym. Symp.*, 54:289–297, 1976.

[50] T. L. Hill. *An Introduction to Statistical Thermodynamics*. Dover, New York, 1960.

[51] C. Hoheisel. *Theoretical Treatment of Liquids and Liquid Mixtures*. Elsevier, 1993.

[52] K. M. Hong and J. Noolandi. Theory of inhomogeneous multicomponent polymer systems. *Macromolecules*, 14(3):727–736, 1981.

[53] K. M. Hong and J. Noolandi. Conformational entropy effects in a compressible lattice fluid theory of polymers. *Macromolecules*, 14(5):1229–1234, 1981.

[54] M. L. Huggins. Theory of solutions of high polymers. *J. Am. Chem. Soc.*, 64(7): 1712–1719, 1942.

[55] M. Iguchi, H. Machida, Y. Sato, and R. L. Smith. Correlation of supercritical CO_2-ionic liquid vapor-liquid equilibria with the ϵ*-modified Sanchez-Lacombe equation of state. *Asia-Pac. J. Chem. Eng.*, 7:S95–S100, 2012.

[56] R. K. Jain and R. Simha. On the statistical thermodynamics of multicomponent fluids: equation of state. *Macromolecules*, 13:1501–1508, 1980.

[57] K. Kamide. *Thermodynamics of Polymer Solutions: Phase Equilibria and Critical Phenomena*. Elsevier, New York, 1990.

[58] P. K. Kilpatrick and S.-H. Chang. Saturated phase equilibria and parameter estimation of pure fluids with two lattice-gas models. *Fluid Phase Equilib.*, 30:49–56, 1986.

[59] J.-H. Kim, T. E. Paxton, and D. L. Tomasko. Microencapsulation of naproxen using rapid expansion of supercritical solutions. *Biotechnol. Prog.*, 12(5):650–661, 1996.

[60] Y. Kim, C. B. Park, P. Chen, and R. B. Thompson. Origins of the failure of classical nucleation theory for nanocellular polymer foams. *Soft Matter*, 7(16):7351, 2011.

[61] Y. Kim, C. B. Park, P. Chen, and R. B. Thompson. Towards maximal cell density predictions for polymeric foams. *Polymer*, 52(24):5622–5629, 2011.

[62] Y. Kim, C. B. Park, P. Chen, and R. B. Thompson. Maximal cell density predictions for compressible polymer foams. *Polymer*, 54(2):841–845, 2013.

[63] M. B. Kiszka, M. A. Meilchen, and M. A. McHugh. Modeling high-pressure gas-polymer mixtures using the Sanchez-Lacombe equation of state. *J. Appl. Polym. Sci.*, 36(3):583–597, 1988.

[64] V. J. Klenin. *Thermodynamics of Systems Containing Flexible-Chain Polymers*. Elsevier, 1999.

[65] R. A. Krenz, T. Laursen, and R. A. Heidemann. The modified Sanchez-Lacombe equation of state applied to polydisperse polyethylene solutions. *Ind. Eng. Chem. Res.*, 48:10664–10681, 2009.

[66] R. H. Lacombe and I. C. Sanchez. Statistical thermodynamics of fluid mixtures. *J. Phys. Chem.*, 80(23):2568–2580, 1976.

[67] S.-T. Lee, C. B. Park, and N. S. Ramesh. *Polymeric Foams: Science and Technology*. CRC Press, Boca Raton, 2006.

[68] G. Li. *Development of a Novel Apparatus for the PVT Visualization and Measurement of Polymer/Gas Solutions*. Ph.D. thesis, University of Toronto, 2008.

[69] G. Li, J. Wang, C. B. Park, P. Moulinie, and R. Simha. Comparison of SS-based and SL-based estimation of gas solubility. *ANTEC 2004, Conf. Proc.*, pages 2566–2575, 2004.

[70] G. Li, H. Li, J. Wang, and C. B. Park. Investigating the solubility of co$_2$ in polypropylene using various EOS models. *Cell. Polym.*, 25(4):237–248, 2006.

[71] G. Li, F. Gunkel, J. Wang, C. B. Park, and V. Altstädt. Solubility measurements of N_2 and CO_2 in polypropylene and ethene/octene copolymer. *J. Appl. Polym. Sci.*, 103(5):2945–2953, 2007.

[72] G. Li, J. Wang, C. B. Park, and R. Simha. Measurement of gas solubility in linear/branched PP melts. *J. Polym. Sci., Part B: Polym. Phys.*, 45(17):2497–2508, 2007.

[73] Y. G. Li and C. B. Park. Effects of branching on the pressure-volume-temperature behaviors of PP/CO_2 solutions. *Ind. Eng. Chem. Res.*, 48(14):6633–6640, 2009.

[74] Y. G. Li, C. B. Park, H. B. Li, and J. Wang. Measurement of the PVT property of PP/CO_2 solution. *Fluid Phase Equilib.*, 270(1-2):15–22, 2008.

[75] Z.-W. Li, Z.-Y. Lu, Z.-Y. Sun, Z.-S. Li, and L.-J. An. Calculating the equation of state parameters and predicting the spinodal curve of isotactic polypropylene/-poly(ethylene-co-octene) blend by molecular dynamics simulations combined with Sanchez-Lacombe lattice fluid theory. *J. Phys. Chem. B*, 111(21):5934–5940, 2007.

[76] X. Liao, Y. G. Li, C. B. Park, and P. Chen. Interfacial tension of linear and branched PP in supercritical carbon dioxide. *J. Supercrit. Fluids*, 55(1):386–394, 2010.

[77] Y. V. Linnik. *Method of Least Squares and Principles of the Theory of Observations*. Pergamon Press, New York, 1961.

[78] H. Machida, Y. Sato, and R. L. Smith. Simple modification of the temperature dependence of the Sanchez-Lacombe equation of state. *Fluid Phase Equilib.*, 297: 205–209, 2010.

[79] S. H. Mahmood, M. Keshtkar, and C. B. Park. Determination of carbon dioxide solubility in polylactide acid with accurate PVT properties. *J. Chem. Thermodyn.*, 70:13–23, 2014.

[80] S. H. Mahmood, C. L. Xin, J. H. Lee, and C. B. Park. Study of volume swelling and interfacial tension of the polystyrene-carbon dioxide-dimethyl ether system. *J. Colloid Interface Sci.*, 456:174–181, 2015.

[81] S. H. Mahmood, C. L. Xin, P. Gong, J. H. Lee, G. Li, and C. B. Park. Dimethyl ether's plasticizing effect on carbon dioxide solubility in polystyrene. *Polymer*, 97: 95–103, 2016.

[82] N. H. March and M. P. Tosi. *Introduction to Liquid State Physics*. World Scientific Publishing Co., Pte, Ltd, Singapore, 2002.

[83] D. W. Marquardt. An algorithm for least-squares estimation of nonlinear parameters. *J. Soc. Ind. Appl. Math.*, 11(2):431–441, 1963.

[84] J. E. Mayer and M. G. Mayer. *Statistical Mechanics*. John Wiley & Sons, Inc., New York, 1940.

[85] M. McHugh and V. Krukonis. *Thermodynamic Modeling of Supercritical Fluid-Solute Phase Behavior*, chapter 5, pages 99–134. Butterworth-Heinemann, Boston, 2 edition, 1994.

[86] A. Michels, B. Blaisse, and C. Michels. The isotherms of CO_2 in the neighbourhood of the critical point and round the coexistence line. *Proc. R. Soc. London, Ser. A*, 160(902):358–375, 1937.

[87] S. P. Nalawade, F. Picchioni, L. P. B. M. Janssen, V. E. Patil, J. T. F. Keurentjes, and R. Staudt. Solubilities of sub- and supercritical carbon dioxide in polyester resins. *Polym. Eng. Sci.*, 46(5):643–649, 2006.

[88] E. Neau. A consistent method for phase equilibrium calculation using the Sanchez-Lacombe lattice-fluid equation-of-state. *Fluid Phase Equilib.*, 203:133–140, Dec 2002.

[89] NIST. Thermophysical properties of fluid systems. URL http://webbook.nist.gov/chemistry/fluid/.

[90] H. Park, C. B. Park, C. Tzoganakis, K. H. Tan, and P. Chen. Surface tension measurement of polystyrene melts in supercritical carbon dioxide. *Ind. Eng. Chem. Res.*, 45(5):1650–1658, 2006.

[91] H. Park, R. B. Thompson, N. Lanson, C. Tzoganakis, C. B. Park, and P. Chen. Effect of temperature and pressure on surface tension of polystyrene in supercritical carbon dioxide. *J. Phys. Chem. B*, 111(15):3859–3868, 2007.

[92] R. K. Pathria. *Statistical Mechanics*. Butterworth Heinemann, Boston, 2 edition, 1996.

[93] A. Péneloux, E. Rauzy, and R. A. Fréze. A consistent correction for Redlich-Kwong-Soave volumes. *Fluid Phase Equilib.*, 8:7–23, 1982.

[94] D.-Y. Peng and D. B. Robinson. A new two-constant equation of state. *Ind. Eng. Chem. Fundam.*, 15(1):59–64, 1976.

[95] D. S. Pope, I. C. Sanchez, W. J. Koros, and G. K. Fleming. Statistical thermodynamic interpretation of sorption/dilation behavior of gases in silicone rubber. *Macromolecules*, 24(8):1779–1783, 1991.

[96] C. I. Poser and I. C. Sanchez. Interfacial tension theory of low and high molecular weight liquid mixtures. *Macromolecules*, 14(2):361–370, March 1981.

[97] M. T. Pottiger and R. L. Laurence. The P-V-T behavior of polymeric liquids represented by the Sanchez-Lacombe equation of state. *J. Polym. Sci., Part B: Polym. Phys.*, 22(5):903–907, 1984.

[98] I. Prigogine. *The Molecular Theory of Solutions*. North-Holland Publishing Company, Amsterdam, 1957.

[99] L. E. Reichl. *A Modern Course in Statistical Physics*. John Wiley & Sons, New York, 1998.

[100] P. A. Rodgers. Pressure-volume-temperature relationships for polymeric liquids: A review of equations of state and their characteristic parameters for 56 polymers. *J. Appl. Polym. Sci.*, 48(6):1061–1080, May 1993.

[101] B. Roffel and B. Betlem. *Process Dynamics and Control: Modeling for Control and Prediction*. John Wiley & Sons, West Sussex, 2006.

[102] M. Rubinstein and R. H. Colby. *Polymer Physics*. Oxford University Press, Oxford, 2003.

[103] I. C. Sanchez and R. H. Lacombe. Theory of liquid-liquid and liquid-vapour equilibria. *Nature*, 252(5482):381–383, 1974.

[104] I. C. Sanchez and R. H. Lacombe. An elementary molecular theory of classical fluids. Pure fluids. *J. Phys. Chem.*, 80(21):2352–2362, 1976.

[105] I. C. Sanchez and R. H. Lacombe. Statistical thermodynamics of polymer solutions. *Macromolecules*, 11(6):1145–1156, 1978.

[106] I. C. Sanchez and C. G. Panayiotou. Equation of state thermodynamics of polymer and related solutions. In S. L. Sandler, editor, *Models for Thermodynamic and Phase Equilibria Calculations*, chapter 3, pages 187–285. Marcel Dekker, Inc., New York, NY, 1994.

[107] I. C. Sanchez and P. A. Rodgers. Solubility of gases in polymers. *Pure and Applied Chemistry*, 62(11):2107–2114, 1990.

[108] K. Sarikhani, K. Jeddi, R. B. Thompson, C. B. Park, and P. Chen. Adsorption of surface-modified silica nanoparticles to the interface of melt poly(lactic acid) and supercritical carbon dioxide. *Langmuir*, 31(20):5571–5579, 2015.

[109] K. Sarikhani, K. Jeddi, R. B. Thompson, C. B. Park, and P. Chen. Effect of pressure and temperature on interfacial tension of poly lactic acid melt in supercritical carbon dioxide. *Thermochim. Acta*, 609:1–6, 2015.

[110] Y. Sato, M. Yurugi, K. Fujiwara, S. Takishima, and H. Masuoka. Solubilities of carbon dioxide and nitrogen in polystyrene under high temperature and pressure. *Fluid Phase Equilib.*, 125(1-2):129–138, 1996.

[111] Y. Sato, K. Inohara, S. Takishima, H. Masuoka, M. Imaizumi, H. Yamamoto, and M. Takasugi. Pressure-volume-temperature behavior of polylactide, poly(butylene succinate), and poly(butylene succinate-co-adipate). *Polym. Eng. Sci.*, 40(12):2602–2609, 2000.

[112] S. Sen Roy and S. Guria. Estimation of regression parameters in the presence of outliers in the response. *Statistics*, 43(6):531–539, 2009.

[113] R. Simha and T. Somcynsky. On the statistical thermodynamics of spherical and chain molecule fluids. *Macromolecules*, 2(4):342–350, 1969.

[114] R. Span and W. Wagner. A new equation of state for carbon dioxide covering the fluid region from the triple-point temperature to 1100 K at pressures up to 800 MPa. *J. Phys. Chem. Ref. Data*, 25(6):1509, 1996.

[115] R. Span, E. W. Lemmon, R. T. Jacobsen, W. Wagner, and A. Yokozeki. A reference equation of state for the thermodynamic properties of nitrogen for temperatures from 63.151 to 1000 K and pressures to 2200 MPa. *J. Phys. Chem. Ref. Data*, 29(6): 1361–1433, 2000.

[116] R. B. Thompson, J. R. MacDonald, and P. Chen. Origin of change in molecular-weight dependence for polymer surface tension. *Phys. Rev. E*, 78(3):030801, 2008.

[117] R. B. Thompson, C. B. Park, and P. Chen. Reduction of polymer surface tension by crystallized polymer nanoparticles. *J. Chem. Phys.*, 133(14):144913, 2010.

[118] D. L. Tomasko, H. Li, D. Liu, X. Han, M. J. Wingert, L. J. Lee, and K. W. Koelling. A review of CO_2 applications in the processing of polymers. *Ind. Eng. Chem. Res.*, 42(25):6431–6456, 2003.

[119] H. Tompa. *Polymer Solutions*. Butterworth, London, 1956.

[120] H. Touchette. Ensemble equivalence for general many-body systems. *EPL*, 96(5): 50010, 2011.

[121] H. Touchette. Equivalence and nonequivalence of ensembles: Thermodynamic, macrostate, and measure levels. *J. Stat. Phys.*, 159(5):987–1016, 2015.

[122] H. Touchette, R. S. Ellis, and B. Turkington. An introduction to the thermodynamic and macrostate levels of nonequivalent ensembles. *Phys. A (Amsterdam, Neth.)*, 340 (1-3):138–146, 2004.

[123] D. Turnbull and M. H. Cohen. Free-volume model of the amorphous phase: Glass transition. *J. Chem. Phys.*, 34(1):120–125, 1961.

[124] N. B. Vargaftik. *Tables on the Thermophysical Properties of Liquids and Gases: in Normal and Dissociated States*. Hemisphere Pub. Corp., Washington, 2 edition, 1975.

[125] G. Vidaurre, V. R. Vasquez, and W. B. Whiting. Robustness of nonlinear regression methods under uncertainty: Applications in chemical kinetics models. *Ind. Eng. Chem. Res.*, 43(6):1395–1404, 2004.

[126] F. Vogt. A self-guided search for good local minima of the sum-of-squared-error in nonlinear least squares regression. *J. Chemom.*, 29(2):71–79, 2015.

[127] K. von Konigslow, C. B. Park, and R. B. Thompson. Evaluating characteristic parameters for carbon dioxide in the Sanchez-Lacombe equation of state. *J. Chem. Eng. Data*, 62(2):585–595, 2017.

[128] K. von Konigslow, R. B. Thompson, and C. B. Park. Polymeric foaming predictions from the Sanchez-Lacombe equation of state: Application to polypropylene-carbon dioxide mixtures. *Phys. Rev. Appl.*, 8(4):044009, 2017.

[129] K. von Konigslow, C. B. Park, and R. B. Thompson. Application of the off-lattice Sanchez-Lacombe equation of state to mixtures relevant to polymeric foaming. In preparation 2017.

[130] J. S. Vrentas and J. L. Duda. Diffusion in polymer-solvent systems. I. Reexamination of the free-volume theory. *J. Polym. Sci., Polym. Phys. Ed.*, 15(3):403–416, 1977.

[131] J. S. Vrentas and J. L. Duda. Diffusion in polymer-solvent systems. II. A predictive theory for the dependence of diffusion coefficients on temperature, concentration, and molecular weight. *J. Polym. Sci., Polym. Phys. Ed.*, 15(3):417–439, 1977.

[132] J. S. Vrentas and J. L. Duda. Molecular diffusion in polymer solutions. *AIChE J.*, 25(1):1–24, 1979.

[133] M. P. Vukalovich and V. V. Altunin. *Thermophysical Properties of Carbon Dioxide*. Collets, Wellingborough, 1968.

[134] T. A. Walker, C. M. Colina, K. E. Gubbins, and R. J. Spontak. Thermodynamics of poly(dimethylsiloxane)/poly(ethylmethylsiloxane) (PDMS/PEMS) blends in the presence of high-pressure CO_2. *Macromolecules*, 37(7):2588–2595, 2004.

[135] N.-H. Wang, K. Hattori, S. Takishima, and H. Masuoka. Measurement and prediction of vapor-liquid equilibrium ratios for solutes at infinite dilution in CO_2+polyvinyl acetate system at high pressures. *Kagaku Kogaku Ronbunshu*, 17(6):1138–1145, 1991.

[136] J. Wu, Y. Zhou, and E. W. Lemmon. An equation of state for the thermodynamic properties of dimethyl ether. *J. Phys. Chem. Ref. Data*, 40(2), 2011.

[137] H. Xie, E. Nies, A. Stroeks, and R. Simha. Some considerations on equation of state and phase-relations - polymer-solutions and blends. *Polym. Eng. Sci.*, 32(22): 1654–1664, 1992.

[138] Y. Xiong and E. Kiran. Miscibility, density and viscosity of poly(dimethylsiloxane) in supercritical carbon dioxide. *Polymer*, 36(25):4817–4826, 1995.

[139] X. Xu, D. E. Cristancho, S. Costeux, and Z.-G. Wang. Density-functional theory for polymer-carbon dioxide mixtures: A perturbed-chain SAFT approach. *J. Chem. Phys.*, 137(5):054902, 2012.

[140] H. Yamakawa. *Modern Theory of Polymer Solutions*. Harper & Row, New York, 1971.

[141] P. Zoller. Analysis of the equation of state of polymer melts in terms of the Ising fluid model. *J. Polym. Sci., Polym. Phys. Ed.*, 18(1):157–160, 1980.

[142] P. Zoller and D. J. Walsh. *Standard Pressure-Volume-Temperature Data for Polymers*. Technomic Publishing Company, 1995.

APPENDICES

Appendix A

Comparison of on-lattice and off-lattice assertions

The molecular theory assertions, as described by Sanchez and Lacombe, are here enumerated. The order in which the assertions are presented does not reflect the original SL presentation. Rather, the order has been changed in order to group structural, entropic, and energetic considerations together, as well as to decouple the fundamental theory assertions from simplifying assumptions. It should be noted that in these assertions, the term "mer" refers to a polymer segment rather than a monomer. The model assertions for the pure fluid are [66, 104, 105]

- (Lattice character) The fluid is assumed to be composed of a "system of N molecules each of which occupies r sites (a r-mer [*sic*]) and N_0 vacant lattice sites (holes). ... The coordination number of the lattice is z." [104]
- (Chain structure)"Each interior mer of a linear chain is surrounded by $z-2$ nearest nonbonded neighbours and two bonded neighbours; mers at the chain ends have $z-1$ nonbonded neighbours and one bonded neighbour." [104]
- (Symmetry) "A r-mer is characterized by a symmetry number σ. For example, for a linear r-mer it is equal to two if the chain ends are indistinguishable and to unity if the chain ends are distinguishable." ("... the exact value of σ is of inconsequential importance.") [104]
- (Flexibility)"A r-mer is also characterized by a "flexibility parameter", δ. It is equal to the number of ways in which the r-mer can be arranged on the lattice after one

of its mers has been fixed on a lattice site. ... It will be assumed that the flexibility parameter δ is independent of temperature and pressure." [104]

- (Preserved close-packed volume) "It will be assumed that the close packed volume rv^* of a molecule is independent of temperature and pressure. The close packed volume of a mer is v^*; it is also the volume of a lattice site." [104]
- (Hole volume) "The volume associated with an empty lattice site (a hole) is also equal to v^*; ..." [104]
- (Nearest neighbour interaction) "The energy of the lattice depends only on nearest-neighbour interactions. ... The only nonzero pair interaction energy is the one associated with nonbonded, mer-mer interactions; hole-hole, hole-mer, and bonded mer-mer pairs are assigned a zero energy. ... The quantity $r\epsilon^*$ is the characteristic interaction energy per molecule in the absence of holes; ϵ^* is also the energy required to create a lattice vacancy (hole)." [104]
- (Fluid characterization) "A pure fluid is completely characterized by three molecular parameters: ϵ^*, v^*, and r, or equivalently, the scale factors T^*, P^*, and ρ^*." [104]

In order to combine molecules from different pure fluids, the lattice construction makes it necessary to add additional "combining rules". The combining rules allow for the population of a mixture lattice with molecules from two different pure fluid lattices. These assertions about the way in which lattices are combined are generally known as mixing rules. The mixing rule assertions are [66, 105]:

- (Volumetric mixing rule) "In general, v^* is some unknown function of v_i^* and the composition of the mixture. ... The close-packed molecular volume of each component is conserved." [66]
- (Energetic mixing rule) "Characteristic pressures are pairwise additive in the close-packed mixtures ... the characteristic pressure P^* is closely related to the physical property of cohesive energy density and our third (energetic mixing) rule insures pairwise additivity of this property in the close-packed state." [105]

Note that the first two original SL combining rules, alluded to in the energetic mixing rule assertion, are not included in the list. The first two combining rules are used to impose a specific mixing rule for the volumetric mixing rule, namely the linear mixing rule. SL admit that such rules are often arbitrary [105]. Only the most general assertion is used here.

Assertion	Justification
(Segment excluded volume) The fluid is composed of polymer molecules, denoted species s, each divided into N_s equal segments of volume v_s that cannot overlap.	Directly from the *lattice character* assertion.
(Preserved close-packed volume) The volume occupied by a polymer molecule is constant, given by the product of the quantities $N_s v_s$, and a characteristic of a given polymer species.	From the *preserved close-packed volume* and *fluid characterization* assertions. If r and v^* characterize the fluid, then the molecular volume rv^* also characterizes the fluid.
(Short-ranged segment interaction) Interactions are limited to those between polymer segments only. The strength of the interactions are assumed to be temperature- and pressure- independent. Interactions are short-ranged, so that they become negligible beyond a segment size. Such interactions are a characteristic of a given polymer species.	From the *nearest-neighbour interaction* and *fluid characterization* assertions. While not necessarily implicit, if r and ϵ characterize the fluid, then both should be invariant. This is confirmed by their treatment in the literature.
(Free volume partition) The fluid contains free volume not occupied by molecular segments. The free is volume partitioned into equal segments of volume v_h. These segments are referred to as "holes".	From the *lattice character* and *hole volume* assertions. Whereas vacancies may not be considered independently of the segments in statistical considerations, the holes in the SL theory are treated as a set of indistinguishable particles in the number of configurations.
(Hole character) Holes are treated as a distinct chemical species rather than simple vacant space. The species contains translational degrees of freedom only.	While not explicitly present in the SL theory assertions, holes are given no internal degrees of freedom.

Assertion	Justification
(Incompressibility) The system of polymer molecules and holes is assumed to fill all space, so that if a given location is not occupied by a polymer segment, it is occupied by a hole.	From the *lattice character* and *hole volume* assertions. The assertions have been rephrased to make clear that holes are treated as indistinguishable particles in statistical considerations.
(Constant hole volume) The volume of a hole v_h is constant and a characteristic of a given polymer species. Changes in free volume correspond solely to changes in the number of holes.	From the *fluid characterization* assertion. While not necessarily implicit, if v^* characterizes a fluid, then it should be invariant. This is confirmed by its treatment in the literature.

Appendix B

Robustness of parameters determined through nonlinear parameter estimation

Caution is needed when extrapolating a model where parameters are determined through nonlinear least squares parameter estimation. Although many other sources of uncertainly affect nonlinear regression, Vidaurre et al. [125] find that uncertainty caused by incomplete data sets has a significant effect on the robustness of the resulting parameters.

In order to illustrate the potential difficulties of nonlinear least squares parameter estimation, a simple example is presented using a contrived model given by equation

$$y(x) = \alpha e^{-\frac{1}{2}\left(\frac{x-\mu}{\sigma}\right)^2}. \tag{B.1}$$

The model is assigned the parameters $\alpha = 1.2$, $\mu = 1.5$, and $\sigma = 0.9$. Virtual data is derived from the model by selecting evenly spaced points along the x-axis, with random error simulated using pseudo-random deviation from the corresponding y points on the curve given by equation B.1. The simulated random error is generated from a normal probability distribution using a fixed standard deviation of $\sigma = 0.02$. In this way, the present example endeavours to include random and limited range parameter estimation errors, while deliberately excluding model error. In an attempt to isolate small sample size error, each data set contains an equal number of $n = 40$ points. Regression is performed using nonlinear least-squares parameter estimation with a Levenberg-Marquardt optimization algorithm [83]. All regressions begin at the same initial choice of parameters given by $\alpha = 2.5$, $\mu = 3.0$, and $\sigma = 1.8$.

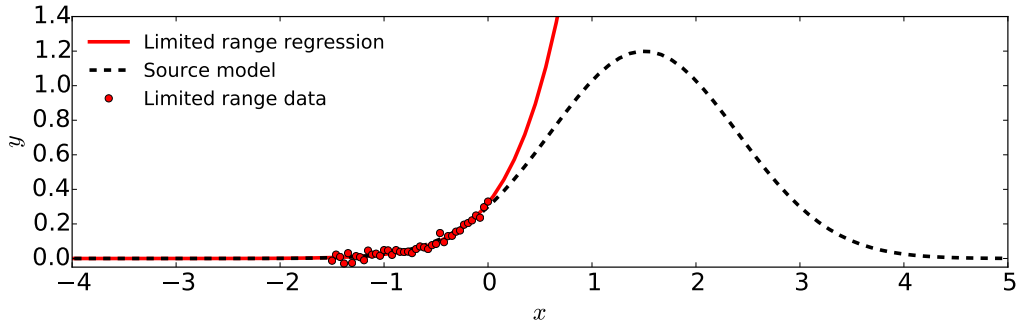

(a)

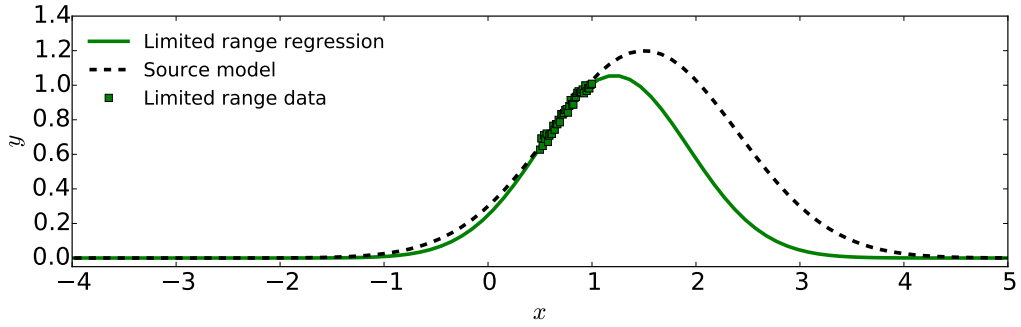

(b)

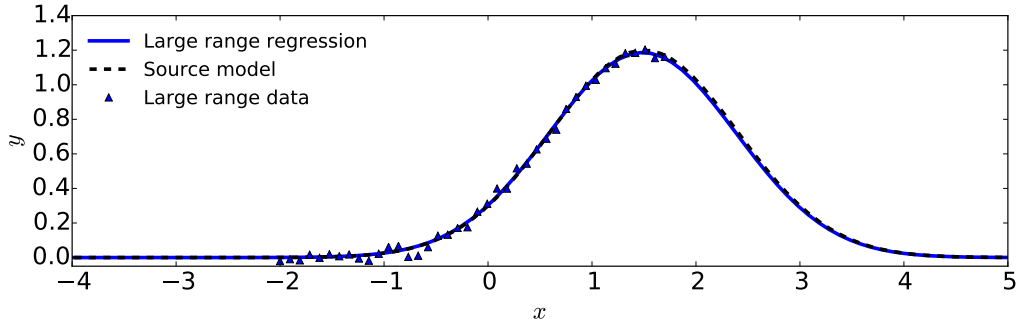

(c)

Figure B.1 Regressions performed using [(a), (b)] data over a limited range and (c) data over a large range. Points represent data and solid lines represent regressions and dashed lines represent the actual source model for the data, as indicated by the legends.

Regression	Data range	α	μ	σ
Limited range (a)	-1.5 to 0	129.3 (10 700%)	5.078 (239%)	1.466 (62.9%)
Limited range (b)	0.5 to 1.0	1.056 (12.0%)	1.214 (19.1%)	0.7129 (20.8%)
Large range (c)	-2.0 to 1.7	1.186 (1.15%)	1.487 (0.868%)	0.8999 (0.0163%)

Table B.1 A comparison of the parameters regressed from data over a limited range and over a large range as shown in figure B.1. Data points were obtained using a pseudo-random distribution about the model given by equation B.1 using the parameters $\alpha = 1.2$, $\mu = 1.5$, and $\sigma = 0.9$. Deviation of the regressed parameters from those of the source model are given in the form of a percent.

Figure B.1 compares the data sets obtained from the model and the resulting regressions. Table B.1 compares the parameters regressed from each data set with those of the source model. Figures B.1a and B.1b show the curves obtained by regression of the limited range data are not consistent, with B.1b producing better agreement than B.1a. Table B.1 reflects this observation, with the parameters for the regression in figure B.1b more closely matching the actual parameters than those of the regression in figure B.1a. This seems to suggest that the proximity of the data to important features of the model, in this case the Gaussian peak, affects the quality of the regression and the robustness of the parameters. Significantly, it is clear that while both figures B.1a and B.1b would produce excellent correlation to the virtual data in the range from which the parameters are derived, extrapolation would prove to be much less successful. On the other hand, the regression in figure B.1c shows excellent agreement with the source model, with table B.1 showing that the parameters regressed from the large range agree closely with those of the source model. More significantly, it is clear that in contrast to the parameters regressed from the limited range data sets, parameters regressed from the larger range allow for successful extrapolation.

In the case of a theoretical model applied to experimentally obtained data, model error, systematic error, and other factors are also present, further complicating regression. As well, in contrast to the present simplified example, the important features of more complex theories may not be known, complicating the strategic choice of range in order to obtain the best possible parameters. Therefore, if one is ignorant of the complete set of features of significance to a theoretical model, then the present example suggests that it is advisable to perform a nonlinear least squares parameter estimation over as large a range as possible.

Glossary

binodal (also **coexistence curve**) the set of points on the equilibrium surface that mark the coexistence of two phases.

blowing agent a substance used for the purpose of creating gaseous voids in the foaming process.

chemical blowing agent a blowing agent that uses thermal decomposition to generate gases.

coarse-graining the modelling of a system of discrete components by using fewer numbers of larger components.

colligative properties solution properties that depend on the concentration of solute but not on the identity of the solute.

configurational partition function the portion of the partition function dependent on position, to the exclusion of momentum, rotation, vibration, etc.

critical point the point on the equilibrium surface at which the binodal and spinodal curves intersect, marking the terminus of a first-order phase transition.

foam a substance composed of gaseous voids in a continuum of dense material.

goodness of fit a measure that characterizes the discrepancy between a model and observed values.

mer a polymer segment in a molecular theory construction that may be equal or larger than the size of a monomer, depending on the level of coarse-graining.

microstate the set of spatial coordinates, internal coordinates, velocities, etc. that describe a system of particles at a given instant.

oligomer a molecule composed of relatively few molecular sub-units.

physical blowing agent a blowing agent that uses thermodynamic phase transition to generate gases.

polymer a molecule composed of a large number of molecular sub-units.

solvent a substance composed of molecules much smaller than those of the polymer with which it is mixed, as considered by Flory-Huggins solution and related theories.

spinodal the set of points on the equilibrium surface near a first-order phase transition curves that mark the boundary between the metastable and unstable states.

state equation (also **equation of state**) an equation establishing a relationship between the state variables at equilibrium.

state variable (also **variable of state**) one property of a set that define the current state of a thermodynamic system.

statistical mechanics a branch of physics using probability theory to derive averaged system properties from assertions about the structure and properties of its constituent particles.

statistical thermodynamics the combined branch of physics aggregating statistical mechanics and thermodynamics.

thermal fluctuation the random deviation of a thermodynamic system from its equilibrium state.

thermodynamic coordinates a set of properties of a thermodynamic system that together represent a thermodynamic state (see **state variable**).

thermodynamic potential a scalar quantity characterizing the state of a thermodynamic system.

thermodynamic response functions quantities derived from the second derivatives of thermodynamic potentials.

thermodynamic state (also **macrostate**) the set of thermodynamic state variables that describe a system at a given instant.

thermodynamics a branch of physics dealing with the relationship between forms of energy.

thermoplastic polymers in bulk material, polymer molecules are held together by inter-polymer coiling and van der Waals forces that increase in mobility with temperature.

thermoset polymers in bulk material, polymers have a complex, connected network structure with little mobility increase with temperature.